The Institute of Paper Chemistry

Appleton, Wisconsin

Doctor's Dissertation

The Effect of the Aglycon and Hydroxyl Orientation on Alkali-Oxygen Degradations of Methyl Glycosides

David O. Hearne

June, 1978

TABLE OF CONTENTS

SUMMARY

Methyl β-D-ribopyranoside (MBR) and methyl β-D-xylopyranoside (MBX) were degraded by molecular oxygen (0.682 MPa partial oxygen pressure) in a Teflon-lined reactor at 120°C and 1.25M sodium hydroxide. The degradations were followed by quantitative gas-liquid chromatography and were analyzed for both degradation rate and product appearance. The glycosidic bond was found to have little effect on the overall rate or pattern of pyranoid ring degradation in oxygen-alkali. Consistent with previous workers (1-3), however, ring hydroxyl orientation dramatically affected the reaction rate. MBR degraded at an initial rate approximately six times the initial degradation rate of MBX. It is postulated that the cis 1,2-diol configuration in MBR favors stabilization via intramolecular hydrogen bonding of the oxyanion formed in the first step of the proposed mechanism of oxygen-alkali degradation of carbohydrates. This stabilization effectively increases the oxyanion concentration in the MBR system leading to an increase in the frequency of initiation reactions and the degradation rate. Consistent with this hypothesis, MBR produced more hydrogen peroxide in oxygen-alkali than did MBX.

Kinetic analysis showed the time dependent orders of MBR and MBX degradation to be 2.75 and 3.5, respectively. Due to similarities in degradation rates and reaction pathways of MBR and MBX, the mechanism for the degradation of the 1,5-anhydroalditols was assumed to be applicable (1-2). This mechanism predicts the degradations to be second order in carbohydrate. The kinetic orders of MBR and MBX were interpreted to imply autoinhibition, i.e., an intermediate in the reaction serves to abnormally slow it down. This autoinhibition is proposed to be the result of a termination reaction between an alpha-hydroxyhydroperoxyl radical and the frequently proposed C-1 radical resulting from anomeric hydrogen atom abstraction. Formation of stable organic peroxides in both methyl glycoside systems supported this hypothesis.

The major acidic reaction products were identified as their per-O-trimethylsilyl derivatives by gas-liquid chromatography-mass spectrometry. The formation of lactic, glycolic, and glyceric acids was qualitatively the same as previously reported in other carbohydrate systems (1-3). A methyl 3-C-carboxy-β-D-tetrafuranoside and isomeric methyl 2-C-carboxy-β-D-tetrafuranosides were identified as major "bound methanol" products. The relative ratios of these methyl C-carboxyfuranosides varied between the MBR and MBX systems thus supporting the previously observed stereoselective formation of these furanoid acids (1). Methoxyacetic acid was observed for the first time as a product of the oxygen-alkali degradation of methyl glycosides. The formation of this product suggests an alternative polysaccharide chain cleavage mechanism to β-alkoxy elimination.

Varied C-3 hydroxyl stereochemistry did not affect glycosidic bond cleavage as determined by a gas-liquid chromatographic methanol analysis. The yields of methanol were identical from both MBR and MBX even though MBR degraded at a much faster rate. The reaction step determining the relative rate of reaction between MBR and MBX apparently occurs prior to the methanol-liberating reaction, a result consistent with the above hypothesis concerning the oxyanion. Although the C-1 radical was postulated to play an important role in autoinhibition, the degradation rate, product, and methanol data implied that C-1 radical formation and decomposition did not represent a major degradative pathway for the methyl glycosides.

INTRODUCTION

PERSPECTIVE

The polluting nature of pulping and bleaching processes utilizing chlorine and sulfur has been widely publicized. Likewise, the potential advantages of delignification with molecular oxygen and alkali are well established. Hindering the full development of oxygen-alkali processes, however, is the harmful degradation of wood polysaccharides in oxygenated, alkaline solutions. This carbohydrate degradation results in a loss of pulp viscosity and mechanical strength.

A potential solution to the carbohydrate degradation problem involves developing an understanding of the degradative reactions. Once the mechanism is understood then the possibility exists to devise methods of intercepting the carbohydrate-degrading reactions. This investigation was designed to examine certain aspects of the degrading mechanism: namely, the effect of the glycosidic linkage on carbohydrate reactivity to oxygen and alkali, and how glycosidic bond cleavage by oxygen-alkali changes with varied ring hydroxyl stereochemistry.

LITERATURE REVIEW

Conventionally the reactions of cellulose and other wood polysaccharides in alkali are divided into two categories — peeling and chain cleavage. The peeling reactions occur at the reducing end of the polymer chain and consist of the stepwise removal of reducing end groups. Chain cleavage involves the breaking of the polymer chain between two inner polymeric units. Similarly, the reactions of wood polysaccharides in oxygen and alkali can be categorized into these two groups — reactions at the reducing end group and chain cleavage reactions. This review will deal only briefly with the reducing end reactions

as they are generally considered to be unimportant in the oxygen-alkali treatment of wood pulps (3-7). Since oxygen-alkali treatment of wood and wood pulps causes significant viscosity loss without adverse yield loss (7) the chain cleavage reactions are the more important ones to understand. The review will present some of the major studies on chain cleavage reactions with emphasis being placed on model compound studies. Finally, an overview of the mechanism of oxygen-alkali degradation of polysaccharides will be presented.

OXYGEN-ALKALI REDUCING END REACTIONS

The apparent stability of oxygen-alkali pulps to alkaline peeling has been attributed to the formation of aldonic acid end groups (4-6,8-11). These end groups prevent the β-alkoxy elimination reaction characteristic of the peeling mechanism. Samuelson and coworkers (4,5) investigated the aldonic acid end groups in cellulose after oxygen bleaching, detecting arabinonic, mannonic, and erythronic acids as the major end groups. Metasaccharinic acids, which are commonly associated with peeling, were found only in minor amounts. Rowell (6) studied the degradation of cellobiose by alkali and oxygen-alkali. In the absence of oxygen, alkali degraded cellobiose completely to monomer units. But when oxygen was present glucosylaldonic acids were produced in up to 27% yields.

Glycosuloses have been postulated as intermediates in the formation of aldonic acid end groups in wood polysaccharides treated by oxygen-alkali (8-11). By comparing the distribution of aldonic acids formed from glucosone and xylosone with the distribution of acid end groups produced respectively from cello-oligosaccharides and xylo-oligosaccharides, Malinen (8) concluded that glycosuloses were likely intermediates in the formation of the aldonic acid end groups.

In summary, some stabilizing effect to peeling reactions seems operative in oxygen-alkali treatments of wood polysaccharides. However, as noted by Malinen (8) some care must be observed in the reaction conditions employed. In his study, hydrocellulose did not always show stability to peeling and the distribution of aldonic acid end groups in these cases differed from the distribution found from glucosone.

CHAIN CLEAVAGE

Chain cleavage and ring opening reactions of polysaccharides have primarily been investigated by using mono- and disaccharide model compounds, most notably methyl β-D-glucopyranoside (MBG). Parameters which have been investigated include number and position of hydroxyls (12,23), the effect of additives (13,14), the importance of peroxidic intermediates (1,2,12-17), and ring hydroxyl stereochemistry (1,2).

Brooks and Thompson (18) noted that oxygen increased the rate of MBG degradation many times over the rate of degradation in the absence of oxygen. The difference was postulated to arise from a lower activation energy for the oxidative reaction than for alkaline hydrolysis. It was proposed that in the presence of oxygen a carbonyl group is introduced to the ring leading to a subsequent β-alkoxy elimination of the C-1 methoxyl group.

McCloskey, et al. (12) examined the oxygen-alkali degradation of MBG and a variety of its methyl ether derivatives. The importance of a free hydroxyl group was emphasized by the fact that methyl 2,3,4,6-tetra-O-methyl β-D-glucopyranoside did not react in oxygen and alkali. Later Millard (1) and Millard, et al. (2) determined that the stereochemistry of the ring hydroxyls was also important to the degradation reaction. Millard examined the oxygen-alkali degradation of 1,5-anhydroxylitol (AX) and 1,5-anhydro-

ribitol (AR). All neighboring hydroxyl orientations in AX are trans while they are cis in AR. The initial degradation rate of AR was ca. 7 times that of AX. Malinen and Sjostrom (3) have noted a similar relationship in reactivity with varied hydroxyl orientation in their limited study of the oxygen-alkali degradation of methyl β-D-glucopyranoside and methyl β-D-mannopyranoside.

McCloskey, et al. (12) were also the first to note that MBG degradation in oxygen-alkali could occur without cleavage of the glycosidic bond. Their data showed that the rate of methanol formation was slower than the rate of MBG degradation. Subsequent acid hydrolysis of the product mixture, however, yielded the unaccounted for methanol. Ericsson, et al. (15) in a later study of the oxygen-alkali degradation of MBG isolated an acidic product containing the methyl aglycon. This product was identified as a methyl 2-C-carboxy-β-D-pentafuranoside and was proposed to be formed via a diketo intermediate (Fig. 1). The diketo intermediate was postulated to arise from the simultaneous introduction of keto groups at C-2 and C-3. The ring can then contract via a benzylic acid type arrangement. Subsequently 2-C- and 3-C-carboxyfuranosides have been identified in a variety of degradations of methyl glycosides with oxygen-alkali (3).

Millard (1,2) in examining the oxygen-alkali reaction of AX and AR identified as products isomeric 1,4-anhydro-2-C-carboxy tetritols which are analogous to the furanoid acids reported by Ericsson, et al. (15). Depending on the alditol examined, the ratio of the two isomers would change, suggesting a stereochemical effect to be operating in their formation. The mechanism of Ericsson (15) could not account for this stereoselectivity and Millard (1,2) offered an alternative mechanism involving an alpha-hydroxyhydroperoxide intermediate.

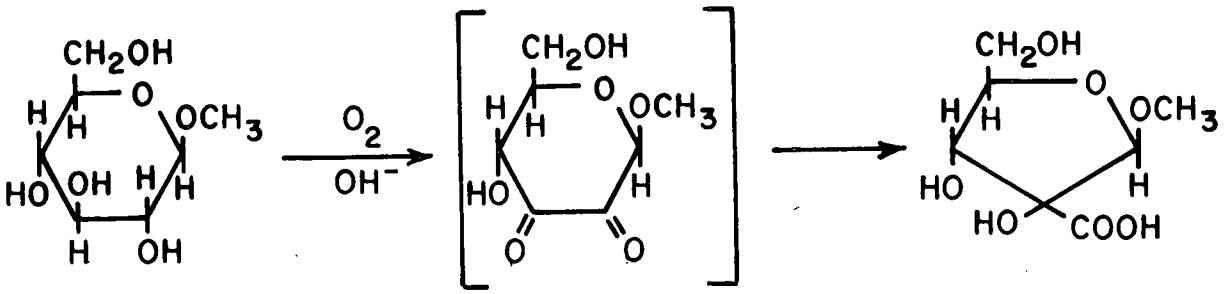

Figure 1. Mechanism Proposed for Formation of Methyl 2-C-Carboxyfuranosides (15)

Hydrogen peroxide has frequently been reported as an intermediate in the degradation of carbohydrates by oxygen and alkali (1,2,12-14,16-18). Sinkey and Thompson (13), in their work with MBG, provided strong evidence for the identity of hydrogen peroxide as an intermediate. The oxygen-alkali degradation of MBG exhibited an induction period during which hydrogen peroxide increased in concentration. Additionally, a rough correlation existed between the end of the induction period and the peak in hydrogen peroxide concentration. These results paralleled the earlier work of Minor and Sanyer (17) on the oxygen-alkali degradation of glucitol. Sinkey (13) also examined the effects of magnesium, iron, and iodide ion on the degradation of MBG. In each case the effect of the additive could be related to the expected behavior of the hydrogen peroxide intermediate in the presence of the additive. Weaver (19) and Ericsson (15), working independently, examined the alkaline hydrogen peroxide degradation of MBG. Their results demonstrated a commonality in products with the products from the oxygen-alkali reaction of MBG.

Sinkey (13) also reported that organic peroxides were formed in the oxygen-alkali degradation of MBG. These peroxides did not appear to be reactive intermediates and were hypothesized to be dialkyl peroxides arising from radical chain termination reactions. Weaver (19) and Weaver, et al. (20)

provided evidence in their study for an intermediate organic peroxide which they proposed to be an alpha-hydroxyhydroperoxide. Millard (1,2) detected an intermediate organic peroxide in the oxygen-alkali degradation of AX. Based upon their experimental evidence this intermediate organic peroxide was also hypothesized to be an alpha-hydroxyhydroperoxide.

In addition to the previously discussed furanoside products, numerous other acids have been reported as products in oxygen-alkali studies, most notably lactic, glycolic, and glyceric acids (1-3,15). Minor concentrations of many other acids such as dibasic acids have been reported. The one characteristic of all of these acids is that they are proposed to be formed via a keto intermediate (1-3,12-15,18).

In summary, model compound studies have generally supported the reaction scheme adapted by Kolmodin and Samuelson (5) for the oxygen-alkali degradation of cellulose (Fig. 2). This mechanism was adapted from the mechanism proposed by Haskins and Hogsed (21) for the depolymerization of cellulose during the aging of alkali cellulose. However, the mechanism of carbonyl formation in the cellulose and how this carbonyl formation is related to hydrogen peroxide and organic peroxides remains unclear.

REACTION MECHANISM

This section will present a current view of the reaction mechanism of oxygen-alkali degradation of carbohydrates. It should be remembered that although many of these reactions are based on experimental observation and analogous autoxidation reactions, they are still largely speculative.

Initiation of oxidative degradation requires the ionization of an hydroxyl to form the carbinolate anion (1,2,12-14,17). The increased electron density provided by the carbinolate ion facilitates hydrogen abstraction

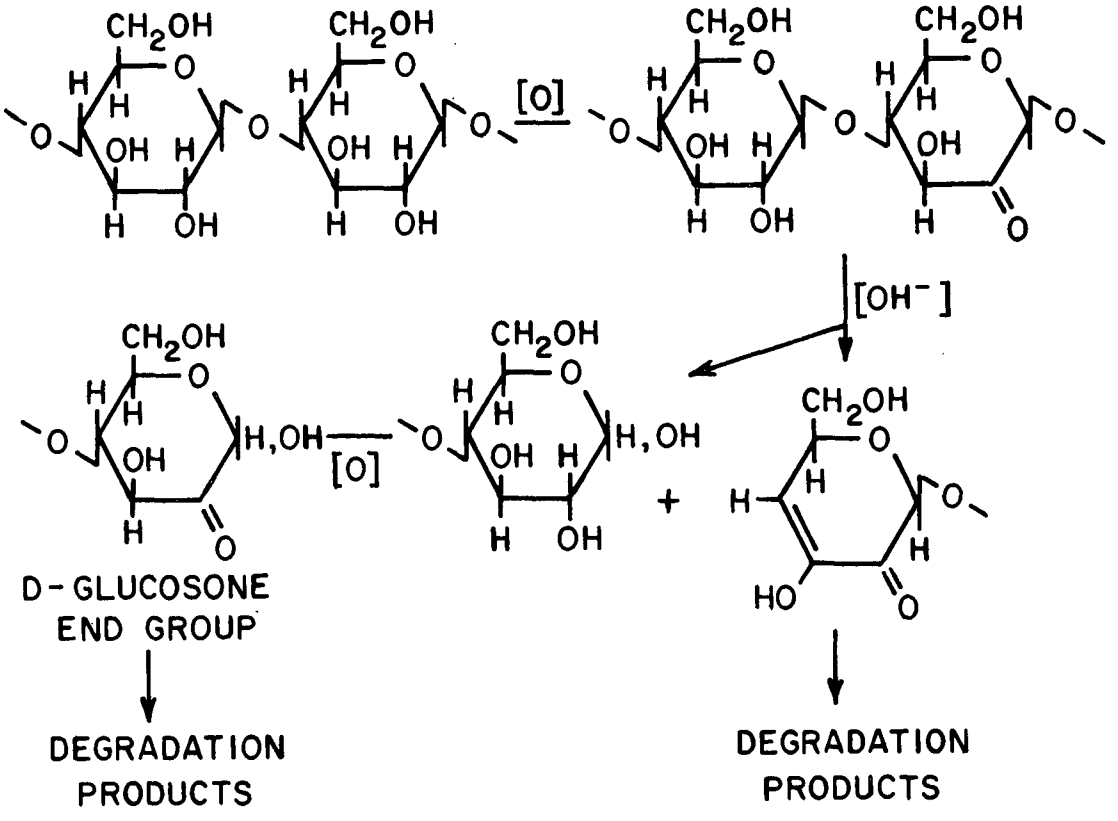

Figure 2. Mechanism for Cleavage of Cellulose by Oxygen in Alkali Proposed by Haskins and Hogsed (21)

by molecular oxygen (Fig. 3). This view is consistent with reactions reviewed by Russell (22) as important in autoxidation.

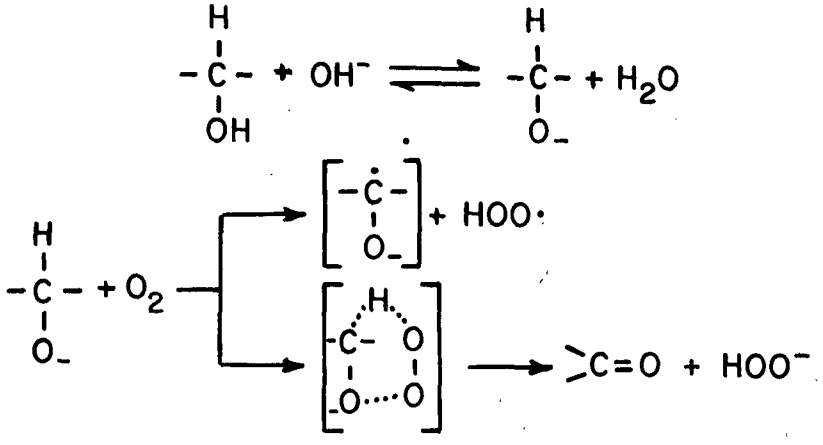

Figure 3. Initiation of Carbohydrate Oxidative Degradation Proposed by McCloskey (23)

The reactions usually show induction periods (1,2,12,13,16,17) during which hydrogen peroxide increases in concentration. Subsequently the carbohydrate degrades rapidly, probably via a free radical mechanism (1,2,12-14). The free radicals are generated by hydrogen abstraction with oxygen (Fig. 3) and metal-catalyzed decomposition of the perhydroxyl anion (1,2,12-14). Intermediate hydroperoxides are hypothesized (1,2,14,17) to arise in a variety of reactions between the carbohydrate and radical species. The hydroperoxides then decompose to acidic degradation products, possibly through carbonyl-containing intermediates (1-3,12-15,18). The presence of organic peroxides in oxygen-alkali reactions has been noted (1,2,13,14) although their structures are as yet undetermined. Studies of the alkaline hydrogen peroxide reaction of MBG suggested the presence of an alpha-hydroxy-hydroperoxide (20,21) and Millard (1,2) has suggested an alpha-hydroxyhydroperoxide as an intermediate in the oxygen-alkali reaction of the 1,5-anhydroalditols. The peroxides noted by Sinkey (13,14) were believed to be dialkyl peroxides arising from termination reactions.

THESIS OBJECTIVES

As noted in the Literature Review, simple glycosides have frequently been used as model compounds in studies of wood polysaccharide degradation by oxygen-alkali. However, little is known as to how the aglycon affects the reactivity of these glycosides. Millard (1,2) recently examined the oxygen-alkali degradation of selected 1,5-anhydroalditols and obtained information on ring cleavage reactions and how these reactions changed with varied hydroxyl orientation. By examining the glycosidic analogs — methyl β-D-ribopyranoside (MBR) and methyl β-D-xylopyranoside (MBX) — of the alditols studied by Millard, information on the effect of the glycosidic bond was obtained.

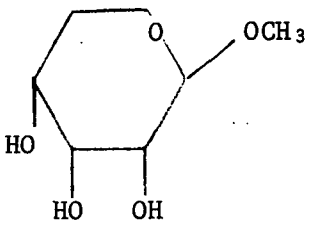

MBR

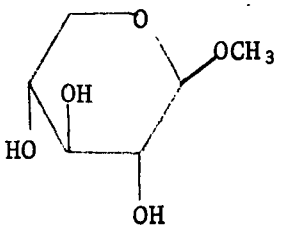

MBX

Differences in reactivity between the alditols and the methyl glycosides were projected because of the following:

1) the glycosidic bond enhances the acidity of the C-2 hydroxyl (24-26),
2) the glycosidic bond enhances radical formation at C-1 through resonance stabilization (27,28), and
3) the methyl aglycon can compete with the ring oxygen as a leaving group in β-alkoxy elimination.

By examining glycosidic bond cleavage and the differences in kinetics and products between the glycosides and the alditols, information was obtained concerning:

1) the impact of the aglycon on pyranoid ring degradation, and
2) the effect of varied hydroxyl orientation on glycosidic bond cleavage.

RESULTS

GLYCOSIDE DEGRADATIONS

GENERAL

To provide a common basis of comparison, the reaction conditions used were the same as employed by previous workers (1,2,12-14): 120°C, 1.25M NaOH, and 0.682 MPa partial oxygen pressure*. All reactions were conducted at a carbohydrate concentration of 0.1M.

The glycoside analyses were conducted by quantitative gas-liquid chromatography (GLC). The glycosides were analyzed as their per-O-acetylated derivatives and n-propyl β-D-xylopyranoside was utilized as an internal standard. The NaOH was purified to minimize metal catalysis (29). The experimental procedures are described in the Experimental section and chromatographic conditions are stated in Appendix I.

Duplicate degradations of both methyl β-D-ribopyranoside (MBR) and methyl β-D-xylopyranoside (MBX) were conducted at the stated conditions. Excellent agreement was found between the duplicated runs as indicated in Fig. 4 (MBX) and Fig. 5 (MBR). The dashed lines in the two figures represent the degradation curves reported for the analogous 1,5-anhydroalditols (1,2). The methyl glycosides showed surprising similarity in reactivity to the alditols. However, minor differences do exist between the degradation curves of the anhydroalditols and the methyl glycosides which are unexplained by experimental error. Thus the glycosidic bond affects the rate of destruction of the pyranoid ring only slightly and the dramatic effect on rate

*Total reactor pressure at 120°C was 1.014 MPa (147.1 psia). This pressure accounted for 0.199 MPa (28.8 psia) water vapor and 0.133 MPa (19.4 psia) nitrogen.

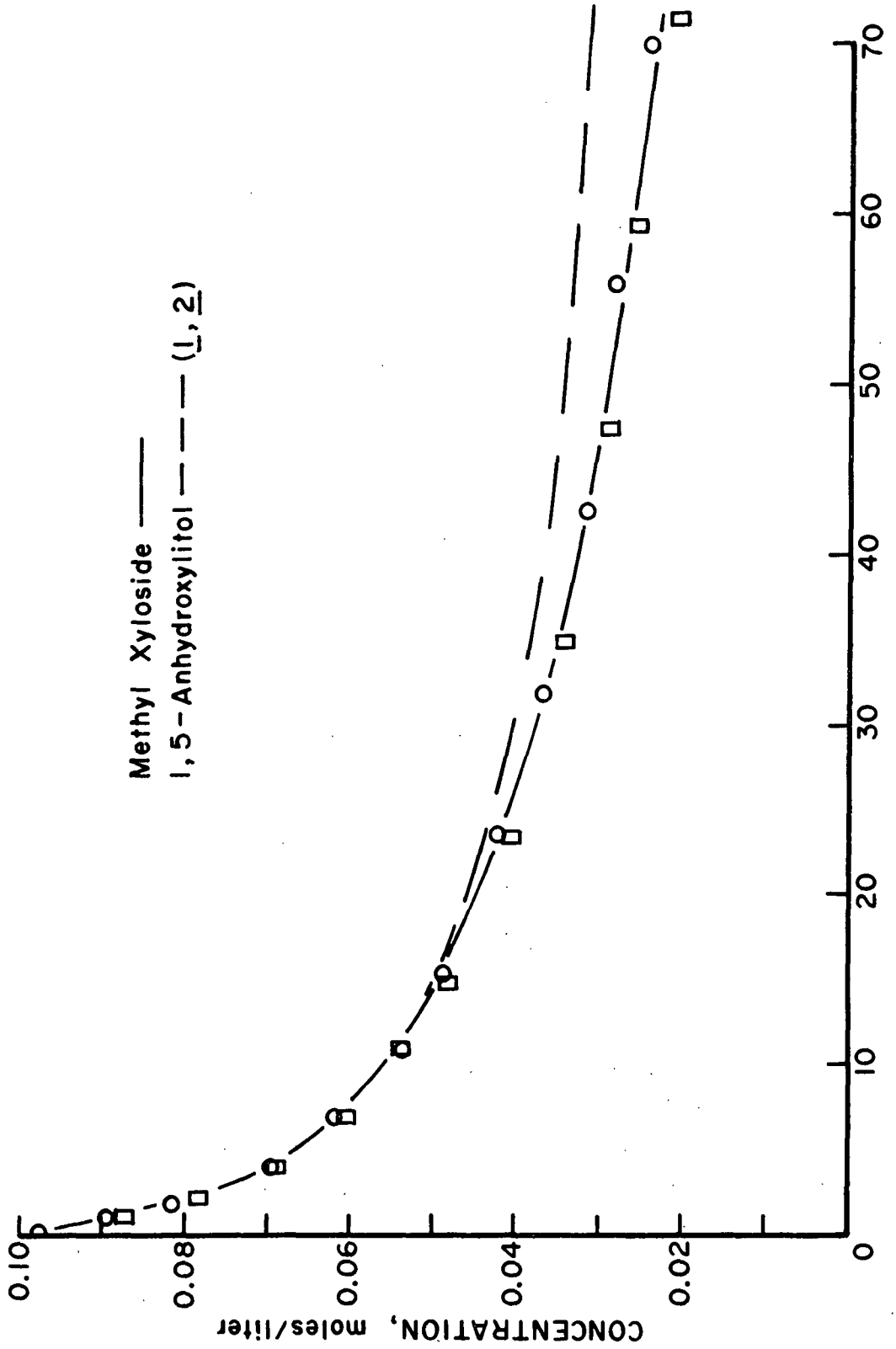

Figure 4. Concentration of Methyl β-D-Xylopyranoside (○- 7MBX, □ - 8MBX) as Function of Time in 1.25M NaOH at 120°C, 0.682 MPa O_2 and 0.1M Carbohydrate Concentration

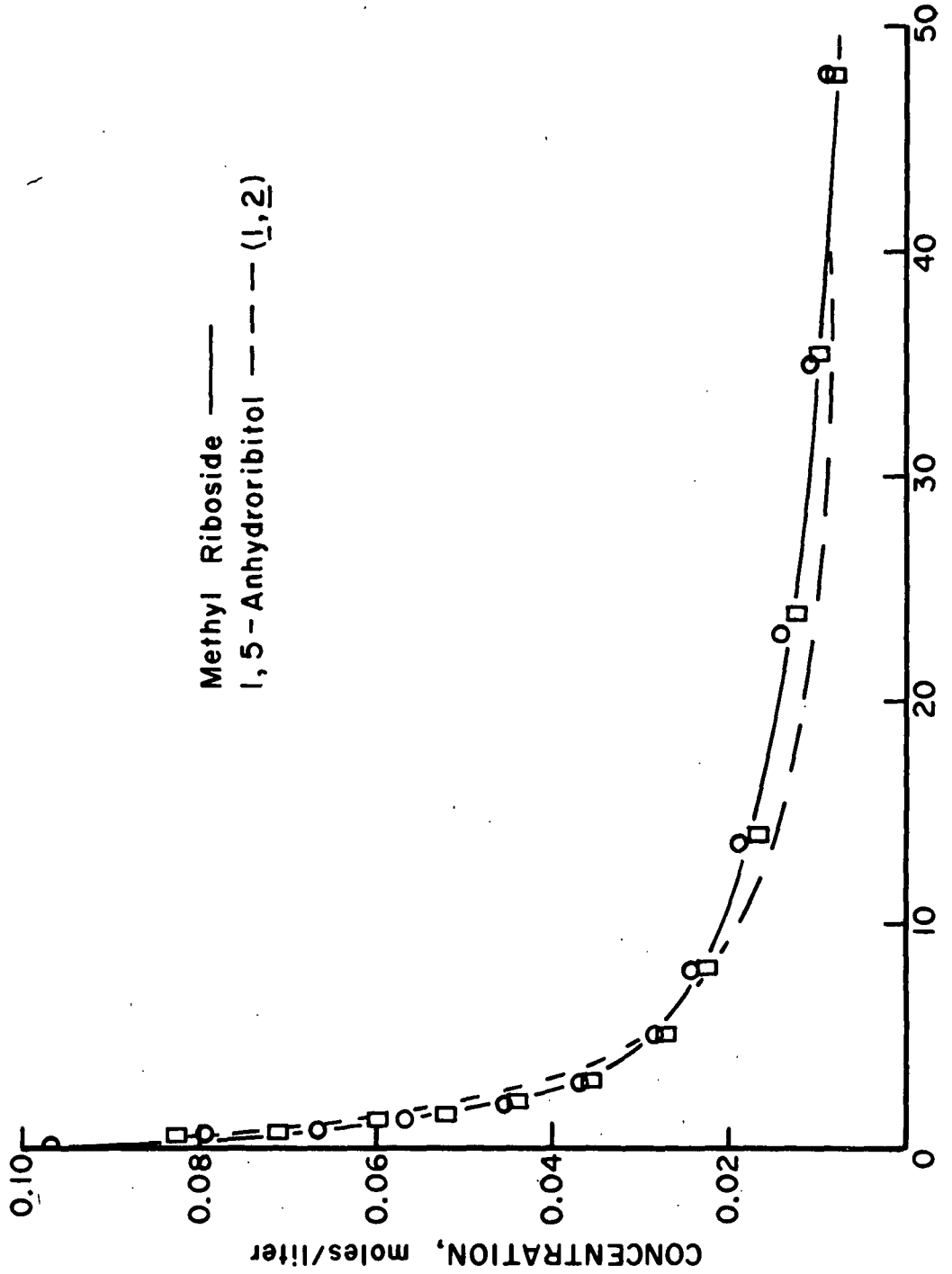

Figure 5. Concentration of Methyl β-D-Ribopyranoside (○- 5MBR,□ - 6MBR) as Function of Time in 1.25M NaOH at 120°C, 0.682 MPa O_2 and 0.1M Carbohydrate Concentration

that Millard (1,2) noted for hydroxyl stereochemistry extends to the methyl glycosides. Neither MBX nor MBR showed any degradation after 72 hr at 120°C and 1.25M NaOH in a nitrogen atmosphere (see Experimental Data, Appendix II).

OXYGEN SOLUBILITY

In studies of oxygen-alkali degradation of carbohydrates, a frequently posed question is whether or not the reaction is oxygen diffusion controlled. Previous workers have interpreted their data to exclude this possibility (2,30,31). Recently an apparatus for determining solution oxygen concentration at elevated pressures was developed (32). By employing this apparatus, solution oxygen concentration was determined at the described reaction conditions.

The experimentally determined saturated oxygen concentration was 2.9 x 10^{-3}M which is 25% higher than the value of 2.2 x 10^{-3}M obtained by a linear extrapolation of Bruhn, et al. data (33). In Table I oxygen dissolution rate is illustrated for conditions of no agitation and with agitation in the presence of carbohydrate. In the presence of 0.1M MBR, ca. 80% of saturation was reached within 6 minutes and saturation was achieved within 30 minutes. As seen in Fig. 5, MBR degrades rapidly and a problem of oxygen diffusion should have shown up as a depressed oxygen concentration during the first 1.5 hr of reaction. Therefore, in agreement with previous studies (2,30,31) it was concluded that oxygen diffusion did not present a kinetic problem. However, under conditions of no agitation the rate of oxygen dissolution was suppressed. This is important because contrary to previous reports (2,31) a threshold stirring rate is necessary to insure adequate oxygen dissolution. To illustrate this fact, degradations were conducted under conditions of limited agitation. The results of these degradations are reported in the section titled Oxygen Deficient Degradations.

TABLE I

OXYGEN SOLUBILITY IN 1.25M NaOH AT 120°C AND 0.682 MPa O_2 PRESSURE

Time, min[b]	Dissolved O_2, x 10^3M
Run OS3[a]	
10	0.8
41	0.9
150	1.4
330	1.7
948	1.9
1554	2.1
Run OS4[c]	
6	2.3
32	3.0
60	2.9
133	2.7
297	3.2
450	3.0

[a]No agitation or carbohydrate.

[b]Pressurized with oxygen at time zero.

[c]With agitation and 0.1M MBR.

REACTION EXOTHERMS

Reaction exotherms have been noted in oxygen-alkali pulping and bleaching experiments (34) and oxygen-alkali treatment of isolated lignin (35). In this work a temperature rise of ca. 1.3°C was noted during the MBR degradations. Very slight exotherms (ca. 0.2-0.3°C) were noted during the MBX degradations, but it was difficult to determine the exact temperature rise as this temperature variation corresponded closely to the control limits of the bath. No temperature rises were noted in the oxygen solubility experiments when carbohydrate was absent. In the case of MBR, the rise in temperature began 5-10 minutes after oxygen was charged to the reactor and reached a maximum after 0.7-1 hr. The temperature remained at this level for ca. 0.5

hr and then slowly declined back to 120°C. This is the first report, to the author's knowledge, of an exotherm during the oxygen-alkali degradation of a carbohydrate.

KINETICS

Background

The kinetics of the methyl glycoside degradations were examined to determine the order of the degradations with respect to glycosidic concentration. A comparison with the kinetics of the oxygen-alkali degradation of the 1,5-anhydroalditols provided information as to the effect of the methyl aglycon of the degradations.

The two most common methods of kinetic order determination are the method of integration and the differential method (36,37). The method of integration employs the integrated form of the rate equation and the data are plotted as dictated by the integrated form after first assuming a reaction order. Because the analysis is conducted on a single reaction plot, the resulting order is with respect to time. The differential method involves plotting the logarithm of the experimentally determined reaction rate against the logarithm of concentration. This yields a line which has a slope equivalent to order. If several reactions are conducted, the initial rates and concentrations can be used to determine the true order. If a single reaction plot is utilized the order determined is said to be with respect to time.

The method of integration allows for a quick check for integral orders, but suffers from sensitivity to slight deviations from integral order (37). Additionally, only in simple reactions do true order and time dependent order correspond. The differential method offers the advantage of not having to assume the reaction order, thereby eliminating the trial and error approach of the method of integration. The disadvantage of the differential

method is that rates must be determined graphically from reaction plots. While errors in rate determination are not significant when applying the differential method to initial rates determined at a wide range of concentrations, errors in rate determination from a single reaction plot can be considerable and cause a loss in sensitivity. A convenient cross-check of order determined by application of the differential method to a single reaction plot is to apply the order thus determined to the method of integration.

In this work the rate of carbohydrate degradation is assumed to be a function of carbohydrate, oxygen, and alkali concentrations as expressed in Equation (1).

$$-\frac{d[A]}{dt} = k[A]^n[OH^-]^m[O_2]^1 \qquad (1)$$

where $[A]$ = glycoside concentration

$-d[A]/dt$ = rate of glycoside disappearance

k = rate constant

$[OH^-]$ = alkali concentration

$[O_2]$ = oxygen concentration

$n,m,1$ = reaction orders

By examining the reactions under conditions of excess oxygen and alkali concentrations such that they are in apparent constant concentration through the course of the reaction, then Equation (2) may be written (36,37):

$$-\frac{d[A]}{dt} = k'[A]^n \qquad (2)$$

where $k' = k[OH^-]^m[O_2]^1$. Kinetic orders determined in this manner are termed psuedo orders. While solution oxygen concentration was not, strictly speaking, in excess relative to carbohydrate concentration, it was continuously introduced into solution by agitation. It has already been shown (see

previous discussion — Oxygen Solubility) that the rate of oxygen dissolution did not affect the degradation rate and therefore the assumption of constant oxygen concentration was valid. Initial alkali concentration was 1.25M NaOH which was an order of magnitude higher than the initial carbohydrate concentration. At long reaction times sufficient concentrations of acidic products are produced to depress the alkali concentration and thus limit the validity of assuming a constant alkali concentration. Millard (1,2), however, showed that this ca. 10-15% drop in alkali concentration did not apparently affect the kinetics.

To apply the differential method, the logarithms of both sides of Equation (2) are taken as shown in Equation (3).

$$\log \{- d[A]/dt\} = \log k' + n \log [A] \qquad (3)$$

Thus, a plot of log rate versus log concentration should yield a line of slope n (order). Application of the method of integration is made by employing the integrated form of Equation (2) which may be written for all n except unity as in Equation (4).

$$k' t (n-1) = \frac{1}{[A]^{(n-1)}} - \frac{1}{[A_o]^{(n-1)}} \qquad (4)$$

where $[A_o]$ = initial concentration. If a plot of time versus $1/A^{(n-1)}$ is linear, the assumed order is correct.

Methyl Glycoside Kinetic Orders

Application of the differential method to the methyl glycosides of this study yielded orders of 2.75 for MBR and 3.47 for MBX (Fig. 6). In contrast, Millard determined orders of 2.0 for 1,5-anhydroribitol (AR) and 3.46 for 1,5-anhydroxylitol (AX) under the same reaction conditions. The orders derived for MBR and MBX by the differential method were supported by applying these

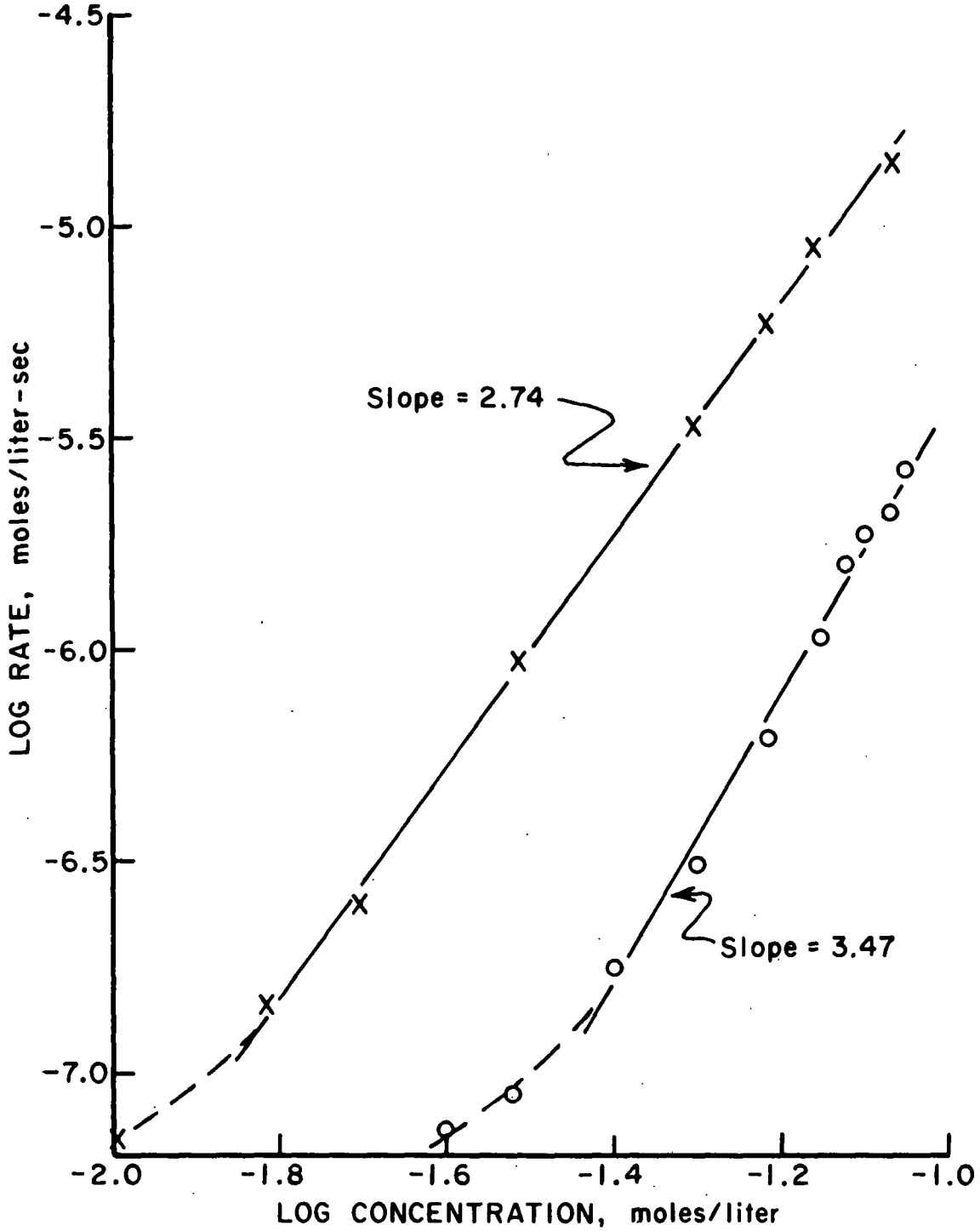

Figure 6. Degradation of 0.1M Glycosides (X - 6MBR, O - 8MBX) in 1.25M NaOH at 120°C and 0.682 MPa O_2. Data Plotted According to the Differential Method

orders to the integrated rate equation. Linear relationships were obtained for both MBR (Fig. 7) and MBX (Fig. 8) although at long reaction times the MBX relationship breaks away from linearity. This divergence from an MBX order of 3.5 is also seen in Fig. 6. A similar but less dramatic break from the derived order was exhibited by MBR.

In comparing the kinetics of the anhydroalditols *versus* methyl glycosides subtle differences were noted. First, although both MBX and AX showed a kinetic order of *ca.* 3.5 through the first 50% of reaction, MBX exhibited a lower reaction order at long reaction times. AX showed no such change in reaction order. This divergence in reaction order occurs at the same point that the reaction plots of MBX and AX begin to diverge (Fig. 4). Secondly, AX showed a tendency to higher reaction orders at the beginning of the reaction while MBX did not. Likewise, the subtle differences in the reaction plots of MBR and AR (Fig. 5) are manifested in differences in kinetic order. It was primarily the difference in kinetic order between MBR (2.75) and AR (2.0) and the difference in organic peroxides, which are reported later, that led to the interpretation of what effect the methyl aglycon has on the degradations. This interpretation is presented in the Mechanism section.

PRODUCTS

METHANOL

To determine the extent of glycosidic bond cleavage and how this cleavage might vary between MBR and MBX, the formation of methanol with time was examined. The methanol was analyzed by quantitative GLC (38) employing ethanol as an internal standard. The method is described in the Experimental section and the GLC conditions are tabulated in Appendix I.

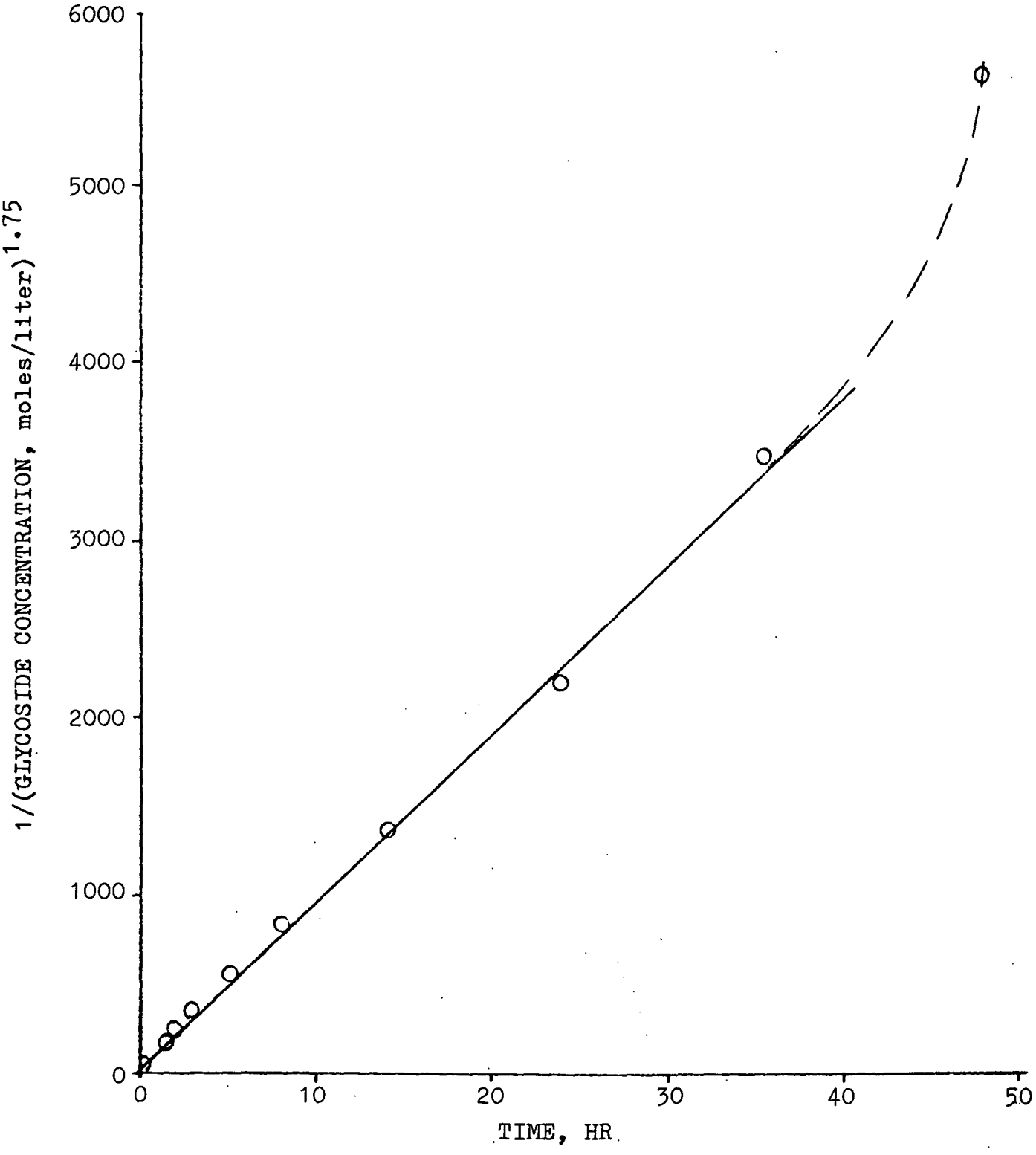

Figure 7. Kinetic Plot of Reaction 6MBR According to the Method of Integration Assuming an Order of 2.75

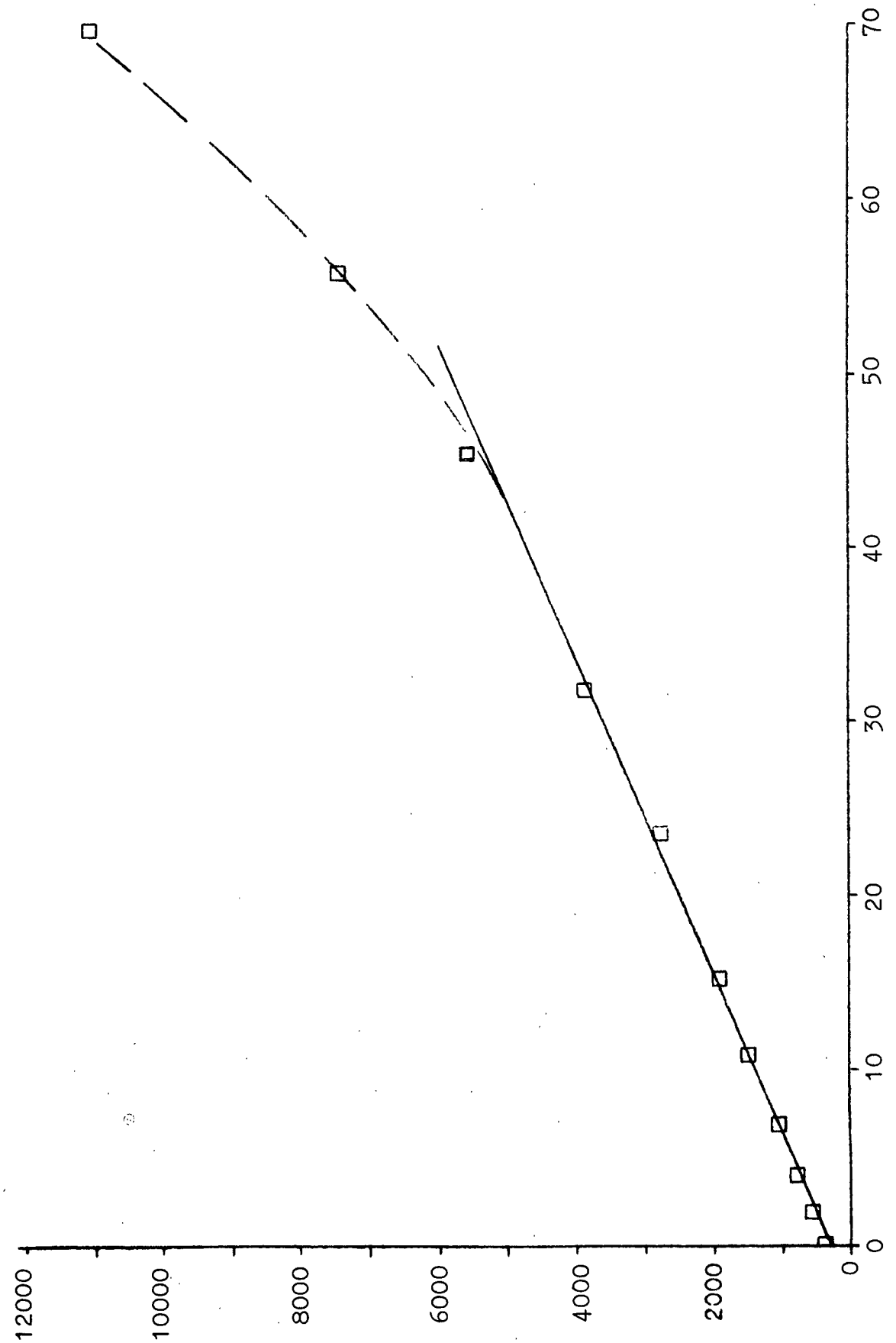

Figure 8. Kinetic Plot of Reaction 7MBX According to the Method of Integration Assuming an Order of 3.5

The yield of methanol from both MBR and MBX was identical. This is illustrated by a plot of methanol yield versus percent reacted glycoside (Fig. 9). For both MBR and MBX, glycosidic bond cleavage can account for ca. 60% of the total degradation. In other words, the percentage of glycosidic bond cleavage is unaffected by the reactivity difference between MBR and MBX and therefore dependent on a common factor. This percentage of glycosidic bond cleavage compares favorably with the data of McCloskey (23) on the formation of methanol from methyl β-D-glucopyranoside. However, Malinen (3) in his study of the oxygen-alkali degradation of several methyl glycosides reported much higher methanol yields (80-95%) and the yields varied with the methyl glycoside degraded. The discrepancy between this work and Malinen's work (3) could be a function of differences in trace metal contamination as suggested by Weaver's data (19). Alternatively, the similarity in methanol yields in this work and McCloskey's work (23) could be fortuitous.

PEROXIDES

General

Hydrogen peroxide and organic peroxides were shown to be different in the oxygen-alkali degradation of AX and AR and it was these differences which allowed Millard (1,2) to explain the differences in kinetics that AR and AX exhibited. Similarily, peroxide formation from the methyl glycosides was monitored to assist in the interpretation of the kinetic and rate data.

Hydrogen peroxide and organic peroxide concentrations were determined by the acidic titanium(IV) sulfate method used by previous investigators (1,2,12-14,39-41). Under strongly acidic conditions hydrogen peroxide will form a complex with titanium(IV) which can be measured colorimetrically. In the presence of strong acid (pH 0-1) organic peroxides will hydrolyze to yield

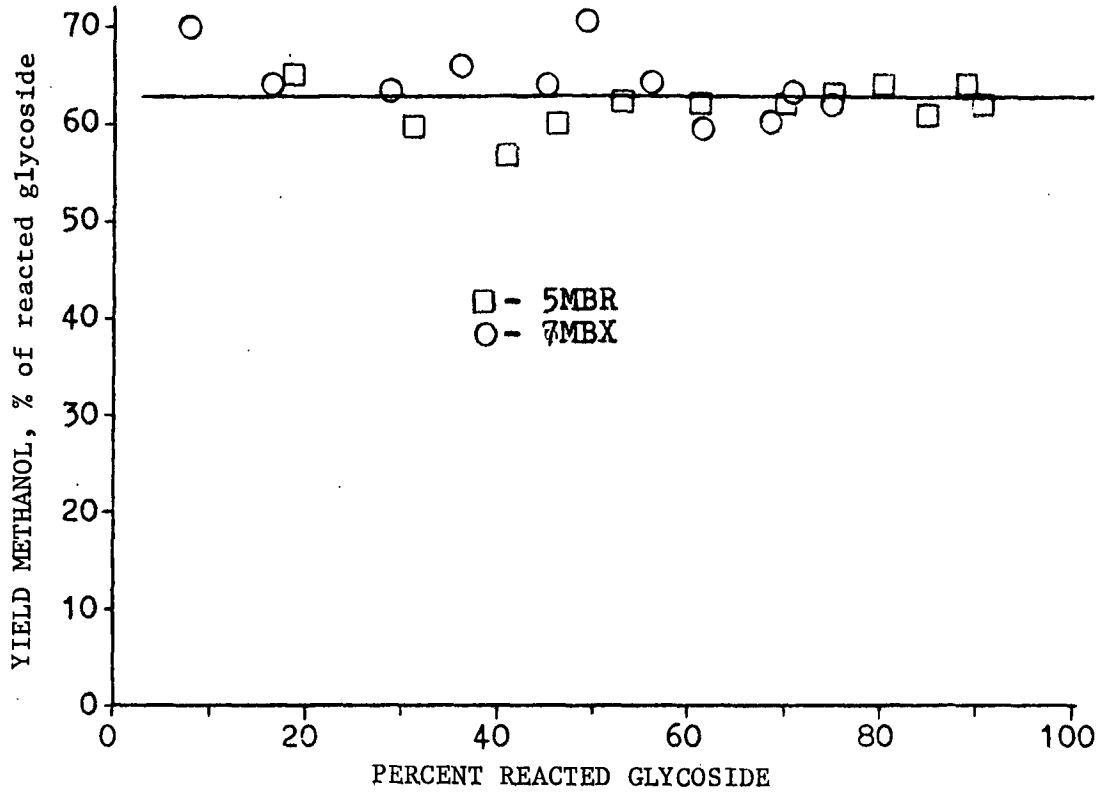

Figure 9. Yield of Methanol as Function of Percent Reaction During Degradation of 0.1M Methyl Glycosides in 1.25M NaOH at 120°C and 0.682 MPa O_2

hydrogen peroxide which can be complexed by titanium(IV). Hydrogen peroxide complexes immediately with the titanium(IV) and therefore the initial absorbance reading is taken as a measure of hydrogen peroxide concentration. Any increase in absorbance with time is taken to be proportional to organic peroxide concentration. Because the organic peroxides can degrade by other paths that do not yield hydrogen peroxide, it has generally been assumed that this method gives a low estimate of organic peroxide concentration (1,2,19). Peroxide concentrations were determined on duplicate runs and excellent agreement was noted (see Appendix II, Experimental Data).

Hydrogen Peroxide

The formation of hydrogen peroxide and organic peroxide in the oxygen-alkali degradation of MBR and MBX is shown in Fig. 10. Hydrogen peroxide from the degradation of MBR is seen to have peaked at a concentration ca. 2.5 times the peak in hydrogen peroxide concentration formed from MBX. The concentration levels of hydrogen peroxide produced and the ratio between hydrogen peroxide from MBR and that from MBX parallels hydrogen peroxide formation from the analogous 1,5-anhydroalditols (1,2). The early peak in hydrogen peroxide concentration relative to total reaction time is consistent with the data of previous investigators (1,2,12-14,17). It is also interesting to note that the hydrogen peroxide curves correlate well with the previously discussed reaction exotherms.

Organic Peroxides

As can be seen from Fig. 10, both methyl glycosides formed organic peroxides which continually increased in concentration. This pattern of organic peroxide formation is in sharp contrast with the trends in organic peroxide formation from the anhydroalditols (1,2). Organic peroxides were only occasionally noted with AR and then only at detection limit levels. Intermediate organic peroxides were formed from AX and their formation and decomposition mirrored hydrogen peroxide formation. Only at longer reaction times (5 hr) were any other organic peroxides detected from AX and then the concentrations were an order of magnitude less than the organic peroxide concentrations noted in this work. This variation in organic peroxides is the most marked difference between the anhydroalditols and the methyl glycosides when they are reacted in oxygen-alkali.

Many attempts were made to detect an early, intermediate organic peroxide in either methyl glycoside degradation. The peroxide tests were

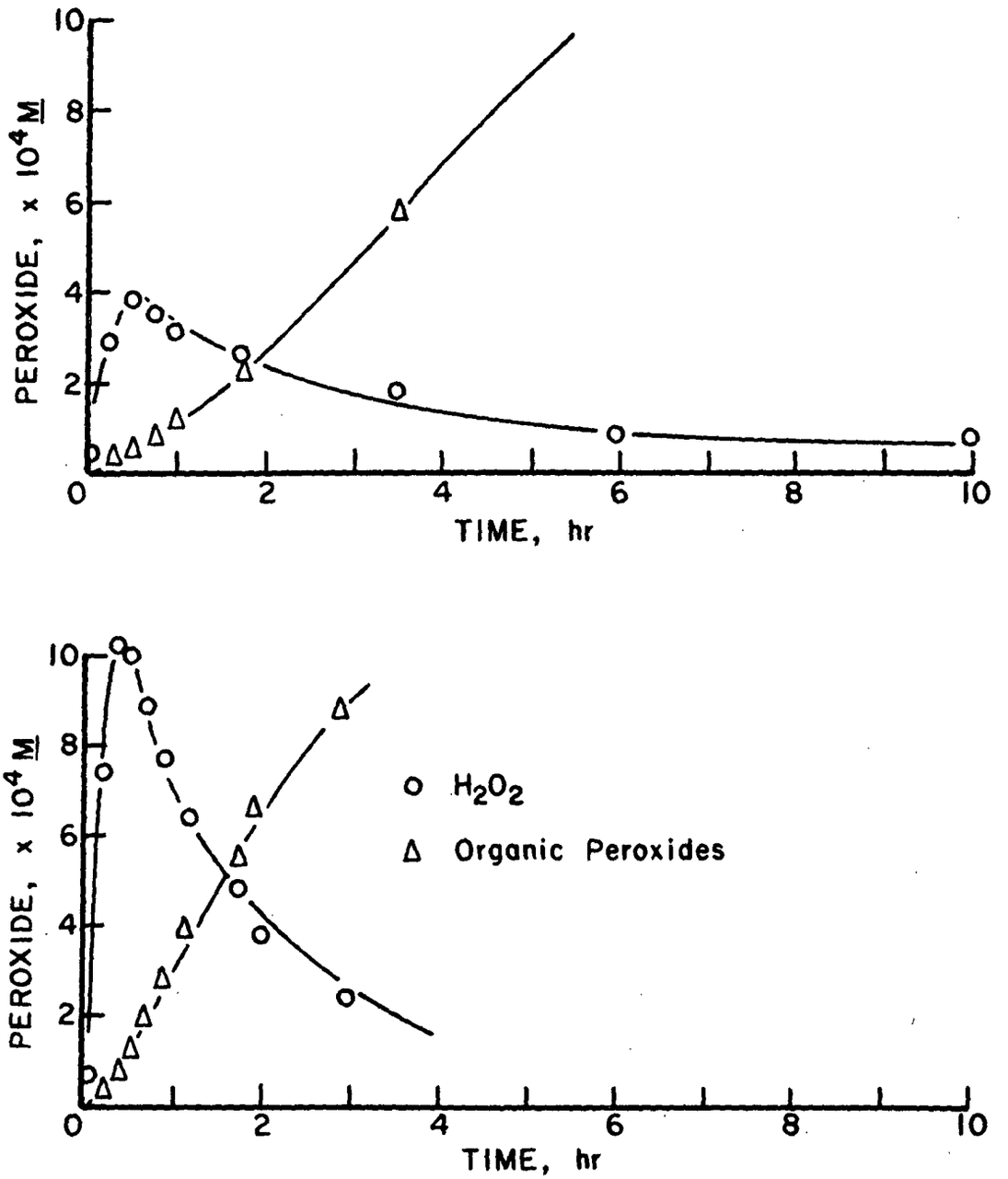

Figure 10. Peroxide Formation During the Degradation of 0.1M Methyl Glycosides in 1.25M NaOH at 120°C and 0.682 MPa O_2

conducted at two pH levels [pH 0 which corresponded to Sinkey's work (13) and pH 1 which corresponded to Millard's work (1,2)]. The AX intermediate peroxide was postulated to be an alpha-hydroxyhydroperoxide, a peroxide which should readily hydrolyze at pH 1. Organic peroxides formed later in oxygen-alkali-carbohydrate degradations are generally considered to be dialkyl peroxides which hydrolyze with much more difficulty (42). In this work, color development at pH 1 always lagged color development at pH 0. Therefore, if an alpha-hydroxyhydroperoxide was produced early in the oxygen-alkali degradation of MBR and MBX, the ratio of absorbance at partial color development at pH 1 to absorbance at full color development at pH 0 might be different early in the reaction than the ratio exhibited at later reaction times. No difference in this ratio was noted between early and late reaction times. The velocity of color development was also examined for variation between early and late reaction times. Time to full color development was approximately the same for all samples, being ca. 24-36 hr at pH 0. This time for full color development compares favorably with the time reported by Sinkey (42) for the hydrolysis of organic peroxides produced in the oxygen-alkali degradation of methyl β-D-glucopyranoside, but differs markedly from the time reported by Millard (1). Millard reported full color development in 20-28 hr at pH 1, suggesting organic peroxides which are much less stable than the organic peroxides detected in this work. Finally to examine the possibility that an alpha-hydroxyhydroperoxide was formed but was hydrolyzed immediately and was being measured as hydrogen peroxide, the peroxides produced from MBX were examined at a test pH of ca. 2. The hydrogen peroxide values measured (see Appendix II, Experimental Data) were comparable to other runs but no organic peroxides were detected after 24 hr of acid hydrolysis. The organic peroxides measured in this work are, therefore,

concluded to be dialkyl peroxides. This does not preclude the existence of an intermediate alpha-hydroxyhydroperoxide in the reaction mechanism, but it does suggest that the methyl aglycon alters the mechanism such that the dialkyl peroxides predominate in the oxygen-alkali degradation of methyl glycosides.

ACIDIC PRODUCTS

General

As explained in the Introduction, differences in reactivity and reaction pathways had been expected between the anhydroalditols and the methyl glycosides. The major acidic degradation products from the oxygen-alkali degradation of MBR and MBX were examined to determine if the methyl aglycon caused either a shift in the type of acidic products formed or a shift in the distribution of the products.

The acidic degradation products were determined as their per-O-trimethylsilyl (TMS) derivatives. These derivatives were identified by GLC (relative retention time) and GLC interfaced with mass spectrometry. The sample work-up procedure was adapted from previous workers (1,2,19,43). Sodium bisulfite was employed in the work-up procedure in an effort to detect an intermediate similar to the one reported by Weaver (19,20).

The acidic products identified in the oxygen-alkali degradation of MBR and MBX were identical for both glycosides and are reported in Table II. A sample chromatogram is shown in Fig. 11. With the exception of methoxyacetic acid, these products (or analogous products) have been identified in previous investigations of the alkaline oxygen degradation of ring carbohydrates (1-3, 15). Methoxyacetic acid was identified as a product of the alkaline hydrogen degradation of methyl β-D-glucopyranoside (19). Although the products of

MBX and MBR were the same, the relative ratios of the "bound methanol" products (products with the methyl aglycon intact) varied between the two methyl glycosides. The methyl C-carboxyfuranosides were examined with time and, as with the 1,5-anhydroalditols (1), evidence for a stereoselective reaction was found. The formation of methoxyacetic acid was also found to vary between the methyl glycosides. No attempt was made to quantify lactic, glycolic, or glyceric acids other than to note that their distribution was qualitatively the same as reported by other investigators (1-3,15). Many other minor products were evident in the GLC chromatogram, but they were not identified.

TABLE II

METHYL GLYCOSIDE DEGRADATION PRODUCTS

Product	Identification Method[a]	Product Identification
1	GLC, MS	Methoxyacetic acid
2	GLC, MS	Lactic acid
3	GLC, MS	Glycolic acid
4	GLC, MS	Glyceric acid
5	MS, PMR	Methyl 3-C-carboxy-β-D-tetrafuranoside
6,7	MS, PMR	Methyl 2-C-carboxy-β-D-tetrafuranoside

[a] GLC — identified by relative GLC retention time as compared to knowns
MS — identified by mass spectrometry
PMR — identified by Fourier transform-proton magnetic resonance spectrometry

Methoxyacetic Acid (1)*

Methoxyacetic acid has been previously reported as a product of the alkaline hydrogen peroxide degradation of methyl β-D-glycopyranoside (19), but never as a product of the oxygen-alkali degradation of a methyl glycoside.

*The circled numbers in the text refer to the chromatography peaks in Fig. 11.

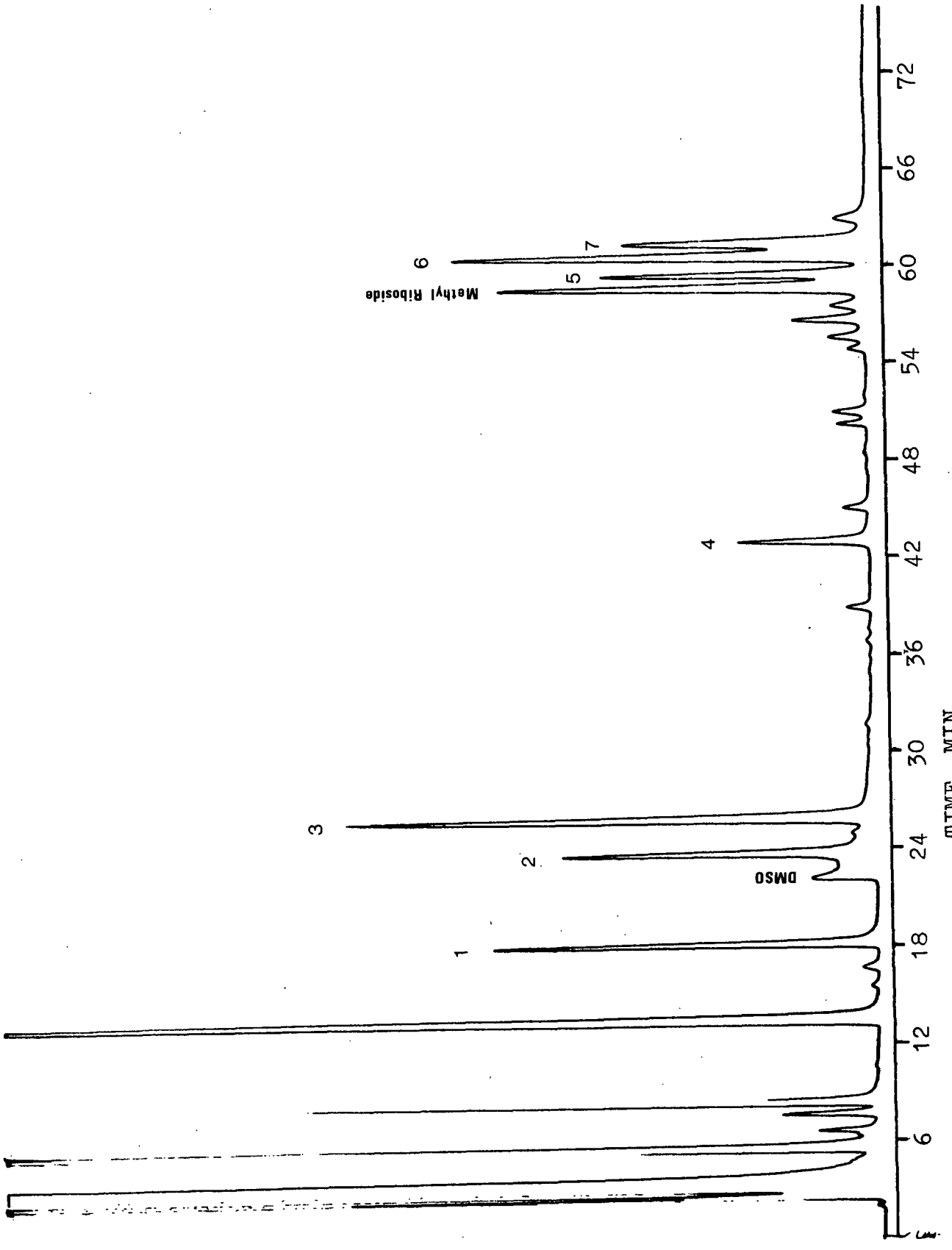

Figure 11. Sample Chromatogram of the Degradation Products of MBR and MBX (6MBR - 90% Reaction of MBR)

By examining the behavior of known methoxyacetic acid subjected to the sample work-up procedure, the identification of product ① as methoxyacetic acid was substantiated and clues provided as to why it had not previously been identified in oxygen-alkali reactions.

The mass spectrum of product ① is shown in Fig. 12 and for comparison a spectrum of known methoxyacetic acid is also presented. Principal fragments are ascribed to m/e 162 (M), m/e 147 ($M-CH_3$), m/e 117 ($M-CH_3OCH_2$), and m/e 89 (M-TMS). As noted in Fig. 12, these spectra were taken on samples derivatized by alternative methods. In Fig. 13, spectra of product ① and known methoxyacetic acid are also presented. These spectra were made from samples which had been carried through the normal work-up procedure employing sodium bisulfite. Note that although strong peaks beyond m/e 162 are exhibited, the same peaks are present in both samples, i.e., m/e 177, m/e 191, and m/e 206.

Although much difficulty was encountered in analyzing product ① , the belief that it is methoxyacetic acid is supported by the fact that known methoxyacetic acid consistently exhibited identical behavior to product ① . A summary of this behavior follows:

1. Methoxyacetic acid and product ① had identical GLC retention times.
2. Although methoxyacetic acid is easily trimethylsilylated by itself, in an artificial product mixture a response for methoxyacetic acid was obtained only when $NaHSO_3$ was used in the sample work-up. Similarily, reaction product samples exhibited product ① only when $NaHSO_3$ treatment was used. The use of $NaHSO_3$ in an artificial product mixture not containing methoxyacetic acid did not give any response resembling product ① .

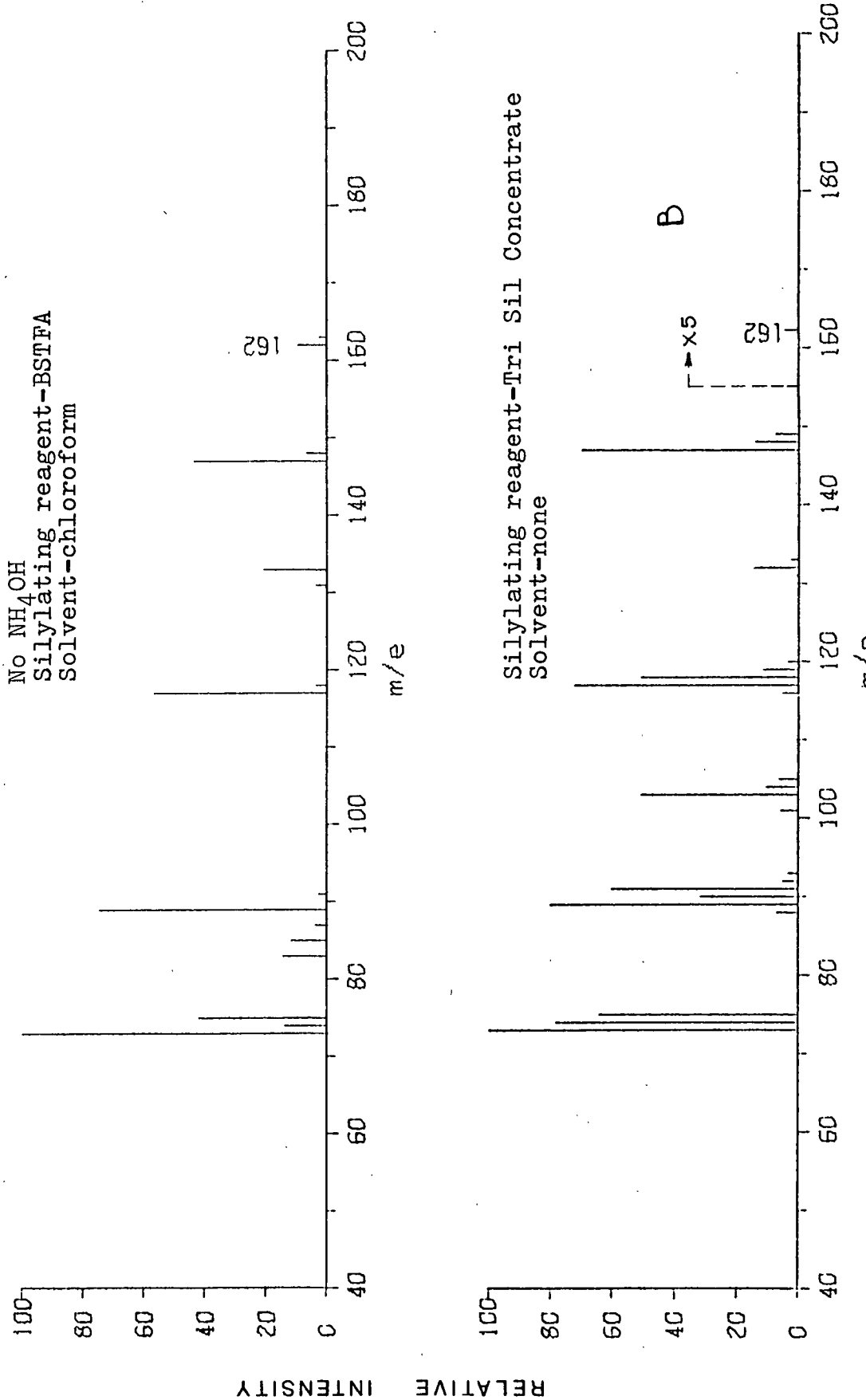

Figure 12. Mass Spectra of the Trimethylsilyl Derivaties of Product ① (Spectrum A) and Known Methoxyacetic Acid (Spectrum B) Using Alternative Derivitization Procedures

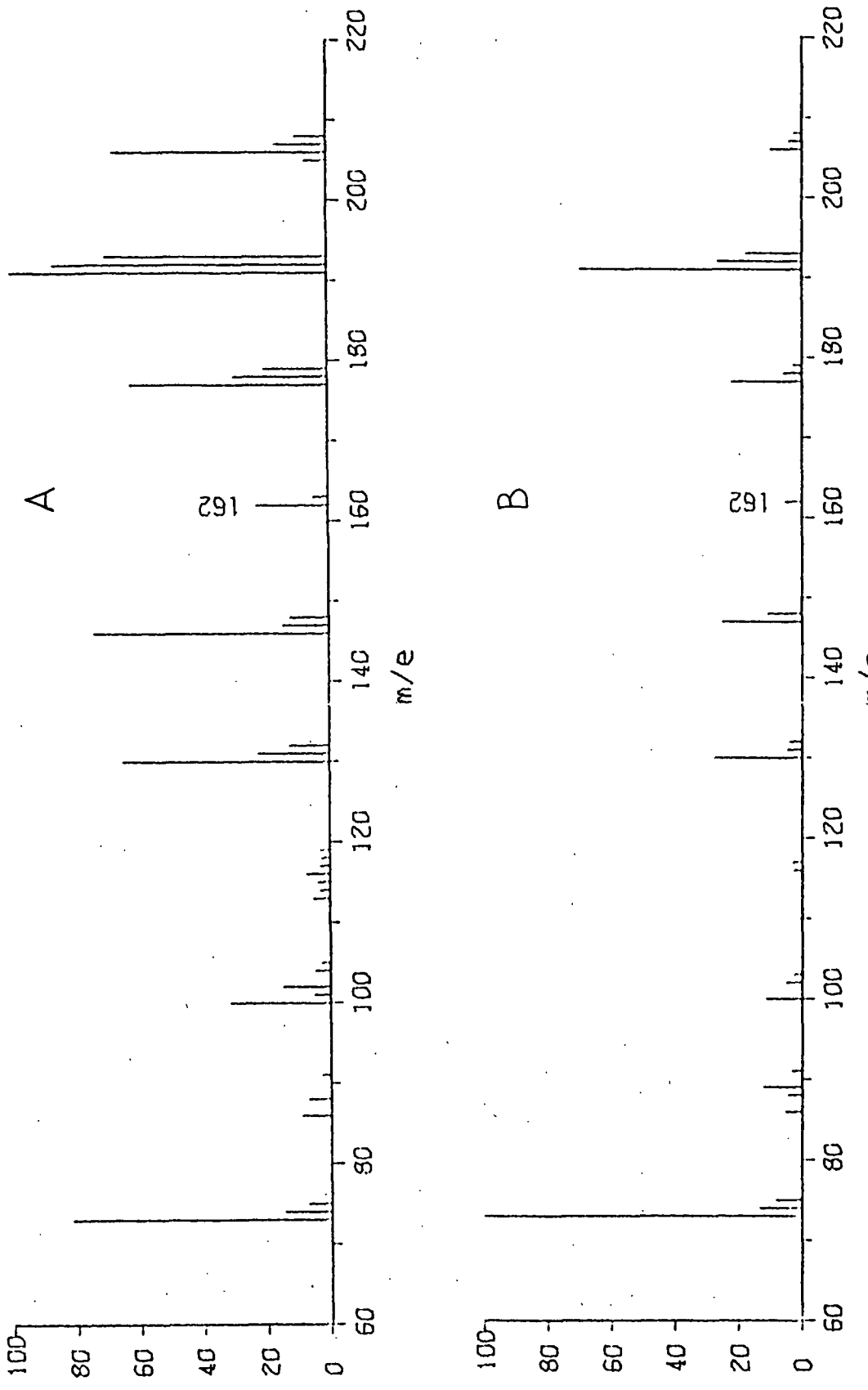

Figure 13. Mass Spectra of the Trimethylsilyl Derivatives of Product ① (Spectrum A) and Known Methoxyacetic Acid (Spectrum B) Using Normal Derivitization Procedure

3. As described above, mass spectra of samples employing $NaHSO_3$ treatment gave identical fragments for both methoxyacetic acid and product ① (Fig. 13).

It is concluded that methoxyacetic acid was identified as a degradation product due to the fortuitous use of $NaHSO_3$. For the same reason, previous workers have not identified it as a product in the oxygen-alkali degradation of methyl glycosides. Finally, as noted in Fig. 12, methoxyacetic acid (as the free acid) can also be derivatized in a product mixture if a strong silylating reagent is used and thus obviate the awkward use of $NaHSO_3$.

Methoxyacetic acid concentration was examined in the final product mixture by two methods — a methanol balance and quantitative GLC. Table III shows very good agreement between the two methods. The methanol balance was done by summing the concentrations of unreacted glycoside, methanol, and the methyl C-carboxyfuranosides and subtracting this figure from initial glycoside concentration. Methoxyacetic acid formation seemed to be favored in the MBX system.

TABLE III

METHOXYACETIC ACID IN FINAL REACTION MIXTURE

Glycoside	Methoxyacetic Acid by Methanol Balance, % yield	Methoxyacetic Acid by GLC, % yield	% Reacted Glycoside
MBR	14	14	90
MBX	25	26	73

Lactic, Glycolic, and Glyceric Acids; ②, ③, ④

Lactic ②, glycolic ③, and glyceric ④ acids have been reported as major products in all product studies of oxygen-alkali-carbohydrate systems (4,10,15,16). Therefore, a discussion of their mass spectra will not be made.

The mass spectra are reported in Appendix III and these spectra are observed to have the same major fragments as the spectra reported in the literature for these acids (44). Qualitatively, the contribution of these acids to the product distribution in this work agreed with the product distributions reported in previous investigations (1-3,15).

Methyl C-Carboxyfuranosides; ⑤, ⑥, ⑦

Three methyl C-carboxyfuranosides were identified in this work as major products from the oxygen-alkali degradation of MBR and MBX. Methyl C-carboxyfuranosides or analogous products have been identified several times in oxygen-alkali reactions of ring carbohydrates (1-3,15). The mass spectra of the three furanosides were essentially identical and a representative spectrum is presented in Fig. 14. The important diagnostic peaks occur at m/e 394 (M), m/e 379 ($M-CH_3$), m/e 334 ($M-COCH_3O-CH_3$), and m/e 291 ($M-CH_2OTMS$). A fragmentation pattern for the major ions is given in Appendix III, Fig. 31.

Following the convention of Ericsson (15) and Malinen (3), products ⑥ and ⑦ were identified as isomeric methyl 2-C-carboxy-β-D-tetrafuranosides and product ⑤ was identified as a methyl 3-C-carboxy-β-D-tetrafuranoside. However, neither Ericsson nor Malinen provided definitive data for the assignment of the 3-C-carboxyfuranoside. Furthermore, although Ericsson (15) adequately characterized the 2-C-carboxyfuranosides formed from the oxygen-alkali degradation of methyl β-D-glucopyranoside, Malinen (3) in his study of other methyl glycosides simply assumed that the same relative retention times were applicable. To eliminate this ambiguity, products ⑤, ⑥, and ⑦ were collected by preparative GLC (see Experimental section) and Fourier transform-proton magnetic resonance (PMR) spectra were taken (Fig. 15 and 16). These spectra demonstrate that the above assignments are correct. The PMR spectrum of product ⑤ shows the anomeric proton as a

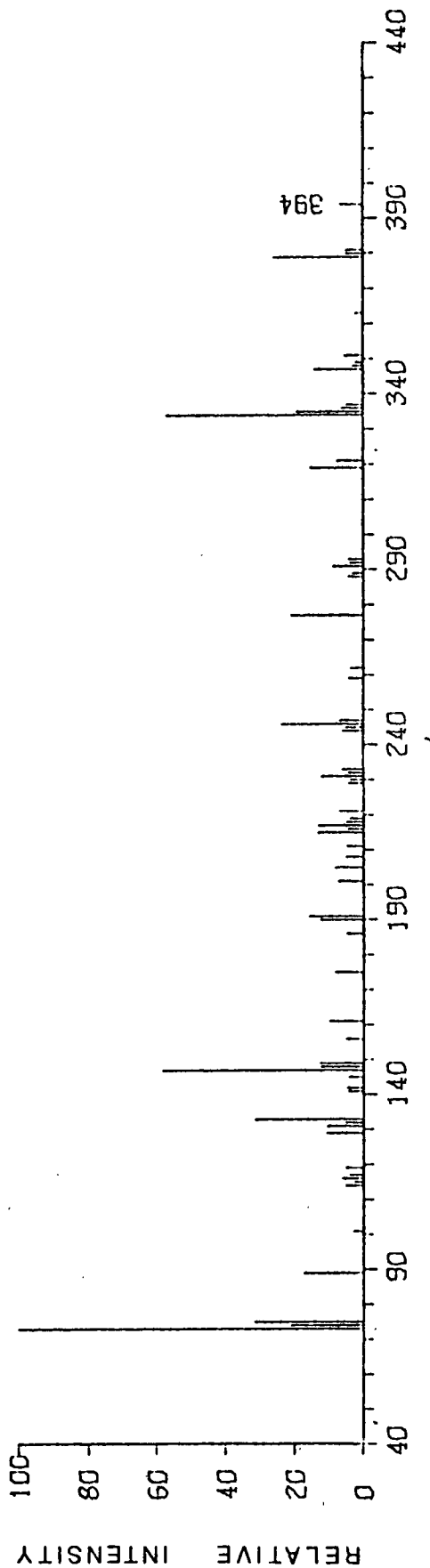

Figure 14. Mass Spectrum of the Trimethylsilyl Derivative of Methyl 2-C-Carboxy-β-D-pentafuranoside (Product ⑦)

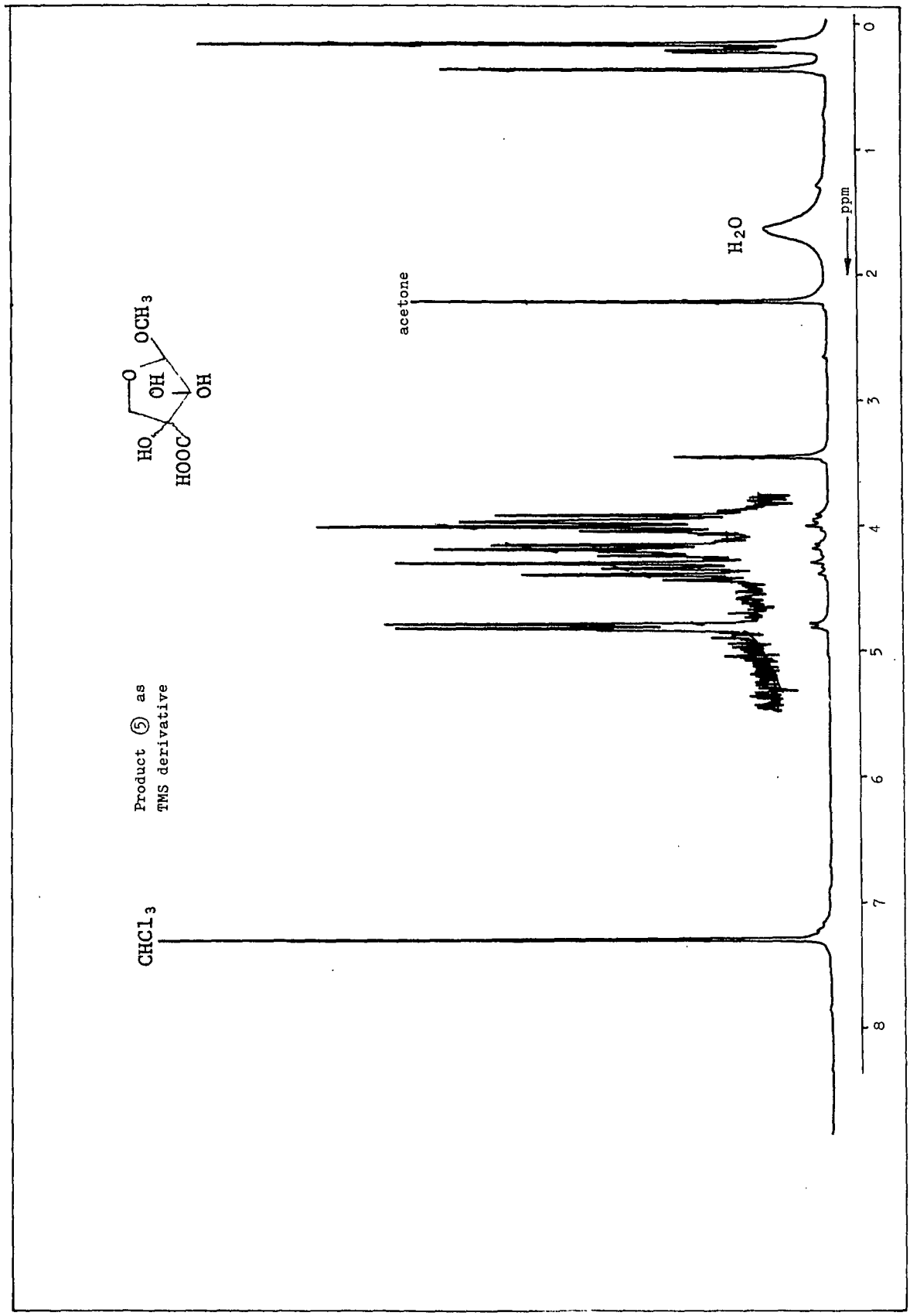

Figure 15. PMR Spectrum of Product ⑤ (Methyl 3-C-Carboxy-β-D-tetrafuranoside

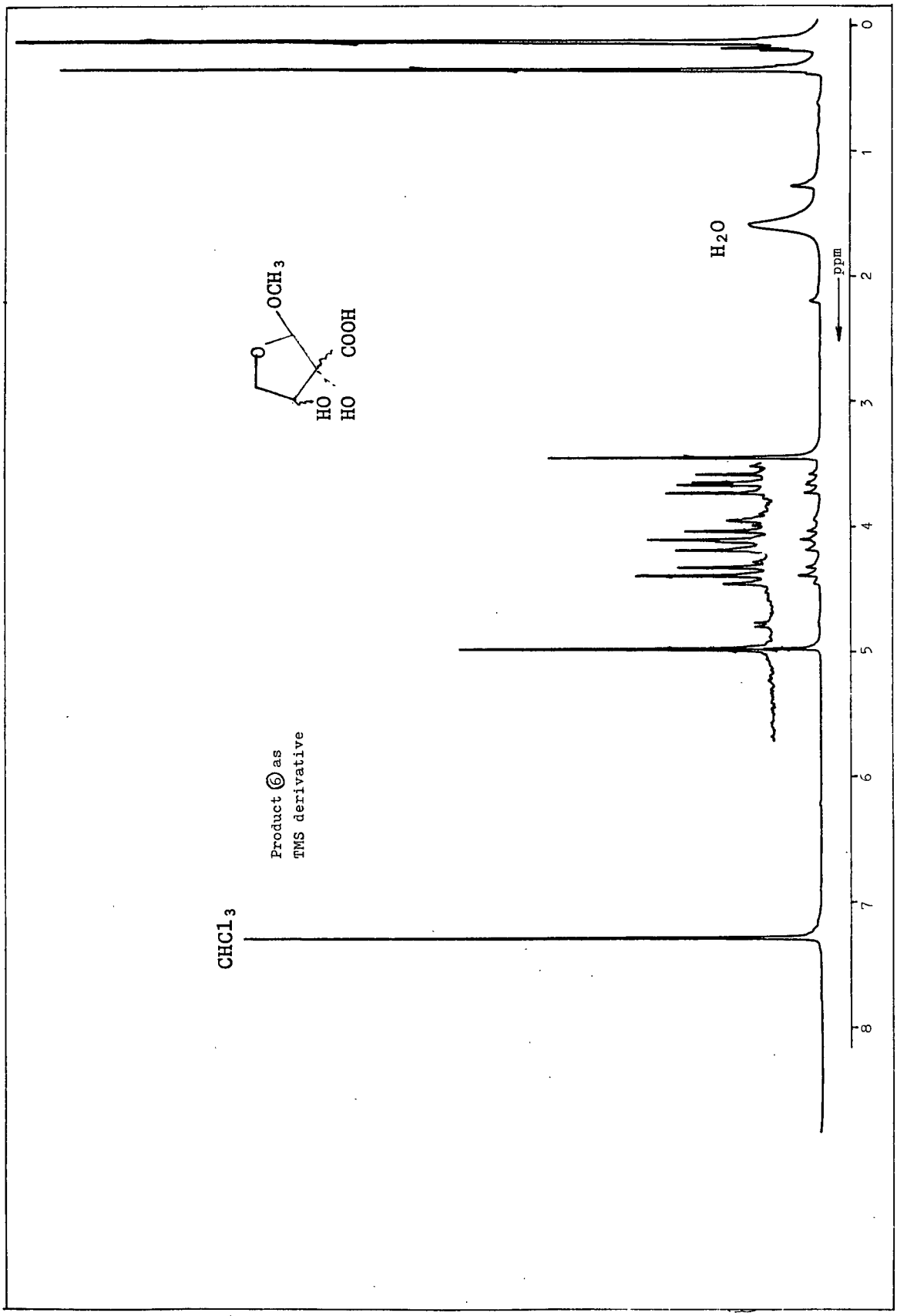

Figure 16. PMR Spectrum of Product ⑥ (Methyl 2-C-Carboxy-β-D-tetrafuranoside)

doublet centered at 4.74 ppm whereas the PMR spectrum of product ⑥ shows the anomeric proton as a singlet at 4.95 ppm. The splitting of the anomeric proton in product ⑤ is due to the ring proton at C-2. Product ⑥ does not have a ring proton at C-2 and therefore no splitting was observed. Under the conditions employed, resolution of products ⑥ and ⑦ was difficult, but a sample was collected which should have consisted mostly of product ⑦. This sample gave the same spectrum as shown in Fig. 16.

The distribution with time of the methyl C-carboxyfuranosides was examined by GLC for both the MBR and MBX degradations. The analysis is an approximation in that molar response factors for ⑤ , ⑥ , and ⑦ relative to n-propyl β-D-xylopyranoside were estimated at 0.9. This estimate was based upon calculated response factors for MBX and MBR. The trends, therefore, in concentration are accurate but the absolute concentration may not be.

Plots of products ⑤, ⑥, and ⑦against percent reacted glycoside are shown in Fig. 17 and 18. Product ⑥ was the most abundant one formed from both glycosides. However, relative to ⑥ the formation of ⑤ and ⑦was enhanced in the methyl riboside degradations. At long reaction times all three products show degradation, with product ⑦ evidencing the most instability at the reaction conditions. This difference in carboxyfuranoside formation between MBR and MBX parallels the observed formation of anhydrotetritol acids from the 1,5-anhydroalditols (1).

OXYGEN-DEFICIENT DEGRADATIONS

Due to problems with the air-driven magnetic stirrer, some degradations were conducted at a condition of very limited agitation. As a result these reactions were diffusion controlled. Because oxygen diffusion is a frequently cited problem in oxygen-alkali pulping and bleaching, the diffusion controlled

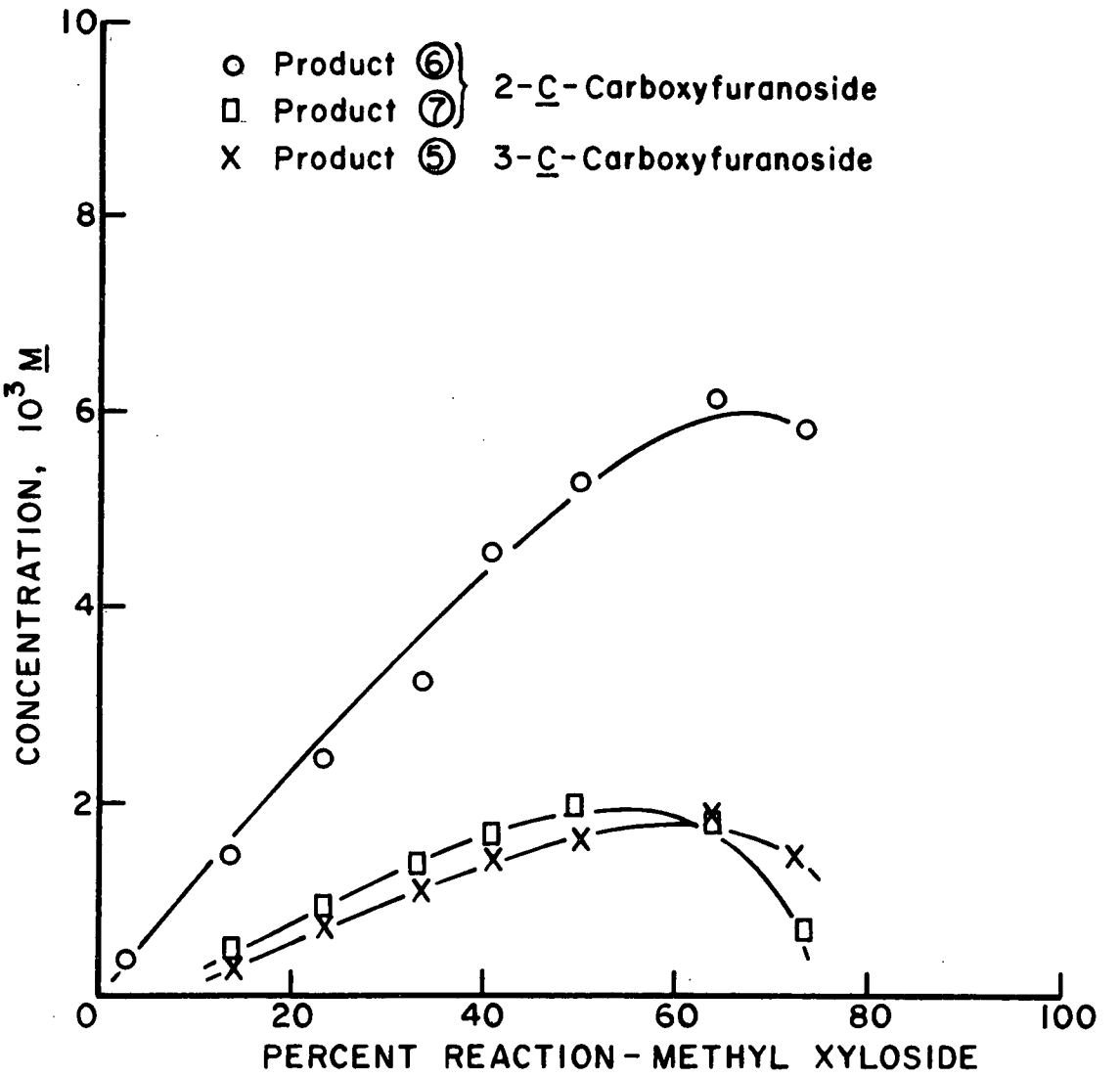

Figure 17. Formation of Methyl C-Carboxyfuranosides in the Degradation of 0.1M Methyl Xyloside in 1.25M NaOH at 120°C and 0.682 MPa O_2

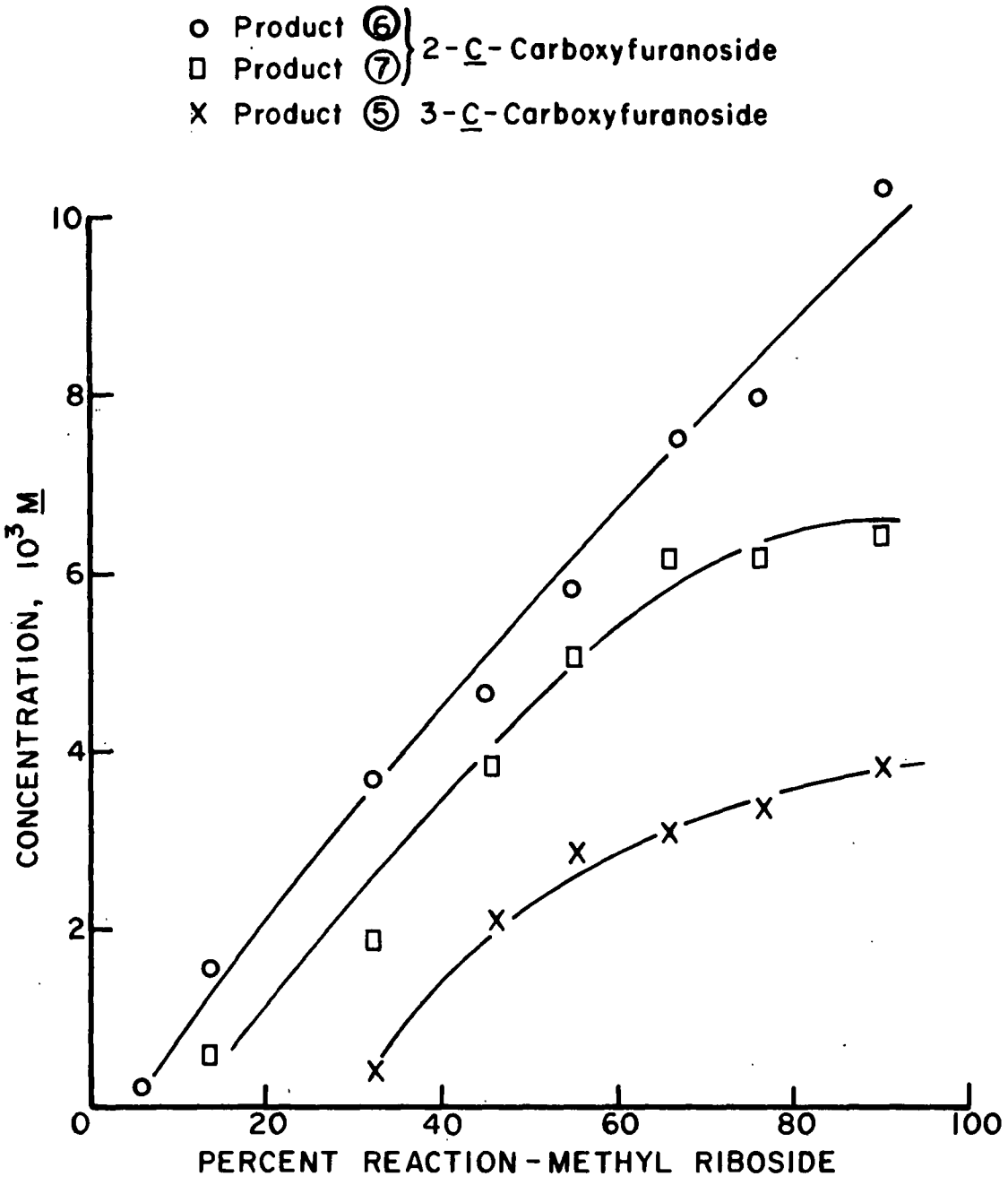

Figure 18. Formation of Methyl C-Carboxyfuranosides in the Degradation of 0.1M Methyl Riboside in 1.25M NaOH at 120°C and 0.682 MPa O_2

reactions were analyzed to examine the possibility of shifts in the reaction mechanism.

Figure 19 shows that the degradation rate of both glycosides under these conditions* was much slower than the kinetic runs (Fig. 4 and 5). The relative rates of degradation between MBR and MBX also shifts significantly. Very long induction periods were noted, while hydrogen peroxide levels were rarely significant. Organic peroxides in significant concentrations were measured; but the values tended to be spurious, probably due to stratification from poor stirring.

As noted for the kinetic runs, methanol formation followed the same pattern as the degradation curves (Fig. 19). Likewise, glycosidic bond cleavage accounted for ca. 60% of the degraded glycoside (see Appendix II, Experimental Data). This result corresponds to the percentage of glycosidic bond cleavage found in the well stirred, kinetic runs. Finally, the formation of the methyl C-carboxyfuranosides was stereoselective, similar to the kinetic runs. In Fig. 20, chromatograms of the methyl C-carboxyfuranosides from the oxygen deficient runs and the kinetic runs are compared at approximately the same percent reaction. Note that the formation of products ⑤ and ⑦ is enhanced in both the MBR kinetic run and in the MBR oxygen-deficient run. Similarly, the other major products were qualitatively the same in relative concentration. Therefore, it is concluded that an oxygen-deficient condition has no effect on the reaction mechanism other than the expected slowing down of the degradation rate.

*Due to an error these runs were conducted at a slightly lower oxygen partial pressure (0.618 MPa) than the kinetic runs.

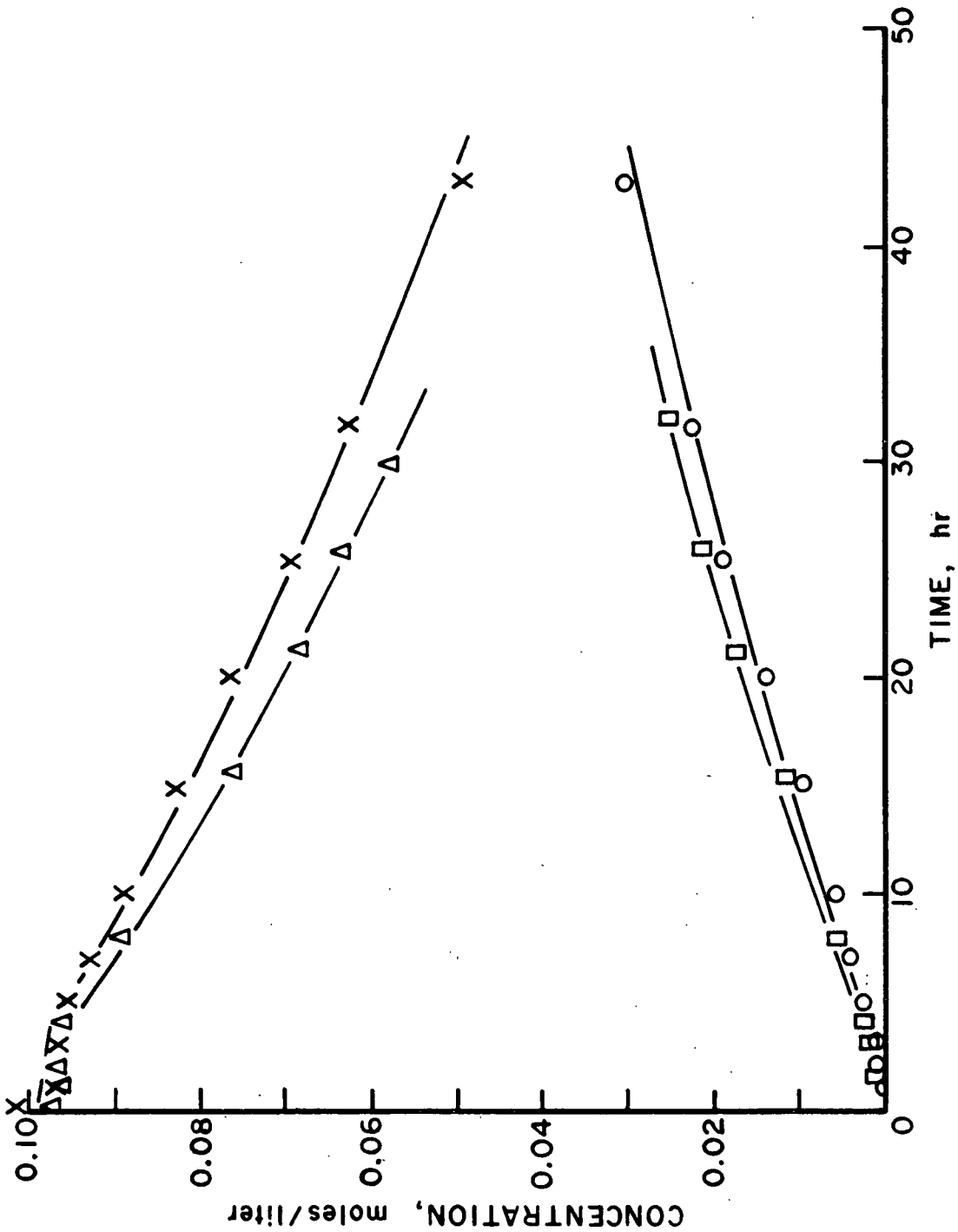

Figure 19. Concentration of Methyl Glycoside (Δ - 3MBR, X - 3MBX) and Methanol (□- 3MBR, ○- 3MBX) as Function of Time in 1.25M NaOH at 120°C, 0.618 MPa O_2, and 0.1M Carbohydrate Concentration

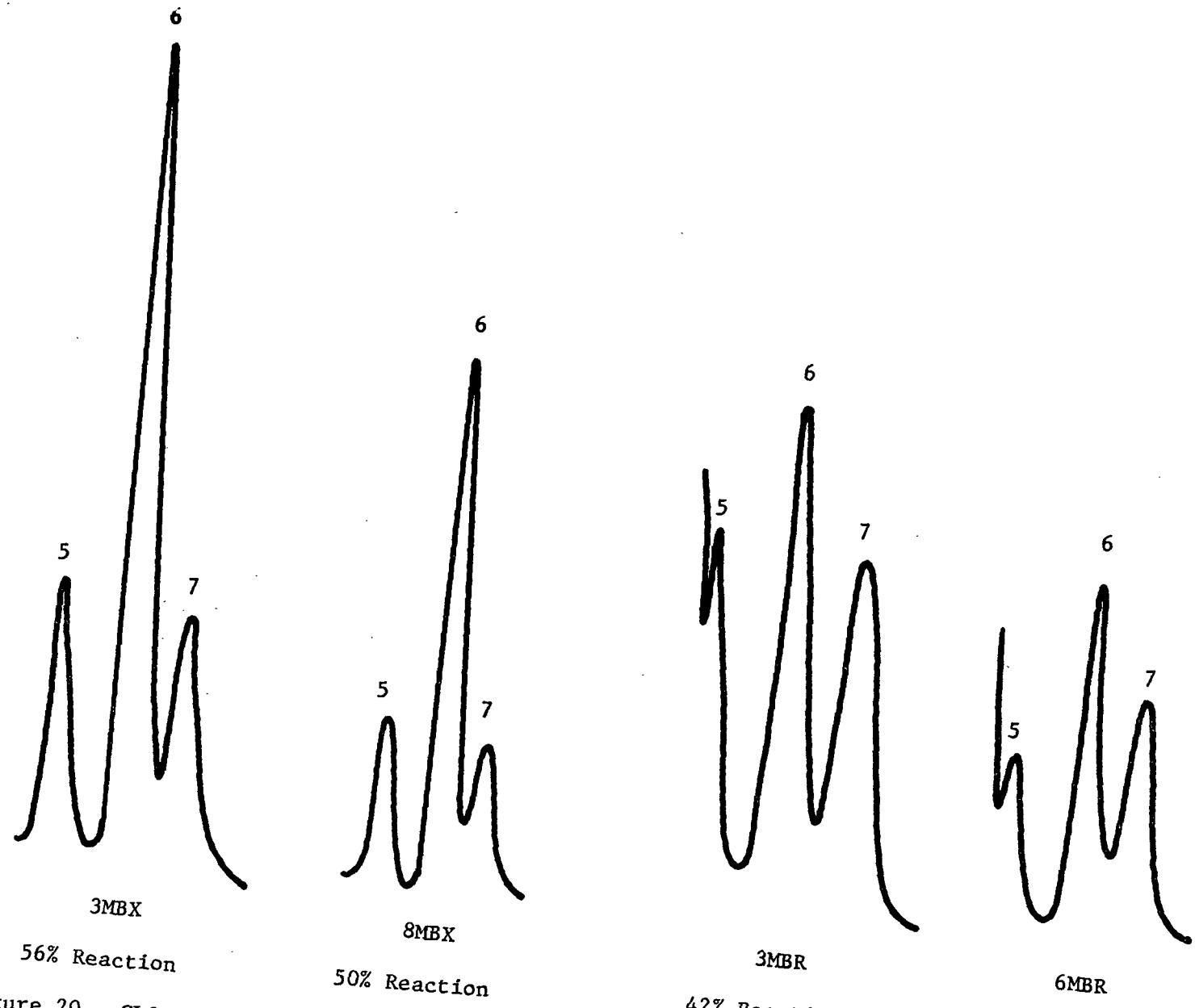

Figure 20. GLC Peaks Comparing Relative Proportions of Methyl C-Carboxyfuranosides Formed in Kinetic Runs (6MBR, 8MBX) Versus Oxygen Deficient Runs (3MBR, 3MBX)

DISCUSSION

INTRODUCTION

The underlying foundation for this work was the study by Millard (1,2) of the oxygen-alkali degradation of 1,5-anhydroxylitol (AX) and 1,5-anhydroribitol (AR). By examining the oxygen-alkali reaction of methyl β-D-xylopyranoside (MBX) and methyl β-D-ribopyranoside (MBR) information was gained as to the impact of the glycosidic bond on the degradation of a pyranoid ring in oxygen-alkali. As a general conclusion, the glycosidic bond was determined to have only a minor effect on the degradation rate and products of model ring carbohydrates having the "ribo" and "xylo" hydroxyl configuration. Therefore, the mechanism proposed by Millard (1,2) for 1,5-anhydroalditol degradation in oxygen-alkali was applied to the methyl glycosides of this study. The minor differences between the 1,5-anhydroalditols and methyl glycosides and their kinetics arise from the methyl aglycon and the effect it has on the termination reactions detailed in Millard's mechanism. This effect will be discussed in this section. Also discussed are 1) the dramatic effect that C-3 hydroxyl orientation has on degradation rate and the relationship between this effect and glycoside acidity, and 2) the distribution of the methyl aglycon among the major degradation products and the implications of this distribution.

MECHANISM

MECHANISM PROPOSED BY MILLARD (1,2)

Because no major differences were encountered between the degradation rates and reaction pathways (excluding organic peroxide formation) of the 1,5-anhydroalditols and the methyl glycosides, the mechanism proposed by

Millard (1,2) for the oxygen-alkali degradation of the 1,5-anhydroalditols was concluded to be equally applicable to the oxygen-alkali degradation of the methyl glycosides. A summary of this mechanism is presented to provide background for the explanation as to why the methyl glycosides exhibited different kinetic orders and organic peroxide formation trends from the 1,5-anhydroalditols.

Equations (5)-(27) represent the reactions used in Millard's derivation of a rate expression for the oxygen-alkali degradation of AR. Several of the reactions are depicted more specifically in Fig. 21, along with the symbols used in Equations (5)-(27).

$$A + OH^- \underset{}{\overset{K_5}{\rightleftharpoons}} A^- + H_2O \qquad (5)$$

$$A^- + O_2 \xrightarrow{k_6} A^{-}\cdot + HOO\cdot \qquad (6)$$

$$HOO\cdot + OH^- \underset{k_{-7}}{\overset{k_7}{\rightleftharpoons}} O_2^{-}\cdot + H_2O \qquad (7)$$

$$O_2^{-}\cdot + H_2O \xrightarrow{k_8} HO\cdot + HOO^- \qquad (8)$$

$$HOO^- + M^{+n+1} \underset{k_{-9}}{\overset{k_9}{\rightleftharpoons}} HOO\cdot + M^{+n} \qquad (9)$$

$$A^{-}\cdot + H_2O \underset{k_{-10}}{\overset{k_{10}}{\rightleftharpoons}} A\cdot + OH^- \qquad (10)$$

$$A + HO\cdot \xrightarrow{k_{11}} A\cdot + H_2O \qquad (11)$$

$$A^- + HO\cdot \xrightarrow{k_{12}} A^{-}\cdot + H_2O \qquad (12)$$

$$A^- + O_2^{-}\cdot \xrightarrow{k_{13}} A^{-}\cdot + HOO^- \qquad (13)$$

$$A^{\cdot -} + O_2 \xrightarrow{k_{14}} AO_2^{\cdot -} \tag{14}$$

$$A^{\cdot} + O_2 \xrightarrow{k_{15}} AO_2^{\cdot} \tag{15}$$

$$AO_2^{\cdot} + OH^- \underset{k_{-16}}{\overset{k_{16}}{\rightleftharpoons}} AO_2^{\cdot -} + H_2O \tag{16}$$

$$AO_2^{\cdot} + M^{+n} \underset{k_{-17}}{\overset{k_{17}}{\rightleftharpoons}} AO_2^{-} + M^{+n+1} \tag{17}$$

$$AO_2^{-} + H_2O \underset{k_{-18}}{\overset{k_{18}}{\rightleftharpoons}} AOOH + OH^- \tag{18}$$

$$AO_2^{-} \xrightarrow{k_{19}} Z + HOO^- \tag{19}$$

$$AOOH + OH^- \underset{k_{-20}}{\overset{k_{20}}{\rightleftharpoons}} AOOH^- + H_2O \tag{20}$$

$$AOOH + OH^- \underset{k_{-21}}{\overset{k_{21}}{\rightleftharpoons}} {}^{-}AOOH + H_2O \tag{21}$$

$$AOOH^- \underset{k_{-22}}{\overset{k_{22}}{\rightleftharpoons}} Z + HOO^- \tag{22}$$

$${}^{-}AOOH \xrightarrow{k_{23}} \text{products} \tag{23}$$

$$AOOH^- \xrightarrow{k_{24}} \text{products} \tag{24}$$

$$Z \xrightarrow{k_{25}} \text{products} \tag{25}$$

$$O_2^{\cdot -} + M^{+n+1} \xrightarrow{k_{26}} O_2 + M^{+n} \tag{26}$$

$$HO^{\cdot} + M^{+n} \xrightarrow{k_{27}} OH^- + M^{+n+1} \tag{27}$$

where M = catalytic metal ion.

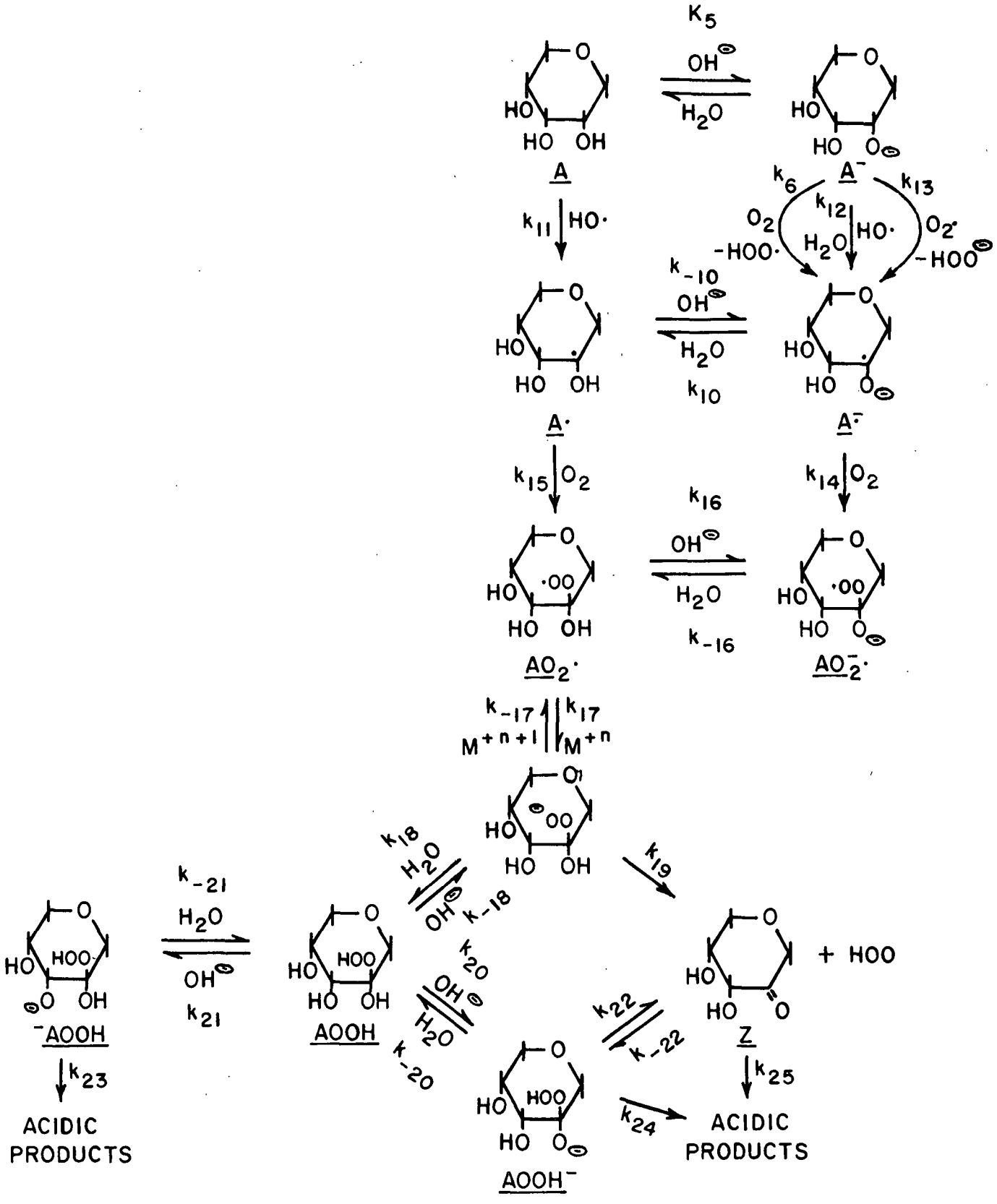

Figure 21. Proposed Mechanism of Degradation of 1,5-Anhydroribitol by Molecular Oxygen in Alkali (10)

This mechanism is unique in that it incorporates a hydroperoxide as an intermediate in the degradation of a carbohydrate by molecular oxygen in alkali. Furthermore, the mechanism postulates the relationship between the hydroperoxide and the keto derivative proposed by many investigators as the precursor to acidic products (3-5,15,18,21). Specifically, the carbonyl is formed from an ionized alpha-hydroxyhydroperoxide [Equations (19) and (22)]. Acidic degradation products can also be produced directly from the ionized alpha-hydroxyhydroperoxide as proposed by Isbell (45) (Fig. 22).

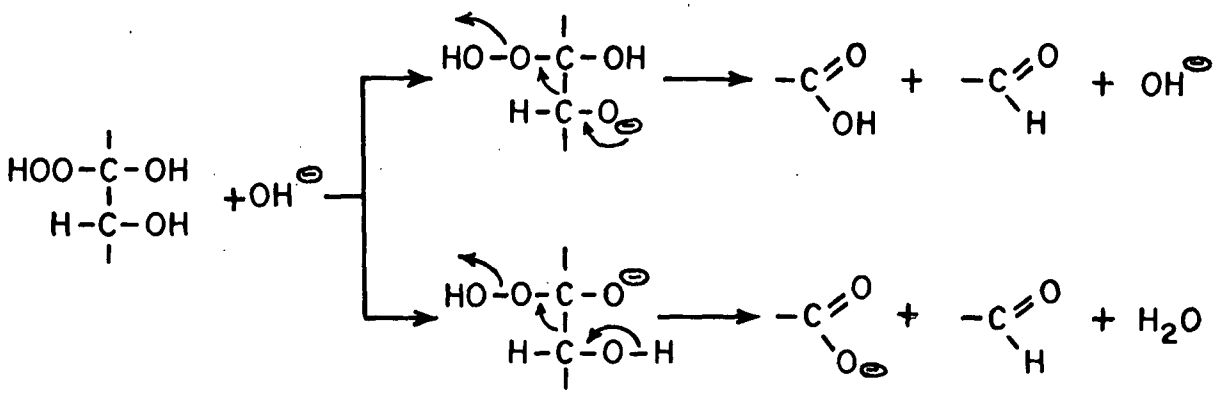

Figure 22. Acidic Degradation Products Formed Directly from Ionized Alpha-hydroxyhydroperoxide as Proposed by Isbell (45)

By applying the steady-state approximation that all radical species are very reactive and therefore present in very small concentrations and that metal ion concentration is also small, Millard (1,2) arrived at the following kinetic expression:

$$-d[A]/dt = K_5k_6[A][OH^-][O_2] + K_5^2k_6k_{13}[A]^2[OH-][O_2]/k_{26}[M^{+n+1}]$$

$$+ K_5k_6k_8[H_2O][A][OH^-][O_2]/k_{26}[M^{+n+1}] \qquad (28)$$

The third term involves reactions associated with the hydroxyl radical. By ignoring the reactions involving the hydroxyl radical, a kinetic expression

was derived which contained the same first two terms but the third term was absent. Millard (1,2) concluded that the hydroxyl radical does not play a major role in the mechanism under the conditions studied. This conclusion was consistent with the postulate that in minimum-metal-catalyzed systems the perhydroxyl (HOO·) and the superoxide (O_2^{-}·) radicals are more important than the hydroxyl radical (46,47). The second term was concluded to dominate at the reaction conditions. The appearance of metal concentration in the denominator causes this term to be large at small metal concentrations. The derived expression breaks down at zero metal concentration and alternative reactions would probably have to be considered. The assumption that the second term predominates (and thus yielding second-order kinetics) was consistent with the data obtained from the oxygen-alkali degradation of AR (1,2). For a more detailed discussion of this mechanism and its derivation the reader is referred to Millard's thesis (1).

AUTOINHIBITION MECHANISM PROPOSED BY MILLARD (1,2)

In the above mechanism, Equations (17), (26), (27) and the reverse of Equation (9) are chain termination reactions. In addition to these reactions, Equations (29) and (30) can be written as chain termination reactions. These reactions are directly analogous to reactions frequently proposed in hydrocarbon autoxidations (22).

$$AO_2\cdot + R\cdot \longrightarrow AOOR \qquad (29)$$

$$2AO_2\cdot \longrightarrow Z + O_2 + AOOH \qquad (30)$$

where Z, AO_2·, and AOOH are specified in Fig. 21. Millard proposed these two reactions as probable chain termination reactions in the oxygen-alkali degradation of AX. It was also argued that Reaction (30) predominated in the AX system.

In the degradation of AX, Millard detected an intermediate organic peroxide which he deduced to be an alpha-hydroxyhydroperoxide (see AOOH in Fig. 21). He further postulated that in the AX system this alpha-hydroxyhydroperoxide could be stabilized via intramolecular hydrogen bonding. This effectively increased the concentration of the radical $AO_2^{\cdot}$ and the significance of termination Reactions (29) and (30). These termination reactions produce only nonradical species resulting in a decrease in carbohydrate degradation. Thus, stabilized $AO_2^{\cdot}$ was a postulated intermediate which serves to inhibit the radical degradation of AX in oxygen-alkali. Reactions that are slowed down by a mechanism-interfering intermediate are termed autoinhibited (37). A characteristic of autoinhibited reactions is that they exhibit time dependent orders higher than true order. Millard's analysis indicated this to be likely in the oxygen-alkali degradation of AX.

AUTOINHIBITION IN METHYL GLYCOSIDE DEGRADATIONS

GENERAL

The time dependent orders for MBR and MBX were determined to be ca. 2.75 and 3.5, respectively. If, as previously stated, it is assumed that MBR and MBX degrade via the mechanism proposed by Millard (1,2) then these kinetic orders suggest that the oxygen-alkali degradation of methyl glycosides is autoinhibited. The oxygen-alkali degradation of ring carbohydrates has generally been reported to be second order in carbohydrate concentration (1,2,23,31,42), although subsequent reanalysis of the data indicated higher time-dependent orders (1,2). Therefore, kinetic orders higher than two might indicate the reactions to be autoinhibited.

In comparing the oxygen-alkali degradation of the 1,5-anhydroalditols with the oxygen-alkali degradation of the methyl glycosides, organic peroxide

formation is seen to differ markedly in the two systems. Stable organic peroxides were produced from the methyl glycosides, suggesting the formation of dialkyl peroxides (12-14). In the degradation of AX, the intermediate organic peroxide was concluded to be an alpha-hydroxyhydroperoxide and stable organic peroxides were detected only in minor concentrations. From this it is concluded that autoinhibition in the methyl glycoside degradations results from an increased probability of Reaction (29) occurring.

If the stable organic peroxides in this work are indeed the result of autoinhibition, then the kinetic orders predict that autoinhibition is more predominant in the MBX system. Such a situation should lead to a higher concentration of organic peroxides from the MBX degradation. This is apparently the case. If the yield of organic peroxides is plotted against percent reaction (Fig. 23), MBX is seen to produce a much higher concentration of organic peroxides at equivalent percent reaction than does MBR.

In autoxidations, Equation (29) is generally considered to be important only at low oxygen pressures and when the intermediate alkyl radical (in this case R·) is stable (22). The following discussion will be addressed to these two points in relation to the oxygen-alkali degradation of methyl glycosides.

STABLE INTERMEDIATE ALKYL RADICAL

A frequently proposed radical in the oxidation of glycosides is the C-1 radical resulting from anomeric hydrogen abstraction (19,27,48). The stability

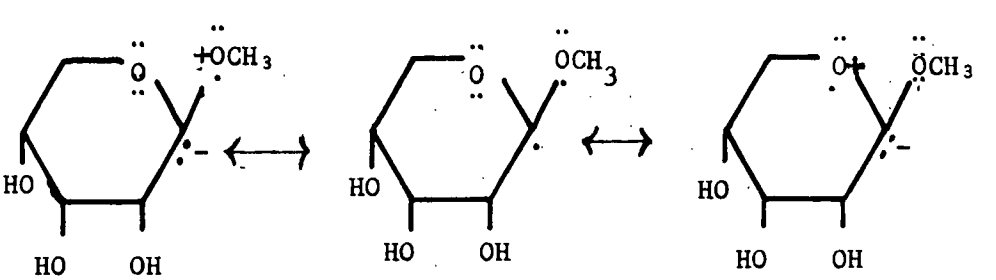

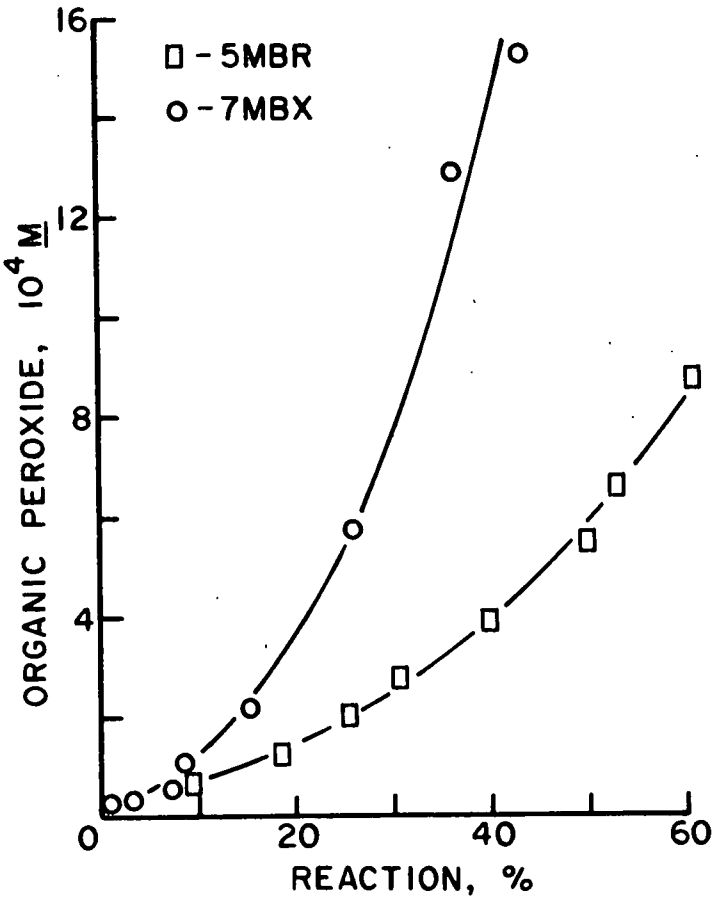

Figure 23. Organic Peroxide Concentration as Function of Percent Reaction in the Degradation of 0.1M Methyl Glycosides in 1.25M NaOH at 120°C and 0.682 MPa O_2

of this radical is enhanced by the adjacent oxygens and their ability to contribute to resonance. Although it will later be argued that formation and decomposition of this radical does not appear to be a major pathway in the degradation of the methyl glycosides (see Fate of Glycosidic Bond), anomeric hydrogen abstraction does provide the necessary stabilized radical for Equation (29). Thus, the C-1 radical is believed to be produced in sufficient concentrations to provide for autoinhibition of the methyl glycoside degradations. The C-1 radical can decompose as shown in Fig. 24 (28). Decomposition (Path A) can yield the methyl radical, a highly reactive radical. It is doubtful that the methyl radical enters into termination reactions owing to its extreme reactivity. Furthermore, no products have

ever been identified from the oxygen-alkali degradation of glycosides which would correspond to C-1 radical decomposition via Path A (3,15,48). The primary radical formed from C-1 radical decomposition via Path B would probably react quickly with molecular oxygen to form a hydroperoxyl radical ($-CH_2OO\cdot$). Similarly, the C-1 radical could react with oxygen to form a tertiary hydroperoxyl radical ($R(R')COO\cdot$).

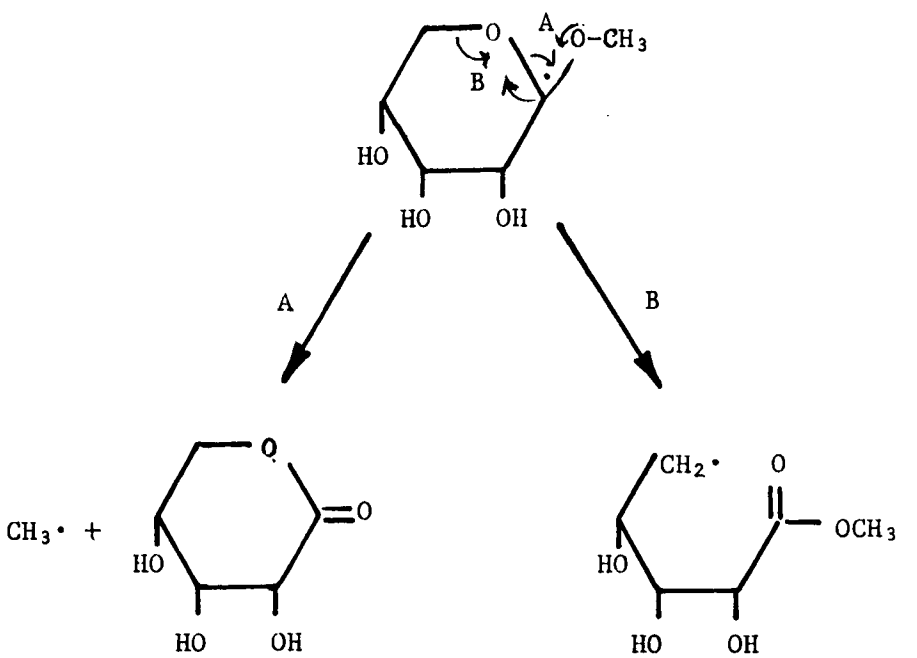

Figure 24. Possible C-1 Radical Decomposition Pathways (28)

Reaction (30) is commonly proposed to proceed through a tetroxide intermediate as illustrated for an analogous reaction between the alpha-hydroxyhydroperoxide radical ($AO_2\cdot$) and the C-1 tertiary hydroperoxyl radical (22). This reaction yields oxygen, a keto glycoside (Z), and a tertiary hydroperoxyorthoester.

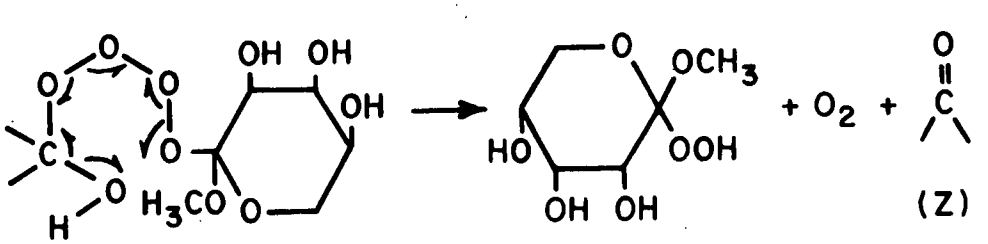

The same reaction with the above primary hydroperoxy radical ($-CH_2OO\cdot$) yields a primary hydroperoxide instead. Reaction (29) between the C-1 radical and $AO_2\cdot$ would form a dialkyl peroxyorthoester. The formation of peroxyorthoesters would

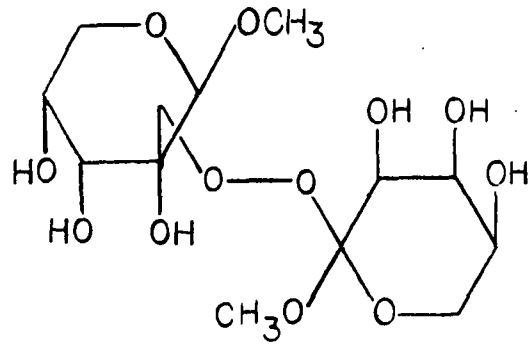

correspond to the stability of the detected organic peroxide in alkaline solution. The question is whether or not peroxyorthoesters would exhibit the same resistance to acid hydrolysis that the detected organic peroxides did. The work of Seyfarth, et al. (49) suggests that they might have this stability. The UV irradiated, oxygen reaction of 2-methyl 1,3-dioxolane yielded 1,3-dioxolan-2-yl hydroperoxide. This hydroperoxide required rather severe conditions (1N H_2SO_4, 20°C, 2 hr) to

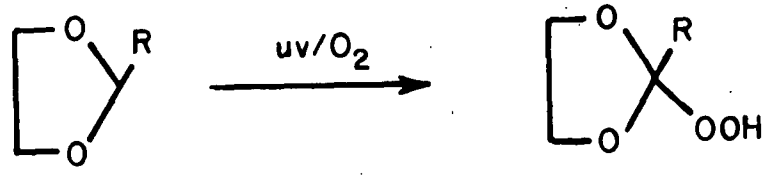

yield hydrogen peroxide. The reaction of this hydroperoxide with hydrogen peroxide yielded bis-(1,3-dioxolan-2-yl) peroxide which was stable to vacuum distillation at 80°C. Thus, it is postulated that autoinhibition in the methyl

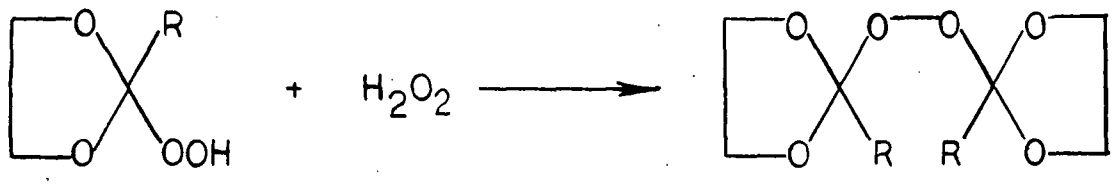

glycosides occurs due to the C-1 radical entering into a termination reaction with $AO_2\cdot$ to yield peroxydiorthoester. The formation of peroxyorthoesters in reactions of $AO_2\cdot$ with $R(R')COO\cdot$ and of hydroperoxides in reactions of $AO_2\cdot$ with $-CH_2OO\cdot$ can be postulated as shown above. These peroxyorthoesters and primary hydroperoxides, however, would not be expected to be as difficult to hydrolyze as the detected organic peroxides were.

So far the methyl glycosides have been unique among the carbohydrates in their ability to form stable organic peroxides during oxygen-alkali degradation. Organic peroxides similar to the ones formed from MBR and MBX were formed from the oxygen-alkali degradation of methyl β-D-glucopyranoside and methyl α-D-glucopyranoside (13,50) while glucitol (17) and mannitol (51) yield hydrogen peroxide but no organic peroxide in oxygen-alkali. The 1,5-anhydroalditols generated hydrogen peroxide and, in the case of AX, an intermediate organic peroxide but not significant concentrations of stable organic peroxides when reacted with oxygen in an alkaline medium (1,2). Cellobiitol, a glycoside, generated hydrogen peroxide readily in oxygen-alkali but does not yield any stable organic peroxides. Presumably, in the case of cellobiitol two factors operate against the envisioned formation of dialkyl peroxides. First, the glucitol aglycon offers more sites for hydrogen abstraction and thus decreases the frequency of anomeric hydrogen abstraction. Secondly, the glucitol aglycon would provide steric hindrance to radical combination.

EFFECT OF OXYGEN PRESSURE

As previously mentioned, Reaction (29) is generally considered to be important only at low oxygen pressures (22). Although this point was not examined in this work, some data of Thompson, et al. illustrate the effect that oxygen pressure has on organic peroxide formation from the oxygen-alkali degradation of methyl β-D-glucopyranoside (14). Figure 25 illustrates

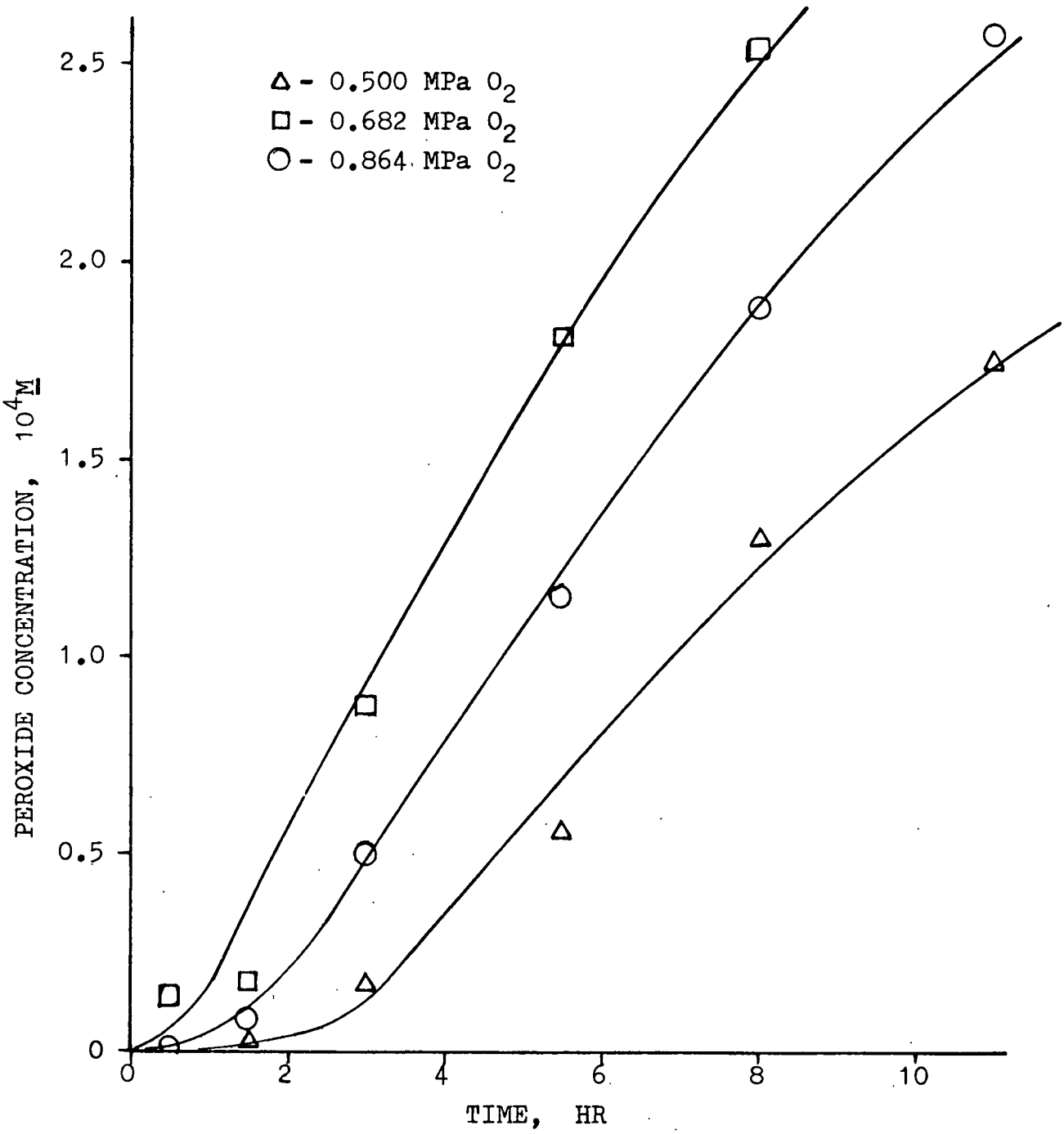

Figure 25. Formation of Organic Peroxides in the Degradation of 0.03M Methyl β-D-Glucopyranoside in 1.25M NaOH at 120°C. Effect of Varied Oxygen Pressure (14)

peroxide formation at three oxygen pressures. In increasing oxygen pressure from 0.5 MPa to 0.864 MPa, organic peroxide formation passes through a maximum. Although these oxygen pressures may not necessarily be considered low, the oxygen pressure only serves to determine the solution oxygen concentration. It is the solution oxygen concentration which ultimately determines whether or not R· is efficiently scavenged by oxygen. Therefore, it is concluded that the solution oxygen concentrations were low enough to allow Reaction (29).

HYDROXYL ORIENTATION RATE EFFECT

GENERAL

Varied C-3 hydroxyl orientation can dramatically affect the rate of degradation of pyranoid rings in oxygen-alkali. This observation has now been made for both the 1,5-anhydroalditols (1,2) and the methyl glycosides. The C-2 epimeric methyl glycosides have also been reported to vary in degradation rate in oxygen-alkali (3). Malinen (3) has suggested that methyl glycosides having cis 1,2-diol configurations can more easily form the frequently proposed alpha-dicarbonyl intermediates. Millard (1,2) did not offer an explanation for the degradation rate differences between AX and AR. Caution must be observed in interpreting the autoinhibition noted by Millard for the AX degradation. Although the AX degradation may have been slower than it would have been in the absence of autoinhibition, this does not preclude different initial rate constants for the respective degradations of AX and AR. The hypothesis presented here is that the degradation rate differences arising in the C-3 epimers of the 1,5-anhydroalditols and the methyl glycosides result from an increase in hydroxyl ionization when neighboring hydroxyls are in a cis configuration. The increase in ionization is believed to be a function of stabilization via intramolecular hydrogen

bonding. The degradation rate increases with increasing oxyanion concentration due to the facilitated hydrogen abstraction to form the oxyanion radical (1,2,23,42).

FACTORS AFFECTING CARBOHYDRATE ACIDITY

The ionization constants for carbohydrates generally are in the range of 10^{-12} to 10^{-14} and are larger than the ionization constants for monohydric aliphatic alcohols (ca. 10^{-16}) (52). The reducing sugars tend to be the most acidic while straight chain alditols, cyclitols, and glycosides of similar molecular weight and hydroxyl content have approximately the same acidity (52). Among similar carbohydrate molecules, however, acidities can vary appreciably with slight structural changes (53,54). For example, methyl α- and β-D-glucopyranoside can be separated on a strongly basic ion-exchange resin (53). In the case of the β-anomer, the dipole moments of the ring and glycosidic oxygens presumably reinforce each other and activate the C-2 hydroxyl to ionization. The α-anomer, however, has the glycosidic oxygen oriented such that it partially cancels the dipole of the ring oxygen thereby diminishing the activation of the C-2 hydroxyl. This example also demonstrates that within a polyhydric molecule the acidity of a specific hydroxyl varies with its environment. Equatorial hydroxyls are considered to be more acidic than axial hydroxyls (55). Upon ionization, the resulting equatorial anion, being less hindered than the axial epimer, is more easily solvated and is therefore more strongly basic. Intramolecular hydrogen bonding can also affect the acidity of hydroxyls (52,54,56,57). If the resultant oxyanion is stabilized by hydrogen bonding, then ionization of the hydroxyl group becomes more favorable. The acidity of the hydrogen-donating hydroxyl is probably lowered due to its bonding with anionic oxygen (52).

METHYL RIBOSIDE AND METHYL XYLOSIDE ACIDITY

The C-2 hydroxyl ionizes most easily in the methyl glycosides due to ring oxygen activation (24-26). The acidity of the C-2 hydroxyl can vary between α- and β-anomers as mentioned above (53), but because MBR and MBX are both β-anomers the effect of ring and glycosidic oxygens should be equivalent in the two glycosides. Evidence in this work, however, has been obtained which indicates that MBR is more acidic than MBX.

In determining a GLC response factor for MBR, the response factor was found to decrease at low MBR concentrations. A series of experiments examining various steps in the sample work-up procedure indicated that MBR was being selectively absorbed on the ion-exchange resin used in the work-up*. The ability of strongly basic resins to ionize and retain methyl glycosides has been demonstrated by Neuberger and Wilson (53). When the MBX response factor was determined, the response factor was constant over the entire range of concentrations examined.

Further evidence supporting the hypothesis that MBR is more acidic than MBX was obtained via ^{13}C-NMR. Spectra were taken of MBR and MBX in both D_2O and D_2O/NaOD (ca. 0.5M NaOD). It was postulated that if MBR is more acidic than MBX, then MBR should show greater ^{13}C peak shifts in alkali than does MBX. Examination of the data in Tables IV and V demonstrates that MBR in alkali exhibits significant shifts in its ^{13}C spectra, while MBX shows only very slight shifts. The assignment of the peaks corresponding to C-1, C-5, and C-6 was made from the off resonance spectra and the expected splitting from the protons that these spectra exhibited. The C-2 peak of MBR and MBX

*The resin used was Amberlite MB-3, consisting of a mixed bed of IR-120 cation resin and IRA-410, a strongly basic anion exchange resin.

TABLE IV

^{13}C PEAK SHIFTS OF METHYL XYLOSIDE IN ALKALI[a]

Carbon	MBX/D_2O, ppm[b]	MBX/D_2O/NaOD, ppm[b]	Shift, ppm[b,c]
C-1	106.9	107.0	0.1
C-3	78.8	78.9	0.1
C-2	76.0	76.1	0.1
C-4	72.3	72.3	0.0
C-5	68.2	68.3	0.1
C-6	60.3	60.3	0.0

[a]Carbohydrate concentrations = 100 mg/0.5 ml D_2O; alkali concentration = 0.59M NaOD.

[b]Relative to 3-(trimethylsilyl)propane sulfonic acid.

[c]Positive shift means downfield shift.

TABLE V

^{13}C PEAK SHIFTS OF METHYL RIBOSIDE IN ALKALI[a]

Carbon	MBR/D_2O, ppm[b]	MBR/D_2O/NaOD, ppm[b]	Shift, ppm[b,c]
C-1	104.4	104.8	0.4
C-2	73.2	73.6	0.4
C-3	70.8	71.3	0.5
C-4	70.7	70.8	0.1
C-5	66.1	66.5	0.4
C-6	59.1	58.9	-0.2

[a]Carbohydrate concentration = 100 mg/0.5 ml D_2O; alkali concentration = 0.53M NaOD.

[b]Relative to 3-(trimethylsilyl)propane sulfonic acid.

[c]Positive shift means downfield shift.

assignment was based upon selective decoupling experiments. All of the above assignments are based on those reported by Bock and Pederson (58). To exclude the possibility of the observed ^{13}C shifts being a function of a salt effect, a ^{13}C spectrum of MBR in 0.5M NaCl/D_2O was obtained. This spectrum had no significant differences between it and the spectrum of MBR in just D_2O.

STABILIZATION OF METHYL GLYCOSIDE OXYANIONS

As indicated in the above discussion, MBR is apparently more acidic than is MBX. In view of the factors affecting carbohydrate acidity, intramolecular hydrogen bonding would seem to be the most plausible contributor to this difference in acidity. The ring oxygen and the glycosidic oxygen have equivalent effects upon the C-2 hydroxyl in both glycosides.

In order to discuss the difference in acidity between MBR and MBX, it is first necessary to develop an understanding of the conformational equilibria of these two glycosides in solution. An estimate of the percentage of each conformer present in solutions of MBR and MBX can be made from the data of Angyal (59) and application of this data to Equation (31).

$$\Delta G^\circ = RT \ln (N_1/N_2) \qquad (31)$$

where ΔG° = difference in conformational free energies of $^4C_1$ and $^1C_4$ conformers

R = gas constant

T = absolute temperature

N_1, N_2 = mole fraction of $^4C_1$ and $^1C_4$ conformers, respectively

It was assumed that ΔG° would be approximately the same at 120°C as it is at 25°. With this assumption MBX was found to have a conformational equilibrium of 0.95:0.05; $^4C_1$:$^1C_4$ at 120°C. At this same temperature MBR was determined to have a conformational equilibrium of 0.68:0.32; $^4C_1$:$^1C_4$. Literature

data indicate that the $^1C_4$ MBR conformer may be even more predominant than this calculation indicates (58). Therefore, in considering the solution reactivity of MBR, both conformers must be examined. However, MBX can be assumed to exist mostly in the $^4C_1$ conformer. Moreover, the frequency of interconversions between the two chair conformers must be greater for MBR.

A principal factor determining hydrogen bond energy is the oxygen-oxygen (O---O) distance (60). The optimum O---O distance varies somewhat depending on the molecular environment but the average for O—H---O$^-$ is 2.75 ± 0.13 A (60). An approximation of the various O---O distances in MBR and MBX was obtained by measurement from Dreiding molecular models. These distances are presented in Table VI. Also presented in the table are O---O distances (indicated in parentheses) obtained from x-ray crystallographic data on MBR (61) and MBX (62). The distances were calculated through the use of the computer program CARTSET (63). No clear distinction between the favorability of hydrogen bond formation in MBR *versus* MBX can be made from the data presented in Table VI.

TABLE VI

OXYGEN-OXYGEN DISTANCES IN METHYL RIBOSIDE (MBR) AND METHYL XYLOSIDE (MBX)

	(O-2)---(O-3), A	(O-3)---(O-4), A	(O-2)---(O-4), A
MBX	2.9[a,b] (2.81)[a,d]	2.9[a,b] (2.91)[a,d]	2.7[b,c] --
MBR	2.7[a,b,c] (2.87)[c,d]	2.7[a,b,c] (2.87)[c,d]	2.7[b,c] (2.77)[c,d]

[a] Distance determined for $^4C_1$ conformer.

[b] Distance determined by measurement from Dreiding molecular models.

[c] Distance determined for $^1C_4$ conformer.

[d] Distance determined by CARTSET program (63) from x-ray crystallographic data on MBR (61) and MBX (62).

Another factor affecting the probability of hydrogen bond formation between neighboring hydroxyls of MBR and MBX involves the spatial orientation of the hydroxyls to the plane of the ring. The dihedral angle between neighboring hydroxyls of MBR and MBX are approximately the same. Yet in MBX neighboring hydroxyls are located trans to the ring plane formed by C-2, C-3, C-5 and the ring oxygen. In MBR the neighboring hydroxyls are oriented cis to the ring plane. In forming a hydrogen bond the O—H---O system shows appreciable contraction of interatomic distances (60). The result of this contraction is to reduce the dihedral angle between the neighboring hydroxyls. With MBX this contraction causes increased puckering of the ring and an increase in the diaxial interaction between hydrogens. In the case of MBR, the ring tends to flatten and no increase in diaxial interactions is observed. An example of this effect was reported by Kuhn (64) in a study of intramolecular hydrogen bonding of 1,2-diols. cis-Cyclohexane-1,2-diol was observed to have more intramolecular hydrogen bonding in solution than did trans-cyclohexane-1,2-diol and Kuhn applied the above discussion as an interpretation of this result. The larger frequency of conversions between MBR chair conformers also assists the formation of O—H---O^- hydrogen bonds. The conversion between the $^4C_1$ and $^1C_4$ conformers involves a number of possible boat, twist-boat, and half-chair intermediate conformers (65). In several of these intermediate conformers of MBR, the dihedral angle between neighboring hydroxyls is reduced. Thus, the contraction in hydrogen bond formation described above is partially accomodated by the conformational equilibrium of MBR.

INTERRELATIONSHIP OF OXYANION AND MECHANISM

To understand the relationship between increased oxyanion concentration and the increased degradation rate, the reader is referred to the previously

discussed mechanism. The proposed mechanism of degradation initiation is via hydrogen abstraction by molecular oxygen from the oxyanion [Equation (6)]. By increasing the concentration of oxyanions, the frequency of initiation reactions is increased. Hydrogen peroxide is generally assumed to be a product of this initiation (1,2,12-14). Experimentally, MBR was observed to form much more hydrogen peroxide than did MBX (Fig. 11). Additionally, the increase in the number of initiation reactions increases the concentration of perhydroxyl radicals. In alkali the perhydroxyl radical ionizes to the superoxide radical (66). In the proposed mechanism (1,2), the superoxide radical also abstracts hydrogen from the oxyanion [Equation (13)]. Thus by increasing the superoxide radical concentration the degradation is accelerated by an increase in radical chain propagating reactions.

FATE OF THE GLYCOSIDIC BOND

GENERAL

As noted in the Literature Review and shown in the Results section, the oxygen-alkali degradation of methyl glycosides can occur without cleavage of the methyl aglycon by forming so-called "bound methanol" products. Glycosidic bond cleavage has been proposed to occur via β-alkoxy elimination from a C-3 keto intermediate (4,7,14,15,17). The formation of the "bound methanol" products has generally been proposed to occur via a dicarbonyl intermediate (3,15), although the recent data of Millard (1) suggested alternative intermediates. This section will attempt to place in perspective the various reaction products containing the methoxyl group and the information that these products yield concerning the mechanism of oxygen-alkali degradation of methyl glycosides.

IMPLICATIONS OF METHANOL FORMATION

The single most abundant product from the oxygen-alkali degradation of MBR and MBX was methanol. In analyzing the methanol data it is concluded that a C-3 keto is the intermediate to glycosidic bond cleavage. This conclusion is derived from the fact that both MBR and MBX produce methanol in approximately 60% yield, yet MBR degrades at an initial rate six times the initial rate of MBX. Since MBR and MBX are C-3 epimers, the C-3 keto derivative of these methyl glycosides would be equivalent and should yield equivalent amounts of methanol upon β-alkoxy elimination. However, a qualification must be made to this discussion as the C-3 keto derivative is not necessarily formed in equal yields from MBR and MBX. Some methanol liberation probably arises from the degradation of secondary products. Yet the linear relationship between percent reaction and methanol yield indicates that the majority of the methanol liberation is probably via β-alkoxy elimination from a keto derivative of the original glycoside.

A second implication of the methanol data involves the previously discussed C-1 radical. It had been originally hypothesized that differences in the degradation patterns of the 1,5-anhydroalditols and the methyl glycosides could arise from the increased probability of C-1 radical formation from the methyl glycosides. However, the overall degradation rates and the major reaction pathways of the methyl glycosides were generally equivalent or analogous to the degradation rates and pathways of the corresponding 1,5-anhydroalditols. Additionally, no major reaction products were identified that would be indicative of C-1 radical decomposition (Fig. 24). This observation was also made by Kano, et al. in a study of the oxygen-alkali degradation of cellobiitol (48). Furthermore, although C-1 radical formation could lead to equivalent methanol yields, MBR would not necessarily be expected to degrade

faster than MBX. Hayday and McKelvey (67) have reported that photochemically induced hydrogen abstraction from 2-methoxy-4-methyltetrahydropyran is preferential to abstraction of an axial "anomeric" hydrogen. The previously discussed conformational analysis indicated that MBX exists predominantly in the conformer ($^4C_1$) having the anomeric hydrogen axially oriented, whereas MBR exists in this conformer to a lesser degree. Assuming the effect noted by McKelvey and Hayday to be applicable, then MBX would be predicted to react faster than MBR if C-1 radical decomposition represented a major pathway. In summary, the C-1 radical is not believed to play a major role in methyl glycoside degradation but, as previously discussed (Autoinhibition in Methyl Glycosides), it is believed to be produced in sufficient concentration to cause autoinhibition in the degradations.

STEREOSELECTIVE FORMATION OF METHYL C-CARBOXYFURANOSIDES

Three methyl C-carboxyfuranosides were identified as major products of the oxygen-alkali degradation of MBR and MBX. Two of these acids (products ⑥ and ⑦) were determined to be isomeric methyl 2-C-carboxy-β-D-tetrafuranosides and the third acid (product ⑤) was identified as a methyl 3-C-carboxy-β-D-tetrafuranoside. Importantly, the relative ratio of formation of these acids varied between the MBR and the MBX systems. This result is in agreement with the previously reported formation of the analogous 1,4-anhydro-2-C-carboxytetritols from AX and AR (1,2). This variation in methyl C-carboxyfuranoside formation from MBR and MBX reemphasizes the observation of Millard (1) that an alpha-dicarbonyl intermediate (3,15) does not adequately account for the observed formation of these furanoid acids. The alpha-dicarbonyl intermediates from MBR and MBX would be identical and the relative ratios of the methyl C-carboxyfuranosides would be expected to be the same from both glycosides.

A mechanism which accounts for this stereoselective formation has been proposed for the oxygen-alkali degradation of the 1,5-anhydroalditols (1,68) and is adapted to the oxygen-alkali degradation of the methyl glycosides in Fig. 26 and 27. These reactions indicate carbonyl formation at C-2 and lead to the methyl 2-C-carboxyfuranosides ⑥ and ⑦. Carbonyl formation at C-4 in MBR can account for the formation of methyl 3-C-carboxyfuranoside ⑤. Formation of a carbonyl at C-3 yields identical intermediates from MBR and MBX thus eliminating any possibility of stereoselective formation of the furanoid acids.

The first step in the proposed mechanism (1,68) involves the reversible addition of hydroxide ion to the carbonyl with the resulting oxyanion being stabilized via hydrogen bonding. The hydroxyl ion adds in a manner such that the oxyanion is cis to the neighboring hydroxyl. This allows for more favorable hydrogen bond formation as discussed previously (see Hydroxyl Orientation Rate Effect). Any of various radical species may then abstract the C-3 hydrogen forming the hydroalkyl radical at C-3. This radical is stabilized to inversion via hydrogen bonding resulting in the stereoselective addition of oxygen to the radical to form the alpha-hydroxyhydroperoxyl radical. Subsequent hydrogen abstraction by this radical yields an alpha-hydroxyhydroperoxide. Methyl C-carboxyfuranoside formation can occur by a semibenzilic type mechanism (69,70) from either the above alpha-hydroxy-hydroperoxide or its conjugate base. The formation of the carbonyl moiety of the carboxylic acid group is concerted with ring contraction. This rearrangement must be from conformations in which the (C-1)-(C-2) bond is antiperiplanar with the carbon-oxygen bond of the hydroperoxide group. The conformations allowing for this are $^{4}C_{1}$ for MBR and $^{1}C_{4}$ for MBX. These conformations also allow for the bulky hydroperoxide group to be equatorial.

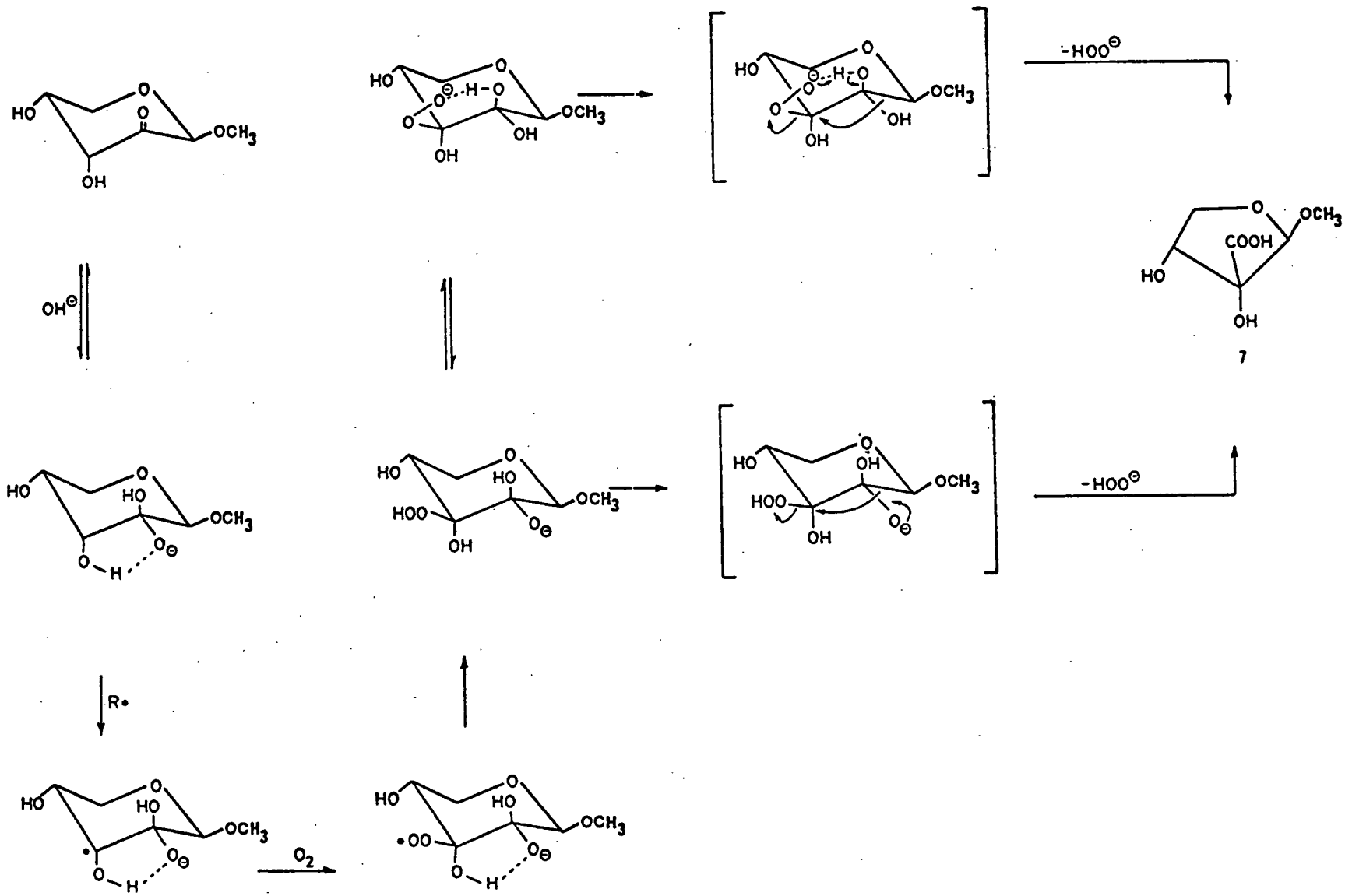

Figure 26. Proposed Mechanism for Stereoselective Formation of Methyl 2-C-Carboxy-β-D-erythrofuranoside According to Millard and Schroeder (1,68)

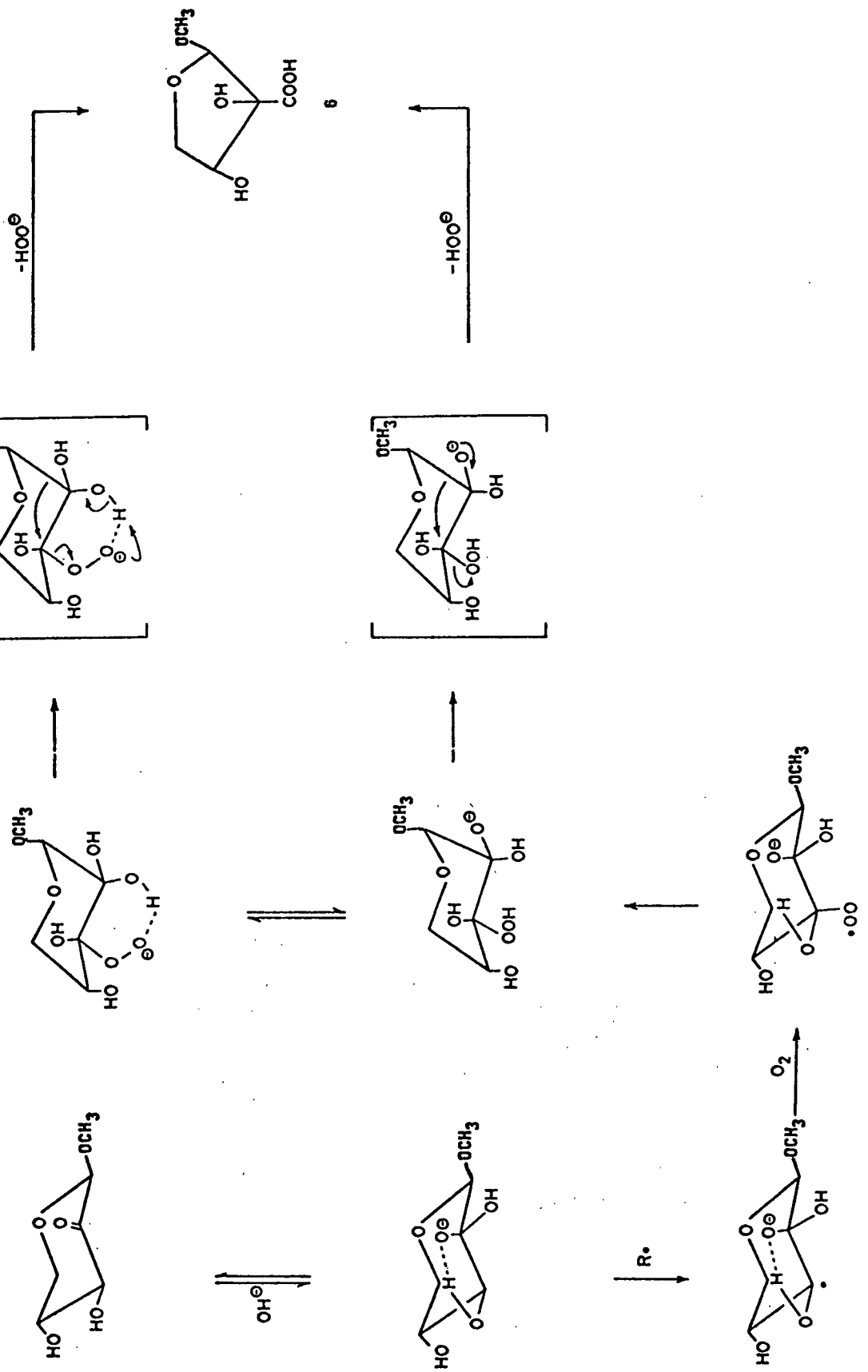

Figure 27. Proposed Mechanism for Stereoselective Formation of Methyl 2-C-Carboxy-β-D-threofuranoside According to Millard and Schroeder (1,68)

Specific assignment of isomeric structure of these acids could not be made based upon the mass spectral or PMR data. However, following the logic of Millard (1), product ⑦ is believed to be methyl 2-C-carboxy-β-D-erythrofuranoside and product ⑤ to be methyl 3-C-carboxy-β-D-erythrofuranoside. Similarily, product ⑥ is believed to be methyl 2-C-carboxy-β-D-threofuranoside. These assignments are consistent with the observation in this work and by previous workers (1-3) that ring carbohydrates having cis 1,2-diol configurations degrade faster in oxygen-alkali than do trans 1,2-diols. Products ⑤ and ⑦ exhibited less stability at the reaction conditions than did product ⑥ (Fig. 16 and 17).

ALTERNATIVE CHAIN CLEAVAGE MECHANISM

Chain cleavage of polysaccharides such as cellulose is usually considered to involve the breakage of bonds at the glycosyl oxygen, i.e., β-alkoxy elimination of either the C-1 or C-4 substituent. However, the detection of methoxyacetic acid in this work indicates that chain cleavage in alkaline oxidative reactions can occur via ring scission. Methoxyacetic acid was previously reported as a product of the alkaline hydrogen peroxide degradation of methyl β-D-glucopyranoside (20), but this is the first report of methoxyacetic acid as a product of the oxygen-alkali degradation of a methyl glycoside. The proposed mechanism of methoxyacetic acid formation (20) (Fig. 28) involves the ring oxygen as a leaving group in β-alkoxy elimination. After the elimination reaction, the resulting α,β-unsaturated molecule can ketonize to an alpha-dicarbonyl. Subsequent oxidative cleavage of this dicarbonyl yields methoxyacetic acid.

Although the above mechanism accounts for methoxyacetic acid formation, it would predict that equivalent amounts of methoxyacetic acid are formed from MBR and MBX. Yet, apparently more methoxyacetic acid is produced from

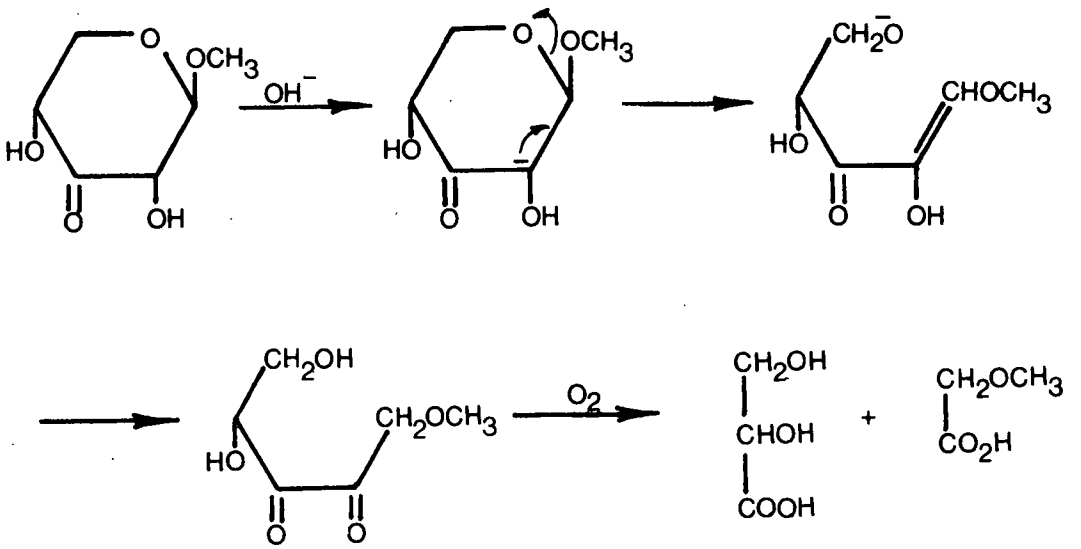

Figure 28. Proposed Formation of Methoxyacetic Acid According to Weaver (9)

MBX than from MBR. Moreover, this difference in methoxyacetic acid formation accounts for the difference in total methyl C-carboxyfuranosides formed in the two systems, while methanol yields from the two glycosides remain the same. This suggests a commonality in intermediates between the formation of methoxyacetic acid and the formation of the methyl C-carboxyfuranosides. However, this commonality is not as yet understood.

CONCLUSIONS

The information gained from the degradation of methyl β-D-ribopyranoside (MBR) and methyl β-D-xylopyranoside (MBX) by oxygen in an alkaline medium indicates that the methyl aglycon has little effect on the overall degradation rate and product formation pattern of a pyranoid ring. The configuration of ring hydroxyls, however, is shown to affect dramatically the degradation rate, thus confirming the observations of earlier workers in other systems (1-3). This effect was postulated to be the result of oxyanion stabilization via intramolecular hydrogen bonding with a neighboring hydroxyl in molecules having a cis 1,2-diol configuration, i.e., MBR. Experimental evidence was obtained which supported this hypothesis.

Because of similarities in degradation rates and reaction pathways between the 1,5-anhydroalditols and the methyl glycosides, the mechanism proposed for the oxygen-alkali degradation of the 1,5-anhydroalditols (1,2) was adapted to the methyl glycosides. This mechanism predicts carbohydrate kinetic orders of 2.0. The time dependent kinetic orders of MBR and MBX were 2.75 and 3.5, respectively, indicating the reactions were autoinhibited. The C-1 radical was postulated to cause the observed autoinhibition through a radical termination reaction with an alpha-hydroxyhydroperoxyl radical ($AO_2\cdot$). In addition to the kinetic orders, autoinhibition was indicated by the formation of stable organic peroxides as would be predicted by a termination reaction between C-1 radical and $AO_2\cdot$. Additionally, the higher kinetic order for MBX (suggestive of more autoinhibition in the MBX system than in the MBR system) corresponded to greater yields of organic peroxides from the MBX degradations.

The varied hydroxyl stereochemistry did not alter the type of products identified from the degradation of MBR and MBX in oxygen-alkali, although the distribution of the "bound methanol" products was affected by hydroxyl stereochemistry. The relative ratio of the identified methyl C-carboxyfuranosides varied between MBR and MBX lending support to the stereoselective mechanism proposed for the 1,5-anhydroalditols (1,68). Methoxyacetic acid was identified as a product of the oxygen-alkali reaction of MBR and MBX. This product has important implications as to an alternative chain cleavage mechanism of polysaccharides in oxidative, alkaline systems.

The orientation of the C-3 hydroxyl did not affect glycosidic bond cleavage as MBR and MBX yielded equivalent amounts of methanol even though their degradation rates differed markedly. Although the C-1 radical was postulated to play an important role in autoinhibition, the degradation rate, product, and methanol data implied that C-1 radical formation and decomposition did not represent a major degradative pathway for the methyl glycosides.

EXPERIMENTAL

GENERAL ANALYTICAL PROCEDURES

Melting points were determined on a Thomas Hoover capillary melting point apparatus. The melting points were corrected against calibration based upon known compounds.

Optical rotations were determined on a Perkin-Elmer Model 141 MC recording polarimeter.

Quantitative visible spectroscopy was done with a Gary Model 15 recording spectrophotometer. A tungsten lamp was utilized as the light source.

Thin-layer chromatography (TLC) was done on microscope slides coated with Silica gel G (Brinkman Instruments, Inc.). Developing solvents were as follows: solvent 1 — chloroform:ethyl acetate, 19:1, v/v; solvent 2 — ethyl acetate. Detection was accomplished with methanolic sulfuric acid spray (20%, v/v) followed by charring.

Quantitative gas-liquid chromatography (GLC) was done on a Varian Aerograph 1200 gas chromatograph equipped with a hydrogen flame ionization detector and a Honeywell Electronic 16 recorder with a Disc integrator. Prepurified nitrogen (Matheson Gas Products) was used as the carrier gas. Column descriptions and operating conditions are given in Appendix I.

Mass spectral analyses were conducted on a Du Pont 21-491 mass spectrometer interfaced via a jet separator to a Varian Aerograph 1400 gas chromatograph equipped with a hydrogen flame ionization detector and a Hewlett-Packard 7128A recorder. Helium (UHP helium, minimum purity 99.999%;

Matheson Gas Products) was used as the carrier gas. Mass spectra were recorded with a Century GPO 460 oscillographic recorder. Chromatographic conditions and mass spectrometer control settings are reported in Appendices I and III.

Nuclear magnetic resonance (PMR and ^{13}C-NMR) spectra were taken with a Joel FX-100 pulse Fourier transform nuclear magnetic resonance spectrometer equipped with a Texas Instrument 980B computer.

Preparative GLC was conducted on a Varian Aerograph 200 gas chromatograph equipped with a thermal conductivity detector and a Cole-Palmer 261 recorder. Prepurified helium (Matheson Gas Products) was used as the carrier gas. Column description and operating conditions are given in Appendix I.

SOLUTIONS AND REAGENTS

Absolute methanol was distilled from magnesium methoxide (71). Dry pyridine was prepared by fractional distillation from sodium hydroxide (72). The triply distilled water was prepared by a method to minimize trace organic contaminants (73).

TITANIUM SULFATE REAGENT (42).

Titanium sulfate (50 g, $TiSO_4 \cdot H_2SO_4 \cdot 8H_2O$, Fisher Scientific Co.) was dissolved in a concentrated sulfuric acid (50 ml) and diluted to 500 ml with triply distilled water. After standing one day, the solution was filtered through a medium porosity, sintered glass filter and stored in a glass bottle.

PURIFIED SODIUM HYDROXIDE

A stock sodium hydroxide solution was purified by a method adapted from Reiner and Poe (29). This was done in an effort to minimize trace metal ion contamination. All glassware used in the purification procedure was cleaned with 35% nitric acid followed by several rinses with triply distilled water.

Reagent grade sodium hydroxide (650 g) and freshly boiled distilled water (1.7 liters) were mixed in a 3 liter round bottom flask. Phenyl 2-pyridyl ketoxime (1.2 g) dissolved in a minimum amount of hot ethanol was added to the sodium hydroxide solution with 10% palladium on charcoal catalyst (0.2 g). The mixture was heated to ca. 100°C and stirred with a Teflon coated magnetic bar. Hydrogen gas was bubbled through the solution for 8 hr, the solution was then stoppered and allowed to cool overnight. The sodium hydroxide was filtered through a medium porosity, sintered glass filter and each liter then extracted with ethanol:isopentyl alcohol; 25:75 (3 x 50 ml). The colored complex easily dissolved into the alcohols.

The sodium hydroxide was returned to the 3 liter round bottom flask with additional phenyl 2-pyridyl ketoxime (1.2 g). The solution was heated as before, but nitrogen was bubbled through the solution. After 12 hr the solution was again stoppered and allowed to cool overnight. The solution was then extracted as before, followed by extraction with chloroform (3 x 150 ml) (42). The last traces of alcohol and chloroform were removed by boiling for 6 hr while bubbling nitrogen through the solution. The cooled sodium hydroxide solution was stored in a paraffin-lined, Teflon-stoppered glass jar under a nitrogen atmosphere. Analysis by GLC showed no ethanol remaining in the caustic and a UV spectrum of the extracted caustic was identical to UV spectra of unextracted caustic thus assuring the removal of the phenyl 2-pyridyl ketoxime.

SODIUM THIOSULFATE SOLUTION

Air dry sodium thiosulfate (16.22 g) and sodium carbonate (0.1 g) were dissolved in a liter of distilled water. This solution was titrated against potassium iodate as a primary standard (71).

GLC INTERNAL STANDARDS

n-PROPYL β-D-XYLOPYRANOSIDE

n-Propyl tri-O-acetyl-β-D-xylopyranoside (39.5 g), kindly provided by Dr. L. R. Schroeder, was dissolved in hot methanol (350 ml). While still hot, 5 ml of 3% sodium methoxide was added. The reaction was monitored by TLC (solvent 2) and was complete after 0.5 hr. The reaction solution was deionized with Amberlite IR-120 cation exchange resin and evaporated *in vacuo* to a sirup (26 g). The sirup was thinned with acetone (25 ml) and placed in a refrigerator where crystallization occurred spontaneously. The n-propyl β-D-xylopyranoside was recrystallized from acetone:diethyl ether, 1:3, v/v to give 22.1 g (93%) yield: m.p. 93-94.5°C; $[\alpha]_D^{29} = -61.6°$ (c 1.0, CH_3OH). Literature: m.p. 92-93°C; $[\alpha]_D^{20} = -58.6°$ (c 2.0, CH_3OH) (74).

ETHANOL

Reagent grade ethanol (95%) was used as an internal standard in the methanol analysis.

MODEL COMPOUNDS

METHYL β-D-XYLOPYRANOSIDE (MBX)

Methyl β-D-xylopyranoside (MBX) was purchased from Pfhanstiehl Laboratories, Inc. (Waukegan, Illinois). MBX was recrystallized from absolute

ethanol (2X), pulverized, and dried in a vacuum oven: m.p. 156-7.5°C; $[\alpha]_D^{20}$ = -65.8° (c 1.134, H_2O). Literature (75): m.p. 156-7°C; $[\alpha]_D^{20}$ = -65.8° (c 9.0, H_2O).

METHYL β-D-RIBOPYRANOSIDE (MBR)

The methyl β-D-ribopyranoside used in this work was synthesized via the tri-O-benzoyl-ribopyranosyl bromide intermediate (Method I). An alternate method (Method II, Fisher glycosidation) was also used and is presented here because it was a better method.

Method I

In a beaker 1,2-dichloroethane (380 ml), dry pyridine (200 ml) and benzoyl chloride (190 ml) were chilled to -20°C by an acetone-dry ice bath (76). D-Ribose (50 g; Pfhanstiehl Laboratories, Waukegan, Illinois) was added slowly and the temperature allowed to rise to 0°C and kept there for 1 hr. The reaction mixture was refrigerated overnight and then allowed to stand at room temperature for 6 hr. The reaction mixture was then poured into ice water and agitated for 0.5 hr. The organic layer was augmented with $CHCl_3$ (700 ml) and separated from the water. The organic layer was washed with ice cold 3N H_2SO_4 (3 x 360 ml), saturated $NaHCO_3$ (2 x 360 ml), and distilled water (3 x 360 ml). The organic layer was then dried over Na_2SO_4, filtered through a carbon bed, and evaporated in vacuo to a clear, pale yellow sirup (230 g) of 1,2,3,4-tetra-O-benzoyl-D-ribopyranose (I).

Sirupy (I) was thinned with 1,2-dichloroethane (400 ml) and allowed to react with 200 ml of 33% (w/w) hydrogen bromide-acetic acid. The reaction was monitored by TLC (solvent 1). After 4 hr, $CHCl_3$ (1000 ml) was added and the reaction mixture washed with ice water (3 x 2000 ml). The organic layer was then dried with $CaCl_2$, filtered, and evaporated in vacuo (35°C) to

a solid. The 2,3,4-tri-O-benzoyl-β-D-ribopyranosyl bromide (II) was recrystallized from diethyl ether to give 136 g (78%): m.p. 147-150°C. Literature: m.p. 151-3°C (76).

Crystalline (II) (105 g) was refluxed (3-4 min) until dissolved in absolute methanol (1000 ml) (46). After overnight refrigeration, crystalline methyl 2,3,4-tri-O-benzoyl-β-D-ribopyranoside (III) formed. Concentration of the mother liquor yielded an additional crop of crystals. Compound (III) was recrystallized from hot ethanol (82 g, 86%): m.p. 108-9°C; $[\alpha]_D^{21} = -69.7°$ (c 1.134, $CHCl_3$). Literature: m.p. 109-10°C; $[\alpha]_D^{21} = -69.5°$ (c 0.820, $CHCl_3$) (76).

Compound (III) (88 g) was suspended in absolute methanol (1000 ml) and $CHCl_3$ (350 ml). Debenzoylation occurred upon addition of 3% sodium methoxide (30 ml). The reaction was monitored by TLC (solvent 2). The reaction solution was extracted with triply distilled water (1 x 500 ml, 2 x 300 ml) until TLC did not show any product in the $CHCl_3$ layer*. The water layer was deionized with Amberlite IR-120 (H^+) resin (30 g) and concentrated in vacuo (40°C) to a sirup (31 g). The sirup was thinned with ethyl acetate (40 ml) and placed in a refrigerator where crystallization occurred. The MBR was recrystallized twice from ethyl acetate (22 g, 73%): m.p. 81-2°C; $[\alpha]_D^{21} = -106.2°$ (c 1.024, H_2O). Literature: m.p. 82-3° (77); $[\alpha]_D^{21} = -105.0°$ (c 0.47, H_2O) (78).

Method II

Absolute methanol (100 ml) was cooled in an ice bath and acetyl chloride (2 ml) slowly added. D-Ribose (10 g) was then dissolved in the acidified methanol and refluxed for 6 hr (78). After the mixture had cooled, the yellow

*The methanol caused difficulty in separation as it partitioned between the two layers. It is recommended that the procedure be modified by first evaporating the reaction solution to sirup before doing the extraction.

solution was decolorized with carbon (3X) and then the pale yellow solution was passed through Amberlite MB-3 (H^+, OH^-) resin. The neutral solution was evaporated *in vacuo* to a sirup (8 g). A portion of this sirup (4 g) was eluted through a Silica gel column (145 g, 60-200 mesh) with ethyl acetate. Fractions (10 ml) were collected and MBR located in Fractions 26-50. Evaporation *in vacuo* of these fractions yielded 1.5 g of sirup which readily gave crystalline MBR. If this alternative method is followed then MBR can theoretically be made in high yields. After the sirup has been column chromatographed and the MBR collected, the column can be stripped and the resulting sirup refluxed again in methanol hydrogen chloride. As shown by Cooper and Bishop (79) an equilibrium will be reestablished with MBR as the predominant glycoside. This mixture can then be put back through the above work-up.

REACTION ANALYSIS

CONDITIONING OF REACTOR AND GLASSWARE

Prior to each reaction run all Teflon surfaces inside the reactor and all glassware used in preparing the reaction solution were washed with Alconox, acetone, distilled water, 35% nitric acid (v/v), and triply distilled water. The reactor and glassware were then allowed to air dry before use.

PREPARATION OF REACTION SOLUTION

Triply distilled water (*ca.* 400 ml) was boiled for 10 min while covered with a watch glass and then placed immediately in a nitrogen atmosphere inside a glove bag. Stock sodium hydroxide solution (*ca.* 33.6 g) was weighed into a volumetric flask (250 ml), the flask purged with nitrogen and placed in the glove bag. After cooling, the triply distilled water was poured into the volumetric flask to mark and thoroughly mixed. The caustic solution was titrated against potassium acid phthalate to a phenophthalein end point.

If necessary, the alkalinity was adjusted until a 1.25 ± 0.005M solution was achieved as determined by triplicate titrations. The reactor was placed in the glove bag and alkaline solution poured into it (ca. 200 ml). By weighing the volumetric flask before and after adding the solution to the reactor, the volume added was calculated from the density of 1.25M NaOH solution (1.0529 g/ml). Carbohydrate was then added to the reactor to achieve the desired concentration. The reactor cover was bolted into place and the solution back-flushed through the sample line with nitrogen (1 min). The reactor was then placed in the oil bath and the bath turned on.

GLYCOSIDE AND METHANOL ANALYSIS

General

After the thermocouple output indicated that the temperature was stable (ca. 3.5 hr for a cold bath), the sample lines were purged by drawing two samples through them (for a description of the sampling procedure see Appendix IV, Reactor System). A time zero sample was taken in duplicate and the reactor pressurized with oxygen. All samples were taken in duplicate into tared 4 ml vials with generally one sample being used for glycoside analysis and one sample for methanol analysis. After each sample, the sample loop was back-flushed with water and acetone and vacuum dried. Prior to each sample, the sample lines were purged twice due to the dead volume between the reactor and the sample valve.

Glycoside Analysis

Each sample size was determined gravimetrically and then internal standard (n-propyl xyloside), as an aqueous solution, was added gravimetrically. The sample was then deionized over an Amberlite MB-3 (H^+, OH^-) resin column (5 ml) and eluted with distilled water (3 x 4 ml). The deionized sample was

then evaporated *in vacuo* to *ca.* 1 ml in a pear shaped flask, transferred to an Erlenmeyer flask (10 ml, GGS) and evaporated *in vacuo* to dryness.

Each sample was dissolved in dry pyridine (0.8 ml) and acetylated at room temperature with acetic anhydride (0.3 ml). After 18 hr of mechanical shaking, ice water (8 ml) was added to each sample and the samples shaken for 0.5 hr. The aqueous mixture was extracted with $CHCl_3$ (2 x 5 ml) and the chloroform extracts washed with 1N HCl (15 ml) and distilled water (10 ml). The chloroform extract was then dried over sodium sulfate, decanted, and evaporated *in vacuo* to dryness. The acetylated glycosides were dissolved in 1 ml of $CHCl_3$ and analyzed in triplicate by GLC (Appendix I, Conditions A).

Methanol Analysis

Each sample size was determined gravimetrically and ethanol internal standard added volumetrically. The samples were then analyzed directly by GLC (38) in triplicate (Appendix I, Conditions B).

To investigate whether or not the sampling method employed would give an accurate picture of liberated methanol, the reactor was charged with a known concentration of methanol in 1.25M NaOH. The reactor was then placed in the oil bath and the experiment conducted at normal reaction conditions. Four samples were taken from the reactor. Between each sample, the headspace was varied in the reactor by emptying approximately 1/4 of the solution. The reactor was allowed to equilibrate for 1 hr between each sample. All of the samples yielded methanol values (by GLC) that agreed within 1.5% of the initial methanol concentration (1.8×10^{-2}M) as determined gravimetrically.

PEROXIDE ANALYSIS

Peroxide Sampling

The peroxide samples were taken through a line which by-passed the glycoside sample loop (Appendix IV, Reactor System). This allowed larger sample sizes to be obtained. Prior to the taking of the peroxide samples the lines were purged with ca. 1 ml of reaction solution. The peroxide sample (ca. 5 ml) was then taken directly into an 8-ml vial.

Peroxide Analysis

The peroxide analysis was conducted using a colorimetric method involving a complex between hydrogen peroxide and titanium(IV) (1,2,12-14,39-41). The initial absorbance of the samples treated with the titanium sulfate reagent was taken as a measure of hydrogen peroxide. With time, absorbance usually increased and the difference between initial and final absorbance was taken as a measure of organic peroxides. A straight-line calibration curve was constructed by analyzing dilute hydrogen peroxide solutions by both the titanium sulfate method and a standard iodide-thiosulfate titration (80) (Fig. 29).

After the peroxide sample was taken from the reactor it was immediately analyzed. An aliquot (1 ml) was added to a 5-ml volumetric flask which contained enough sulfuric acid to give a final pH of either 0 or 1. Duplicate analyses were conducted at each pH level. After adding the sample and shaking, 3 drops of the titanium sulfate reagent were added to each flask*. Distilled water was added to the mark and the absorbance of each sample was then taken at 400 nm within 5 minutes of the sampling time. The absorbance

*To avoid precipitation of the titanium sulfate, the sample must be acidified before the titanium sulfate reagent is added.

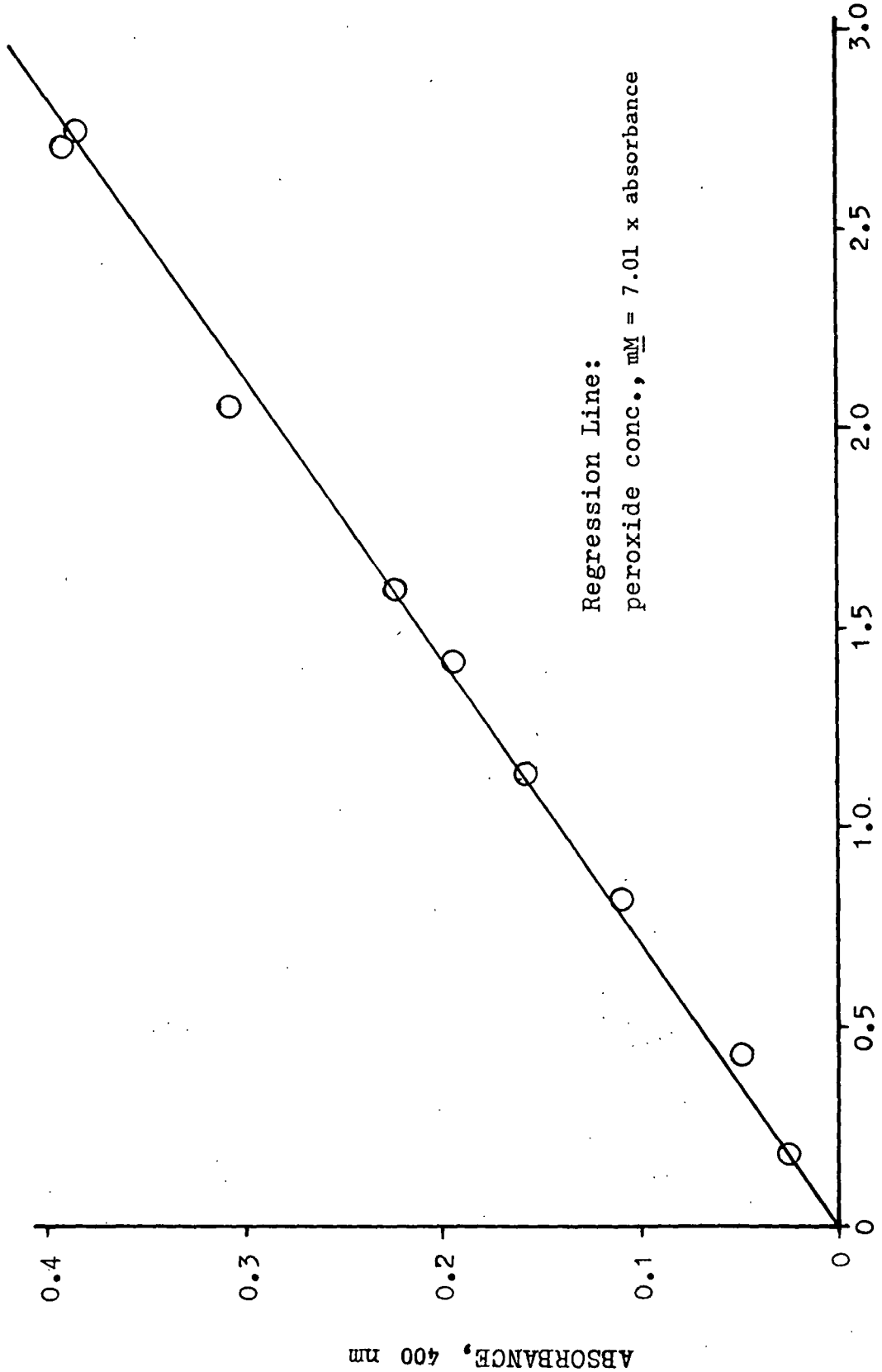

Figure 29. Absorbance at 400 nm vs. Peroxide Concentration as Determined by the Standard Iodometric Titration Technique

increase over a period of 2 days was followed with the maximum in absorbance for the pH 0 samples occurring at 24-36 hr. When the pH 0 samples reached maximum absorbance, the pH 1 samples had an absorbance value of 40-70% of the pH 0 value. The volume of acid necessary to achieve the desired pH was predetermined by a pH meter. All absorbance measurements were made against a distilled water reference as this gives the same result as a titanium sulfate reagent reference (42).

PRODUCT ANALYSIS

Product Sampling and Derivitization

The product samples were taken through the same by-pass line as employed for the peroxide samples (Appendix I, Reactor System). Prior to the taking of each sample the lines were purged with reaction solution (ca. 1 ml). The samples (ca. 4 ml) were taken directly into tared 8-ml vials containing 1M $NaHSO_3$ (1 ml). The sample sizes were determined gravimetrically and then internal standard (n-propyl xyloside, as an aqueous solution) was added gravimetrically. Each sample was then deionized through an Amberlite IR-120 (H^+) column (10 ml) and eluted with distilled water (3 x 8 ml). The pH of the deionized sample was immediately adjusted to ca. 7-8 by the addition of NH_4OH. The sample was then concentrated in vacuo (35°C) to ca. 1 ml in a pear shaped flash and transferred to a 4-ml screw-top vial. The sample was then evaporated in vacuo (35°C) to dryness and vacuum evaporated (2X) with 1,2-dichloroethane to remove the last traces of water.

Approximately 30 to 50 mg portions of the product samples were transferred to 4-ml vials fitted with septa and the sample residue dissolved in dimethylsulfoxide (0.5 ml, silylation grade, Pierce Chemical Co.). To assist dissolution, the mixture was heated in a block heater (65°C, 15 min).

The mixture was then treated with Tri-Sil Concentrate (0.5 ml, Pierce Chemical Co.) and mechanically shaken for 12 hr. The top layer was then analyzed by either GLC (Appendix I, Conditions C), GLC-MS (Appendix III), or preparative GLC-PMR (Appendix I, Conditions D). One sample, from which methoxyacetic acid was identified, was subjected to an alternative work-up procedure. No bisulfite or NH_4OH was used and the sample was derivatized as a $CHCl_3$ solution with BSTFA (Pierce Chemical Co.).

Mass Spectral Analysis

The major reaction products were identified principally by GLC-MS (see Appendix III for mass spectrometer settings) as their TMS derivatives. Mass calibration was achieved through the use of an internal standard, Perflurokerosene (high mass; PCR, Inc., Gainesville, Florida). The fragmentation patterns of MBR and MBX were assigned by comparison with the fragmentation pattern of methyl 2,3,4-tri-O-methyl-α-L-arabinopyranoside as discussed by Kochetkov and Chizhov (81). The mass spectra and relative abundance data of the identified compounds are reported in Appendix III.

Time Distribution of Products

The concentration of the methyl C-carboxyfuranosides was examined as a function of time by quantitative GLC. The response factor of these furanoid acids relative to PBX was estimated to be 0.9. This estimate was based upon the calculated response factors of MBR and MBX relative to PBX (Appendix I, Table VII). The product samples were derivatized as previously described and the GLC conditions are given in Appendix I. A sample chromatogram of the products is shown in Fig. 12.

Preparative GLC-PMR Analysis

The assignment of the carboxyl function position in the methyl C-carboxyfuranosides was accomplished by isolating the products by preparative GLC and taking PMR spectra. An aliquot of run OS-4 (ca. 25 ml) was passed over an Amberlite IR-120 (H^+) column (12 ml) and eluted with distilled water (75 ml). After deionizing the pH was adjusted from 3 to 8 with 1N NaOH. This solution was then eluted over an Amberlite IRA-400 (OH^-) column at a rate of 1.5 ml/min, followed by elution with distilled water (1 liter) at a rate of 3.0 ml/min. The acids were then displaced from the column via elution with 1M $NaHCO_3$ (1500 ml) at 3.0 ml/min.* The bicarbonate eluate was deionized batchwise with Amberlite IR-120 (H^+) until the pH reached ca. 3-4. The pH was then brought back to ca. 7-8 with NH_4OH. This solution was then evaporated and derivatized as previously discussed (see Product Sampling and Derivatization).

The products were then separated by GLC (Appendix I, Conditions D) employing a thermal conductivity detector for peak detection. As the methyl C-carboxyfuranosides eluted from the gas chromatograph, they were collected in glasswool-packed glass tubes cooled by an ice bath. The samples were washed from the tubes with $CDCl_3$ into NMR tubes and analyzed within one hour by FT-PMR.

OXYGEN SOLUBILITY

The solubility of oxygen at the reaction conditions was determined by employing equipment developed by Green and Thompson (32). Reaction solutions

*The use of $NaHCO_3$ should be avoided if possible as it leads to severe deionizing problems. NaOH should be able to elute all but the dicarboxylic acids of the acids encountered in oxygen-alkali-methyl glycoside studies (15).

were withdrawn from the reactor by an hydraulic piston which then transferred the solution into a pressurized trap (N_2, 200-250 psig). In the trap, the reaction solution was allowed to react with Winkler solutions (82) while the nitrogen pressure insured that the oxygen would not come out of solution. The final sodium thiosulfate titration was done at atmospheric pressure.

ACKNOWLEDGMENTS

The author greatly appreciates the guidance and support of this work by the advisory committee: Drs. S. N. Thompson, Chairman; L. R. Schroeder and R. D. McKelvey. Special gratitude is extended to Drs. Thompson and Schroeder for numerous helpful conversations and votes of confidence. The author also acknowledges the invaluable assistance given by numerous faculty and staff members.

The generous financial support provided by the member companies of The Institute of Paper Chemistry was greatly appreciated.

The atmosphere of friendship provided by the faculty, staff, fellow students and their wives and children, made this work more enjoyment than drudgery.

Finally I especially thank the following persons who encouraged me in my work: to the parents of my wife and me for their continued support; to my sons, David and Walt, who were a welcomed distraction; and most importantly to my wife, Claire, for her unending encouragement and support of my cause.

LITERATURE CITED

1. Millard, E. C. The degradation of selected 1,5-anhydroalditols by molecular oxygen in alkaline media. Doctoral Dissertation. Appleton, WI, The Institute of Paper Chemistry, 1976.

2. Millard, E. C., Schroeder, L. R., and Thompson, N. S., Carbohyd. Res. 56:259(1977).

3. Malinen, R., and Sjostrom, E., Cellulose Chem. Technol. 9:231(1975).

4. Samuelson, O., and Stolpe, L., Tappi 52(9):1709(1969).

5. Kolmodin, H., and Samuelson, O., Svensk Papperstid. 73(4):93(1970).

6. Rowell, R. M., Pulp Paper Mag. Can. 72:T236(1971).

7. Ericsson, B., Lindgren, B. O., and Theander, O., Svensk Papperstid. 74:757(1971).

8. Malinen, R., Paperi Puu 57(4a):193(1975).

9. Lindberg, B., and Theander, O., Acta Chem. Scand. 22:1782(1968).

10. Kolmodin, H., and Samuelson, O., Svensk Papperstid. 76:71(1973).

11. Ericsson, B., Lindgren, B. O., and Theander, O., Cellulose Chem. Technol. 7:581(1973).

12. McCloskey, J. T., Schroeder, L. R., Sinkey, J. D., and Thompson, N. S., Paperi Puu 57:131(1975).

13. Sinkey, J. D., and Thompson, N. S., Paperi Puu 56:473(1974).

14. McCloskey, J. T., Sinkey, J. D., and Thompson, N. S., Tappi 58(2):56 (1975).

15. Ericsson, B., Lindgren, B. O., and Theander, O., Cellulose Chem. Technol. 8:363(1974).

16. Samuelson, O., and Stolpe, L., Svensk Papperstid. 72:661(1969).

17. Minor, J. L., and Sanyer, N., J. Polymer Sci., Part C, 36:73(1971).

18. Brooks, R. D., and Thompson, N. S., Tappi 49:362(1966).

19. Weaver, J. W. The alkaline hydrogen peroxide reaction of methyl β-D-glucopyranoside and methyl 4-O-methyl β-D-glucopyranoside. Doctoral Dissertation. Appleton, WI, The Institute of Paper Chemistry, 1976.

20. Weaver, J. W., Schroeder, L. R., and Thompson, N. S., Carbohyd. Res. 48:C5(1976).

21. Haskins, J. F., and Hogsed, M. J., J. Org. Chem. 15:1264(1950).

22. Russell, G. A., J. Chem. Educ. 36:111(1959).

23. McCloskey, J. T. The degradation of methyl β-D-glucopyranoside by oxygen in alkaline solution. Doctoral Dissertation. Appleton, WI, The Institute of Paper Chemistry, 1971.

24. Rendleman, J. A., Adv. Carbohyd. Chem. 21:209(1966).

25. Rowland, S. P., Carbohyd. Res. 17:393(1971).

26. Saric, S. P., and Schofield, R. K., Proc. Royal Soc. (London) (A), 185:431(1946).

27. Church, J. A. The autoxidation of methyl glycopyranosides. Doctoral Dissertation. Appleton, WI, The Institute of Paper Chemistry, 1964.

28. McKelvey, R. D., Carbohyd. Res. 42:187(1975).

29. Reiner, D., and Poe, D. P., Anal. Chem. 49(6):889(1977).

30. Dewilt, H. G. J., and Kuster, B. F. M., Carbohyd. Res. 19:5(1971).

31. Tanner, F. W. Model studies on the effect of oxygen in the alkaline hydrolysis of glucosidic bonds. Master's Dissertation. North Carolina State University, Raleigh, NC, 1973.

32. Green, J. W., and Thompson, N. S., unpublished work.

33. Bruhn, G., Gerlach, J., and Pawlek, F., Z. Anorg. Allgem. Chem. 337(1-2):68(1965).

34. Thompson, N. S., personal communication.

35. Crozier, T. C. Studies on the oxidative activation of loblolly pine dioxane lignin toward degradation with oxygen-alkali. Doctoral Dissertation. Appleton, Wisconsin, The Institute of Paper Chemistry, 1978.

36. Frost, A. A., and Pearson, R. G. Kinetics and mechanism. 2nd ed., Chap. 2, New York, Wiley and Sons, 1961.

37. Laidler, K. J. Chemical kinetics. 2nd ed., Chap. 1, McGraw-Hill, New York, 1965.

38. Sims, E. W., J. Chromat. Sci. 14:65(1976).

39. Satterfield, C. N., and Bonnell, A. H., Anal. Chem. 27:1175(1955).

40. Marklund, S., Acta Chem. Scand. 25:21(1971).

41. Pobiner, H., Anal. Chem. 33(10):1423(1961).

42. Sinkey, J. D. The function of magnesium compounds in an oxygen-alkali-carbohydrate system. Doctoral Dissertation. Appleton, WI, The Institute of Paper Chemistry, 1973.

43. Verhaar, L. A., and DeWilt, H. G., J. Chromat. 41:168(1969).

44. Peterson, G., Tetrahedron 26:3413(1970).

45. Isbell, H. S., Adv. Chem. Ser. 117:71(1975).

46. Ericsson, B., Lindgren, B. O., Theander, O., and Petersson, G., Carbohyd. Res. 23:323(1972).

47. Michie, R. I. C., and Neale, S. M., J. Polymer Sci., Part 2a:2063(1964).

48. Kano, T., Ishizu, A., Hosoya, S., and Nakano, J., J. Soc. Fiber Sci. Technol. Japan 30(5/6):T260(1974); Jap.; ABIPC 45:A5534.

49. Seyfarth, H. E., Rieche, A., and Hesse, A., Chem. Ber. 100:624-8(1967); Angew Chem. Intern. Ed. Engl. 5:253(1965).

50. McCloskey, J. T., Sinkey, J. D., and Thompson, N. S. Nonsulfur Pulping Symposium, Madison, WI, 1975.

51. Thompson, N. S., unpublished data.

52. Rendleman, J. A., Adv. Chem. Ser. 117:51(1975).

53. Neuberger, A., and Wilson, B. M., Carbohyd. Res. 17:89(1971).

54. Izatt, R. M., Rytting, J. H., Hanson, L. D., and Christensen, J. J., J. Chem. Soc. 88:2461(1966).

55. Kabayama, M. A., Patterson, D., Can. J. Chem. 36:563-73(1958).

56. Norrman, B., Acta Chem. Scand. 22:1623(1968).

57. Roberts, E. J., Wade, C. P., and Rowland, S. P., Carbohyd. Res. 21:357 (1972).

58. Bock, K., and Pederson, C., Acta Chem. Scand. B29:258(1975).

59. Angyal, S. J., Aust. J. Chem. 21:2737(1968).

60. Vinogradov, S. N., and Linnell, R. H. Hydrogen bonding. Chap. 7, New York, Van Nostrand Reinhold Co., 1971.

61. Hordvik, A., Acta Chem. Scand. B28(2):261(1974).

62. Brown, C. J., Cox, G., and Llewellyn, F. J., J. Chem. Soc. (A), 1966:922.

63. Wells, H. A., Jr. An investigation of the vibrational spectra of glucose, galactose, and mannose. Doctoral Dissertation. Appleton, WI, The Institute of Paper Chemistry, 1977.

64. Kuhn, L. P., J. Am. Chem. Soc. 74:2492(1952).

65. Stoddart, J. F. Stereochemistry of carbohydrates. p. 54-8. Toronto, Wiley-Interscience, 1971.

66. Behar, D., Czapski, G., Rabini, J., Dorfman, L. M., and Schwarz, H. A., J. Phys. Chem. 74:3209(1970).

67. Hayday, K., and McKelvey, R. D., J. Org. Chem. 41:2222(1976).

68. Schroeder, L. R., personal communication.

69. March, J. Advanced organic chemistry: reactions, mechanisms, and structure. p. 804-9. New York, McGraw-HIll, 1968.

70. Carey, F. A., and Sundberg, R. J. Advanced organic chemistry. Part B: Reactions and synthesis. p. 324-8. New York, Plenum, 1977.

71. Skoog, D. A., and West, D. M. Fundamentals of analytical chemistry. 835 p., 2nd ed., New York, Holt, Rinehart, and Winston, 1969.

72. Perrin, D. D., Armarego, W. L. F., and Perrin, D. R. Purification of laboratory chemicals. 362 p., New York, Pergamon Press, 1966.

73. Bauer, N., and Lewin, S. Z. In Weissberger's Techniques in organic chemistry. Vol. I, Part 1, p. 136., New York, Interscience, 1959.

74. Debruyne, C. K., and Loontinens, F. G., Nature 209:396(1966).

75. Fischer, E., Ber. 28:1157(1895).

76. Jeanloz, E. L., Fletcher, H. G., Jr., and Hudson, C. S., J. Am. Chem. Soc. 70:4055(1948).

77. Durette, P. L., and Horton, D., Carbohyd. Res. 18:403(1971).

78. Jackson, E. L., and Hudson, C. S., J. Am. Chem. Soc. 63:1229(1941).

79. Bishop, C. T., and Cooper, F. P., Can. J. Chem. 41:2743(1963).

80. Kolthoff, I. M., and Sandell, E. B. Textbook of quantitative inorganic chemistry. 3rd ed., p. 574, New York, MacMillan, 1956.

81. Kochetkov, N. K., and Chizhov, O. S., Adv. Carbohyd. Chem. 21:29(1966).

82. American Public Health Association. Standard methods for the examination of water and waste water. p. 474, New York, APHA, 1971.

83. Brandon, R. E. Alkaline degradation of 1,5-anhydrocellobiitol. Doctoral Dissertation, Appleton, WI, The Institute of Paper Chemistry, 1973.

APPENDIX I

GAS-LIQUID CHROMATOGRAPHY

Quantitative GLC was accomplished through the use of an appropriate internal standard. Molar response factors relative to the internal standards were calculated according to Equation (32).

$$F_x = A_r \times M_r \tag{32}$$

where F_x = response factor for compound X relative to the internal standard

A_r = ratio of peak area of compound X to the peak area of the internal standard

M_r = mole ratio of the internal standard to compound X

The response factors were experimentally determined by preparing a series of solutions with varied molar ratios and subjecting the solutions to the appropriate work-up procedure. The solutions were then analyzed by GLC in triplicate and the response factor calculated as an average of the values obtained.*

Table VII lists the various GLC conditions used in this work and Table VIII gives GLC retention times and response factors of various compounds associated with this work.

Through the use of Equation (33) the response factors were used to calculate the concentration of compound X in the reaction samples.

$$[X] = 10^3 \, (A_r) \, (IS) \, \rho/(S) \, (F_x) \tag{33}$$

*This assumes that the response factor was constant over the range of molar ratios and concentrations examined. Although the response factors did not seem to be affected by molar ratio, at lower concentrations of MBR and methanol deviation from the reported response factors occurred. However, these concentration ranges were not, generally, experienced in this work.

where [X] = concentration of compound X, moles/liter

ρ = density of reaction mixture, g/ml

S = reaction sample, g

IS = internal standard, moles

TABLE VII

GAS-LIQUID CHROMATOGRAPHIC CONDITIONS

Conditions	A	B	C	D[d]
Column type	SE-30[a]	Carbowax 20M[b]	OV-17[c]	OV-17[e]
Derivative	Acetylated	Underivatized	Trimethyl-silylated	Trimethyl-silylated
Column temp. programming, °C	170	70	60→160 @ 2°/min	60→150 @ 2°/min
Injector temp., °C	260	150	260	200
Detector temp., °C	260	265	260	200
N_2 flow rate, ml/min	15	35	20	20

[a] Stainless steel column (5 ft x 0.125 inch) rigged for on-column injection and packed with 10% SE-30 on 60/80 mesh DMCS-AW Chromosorb W.

[b] Stainless steel column (4 ft x 0.125 inch) rigged for off-column injection and flash vaporization and packed with 5% Carbowax 20M on 80/100 mesh Chromosorb 101.

[c] Stainless steel column (15 ft x 0.125 inch) rigged for on-column injection and packed with 3% OV-17 on 80/100 mesh Supelcoport.

[d] Thermal conductivity bridge detector — 100 ma current.

[e] Stainless steel column (10 ft x 0.25 inch) rigged for on-column injection and packed with 5% OV-17 on 80/90 mesh Anakrom ABS.

TABLE VIII

RETENTION TIMES (T_r) AND RESPONSE FACTORS (F_x)

Conditions	Compound	T_r, min	F_x
A	Methyl β-D-xylopyranoside	7.2	0.774 ± 0.011[a]
	Methyl β-D-ribopyranoside	7.7	0.756 ± 0.013[a]
	n-Propyl β-D-xylopyranoside	12.3	1.000[a]
B	Methanol	2.9	0.535 ± 0.008[b]
	Ethanol	7.8	1.000[b]
C	Methoxyacetic acid	14.5	1.044 ± 0.040[a,c]
	Lactic acid	19.4	
	Glycolic acid	21.4	
	Glyceric acid	38.4	
	Methyl β-D-ribopyranoside	55.0	0.894 ± 0.019[a]
	Methyl 3-C-carboxy-β-D-tetrafuranoside	56.1	0.900[d]
	Isomeric methyl 2-C-carboxy-β-D-tetrafuranosides	57.8 58.9	0.900[d] 0.900[d]
	Methyl β-D-xylopyranoside	62.9	0.881 ± 0.016[a]
	n-Propyl β-D-xylopyranoside	90.9	1.000[a]

[a]Calculated relative to n-propyl β-D-xylopyranoside at the specified conditions.

[b]Calculated relative to ethanol at the specified conditions.

[c]Calculated from triplicate injections of a single sample.

[d]Estimated response factor.

APPENDIX II

EXPERIMENTAL DATA

TABLE IX

DEGRADATION OF METHYL β-D-XYLOPYRANOSIDE (MBX) (ca. 0.1M) IN 1.25M NaOH AT 120°C, 0.682 MPa O_2

Time, min	MBX, x 10^2M	MeOH, x 10^3M	Mole %, MeOH
	Reaction 7MBX		
0	9.77	--	--
15	9.61	1.2	75
30	9.43	3.6	106
60	8.95	5.7	70
120	8.14	10.4	64
240	6.98	17.5	63
420	6.19	23.6	66
660	5.36	27.8	63
930	4.94	34.3	71
1428	4.21	35.4	64
1914	3.70	36.0	59
2730	3.17	39.6	60
3360	2.82	44.0	63
4200	2.41	45.7	62
	Reaction 8MBX		
0	9.57	--	--
20	9.44	0.9	69
40	9.11	3.3	72
60	8.69	6.3	71
120	7.79	10.3	58
240	6.88	17.0	63
420	5.99	23.6	66
660	5.31	29.7	70
900	4.79	33.4	69
1410	4.05	38.2	69
2100	3.41	39.6	64
2850	2.94	41.7	63
3540	2.58	45.3	65
4290	2.25	45.8	63

TABLE X

DEGRADATION OF METHYL β-D-RIBOPYRANOSIDE (MBR) (ca. 0.1M) IN 1.25M NaOH AT 120°C, 0.682 MPa O_2

Time, min	MBR, x 10^2M	MeOH, x 10^3M	Mole %, MeOH
	Reaction 5MBR		
0	9.66	--	--
10	9.30	3.7	103
30	7.90	11.4	65
50	6.65	17.8	59
70	5.68	22.5	57
90	5.20	26.5	59
120	4.54	31.6	62
175	3.72	36.6	62
300	2.85	42.1	62
480	2.37	45.8	63
810	1.91	49.5	64
1380	1.46	49.7	61
2100	1.11	53.7	63
2880	0.88	54.1	62
	Reaction 6MBR		
0	9.65	--	--
5	9.65	0.7	--
30	8.25	10.7	76
50	7.07	14.5	56
70	5.94	22.0	59
90	5.20	25.3	57
120	4.34	30.9	58
177	3.51	35.7	58
300	2.70	43.1	62
480	2.15	49.4	66
840	1.62	51.3	64
1440	1.23	49.8	59
2130	0.94	53.0	61
2880	0.72	50.1	56

TABLE XI

DEGRADATION OF METHYL β-D-XYLOPYRANOSIDE AND METHYL β-D-RIBOPYRANOSIDE IN 1.25M NaOH AT 120°C AND 0.682 MPa O_2[a]

Time, min	MBX, x 10^2M	MeOH, x 10^3M	Mole %, MeOH
	Reaction 3MBX		
0	10.18	0.0	--
60	9.70	0.5	13
120	9.75	1.0	30
180	9.68	1.3	33
308	9.60	2.5	52
420	9.30	3.8	54
600	8.92	6.0	52
890	8.30	9.8	55
1200	7.64	14.0	57
1530	6.95	19.1	61
1900	6.25	22.6	59
2582	4.92	30.8	60
	Reaction 3MBR		
0	9.83	0.0	--
70	9.64	0.4	21
120	9.71	0.6	50
250	9.63	1.9	95
480	8.87	5.1	53
942	7.65	11.1	51
1295	6.86	16.4	55
1560	6.31	21.2	60
1800	5.74	24.0	59

[a]Oxygen deficient degradations, i.e., limited agitation.

TABLE XII

DEGRADATION OF METHYL β-D-XYLOPYRANOSIDE (MBX) (ca. 0.1M) IN 1.25M NaOH AT 120°C, 0.0 MPa O_2 (N_2 atmosphere)

Time, min	MBX, x 10^2M	Time, min	MBX, x 10^2M
	Reaction 10MBX		
0	9.66	2375	9.57
370	9.61	3080	9.68
1025	9.89	3840	9.61
1640	9.69	4380	9.50

TABLE XIII

DEGRADATION OF METHYL β-D-RIBOPYRANOSIDE (MBR) (ca. 0.1M) IN 1.25M NaOH AT 120°C, 0.0 MPa O_2 (N_2 atmosphere)

Time, min	MBX, x 10^2M	Time, min	MBX, x 10^2M
	Reaction 7MBR		
0	10.18	2420	10.02
365	10.27	2990	10.11
1015	10.20	3860	10.04
1550	10.14	4360	10.19

TABLE XIV

PEROXIDE FORMATION DURING DEGRADATION OF METHYL β-D-XYLOPYRANOSIDE (MBX) (ca. 0.1M) IN 1.25M NaOH AT 120°C, 0.682 MPa O_2

Time, min	H_2O_2, x 10^4M	Organic Peroxides, x 10^4M
	Reaction 7MBX	
4	0.4	0.3
15	2.9	0.3
30	3.8	0.5
45	3.6	0.8
60	3.2	1.1
105	2.7	2.2
210	1.8	5.8
420	0.9	12.4
600	0.8	15.3
	Reaction 8MBX	
10	2.0	--
20	3.5	0.2
30	3.8	0.4
40	3.9	0.7
50	3.7	0.6
60	3.5	0.8
75	3.4	1.3
105	2.7	2.3
180	2.2	4.7
300	1.5	8.5
	Reaction 9MBX[a,b]	
5	1.1	
15	1.6	
30	2.3	
40	3.2	
50	3.1	
65	2.8	
85	1.8	
110	1.3	

[a] Peroxides determined at test pH of 1.9.

[b] No organic peroxides detected after 36 hr of hydrolysis.

TABLE XV

PEROXIDE FORMATION DURING DEGRADATION OF METHYL β-D-RIBOPYRANOSIDE (MBR) (ca. 0.1M) IN 1.25M NaOH AT 120°C, 0.682 MPa O_2

Time, min	H_2O_2, x 10^4M	Organic Peroxides, x 10^4M
	Reaction 5MBR	
2	0.7	--
10	7.4	--
20	10.2	0.7
30	10.1	1.2
40	8.9	2.0
50	7.7	2.8
68	6.4	3.9
105	4.8	5.4
117	3.8	6.6
172	2.5	8.7
	Reaction 6MBR	
5	2.3	--
15	7.2	0.6
30	8.2	1.2
50	8.8	2.2
70	7.6	3.6
90	6.3	4.3
150	3.3	7.3

TABLE XVI

PRODUCT DISTRIBUTION FROM THE DEGRADATION OF 0.1M METHYL XYLOSIDE AND METHYL RIBOSIDE IN 1.25M NaOH AT 120°C and 0.682 MPa O_2

Time, hr	% Reacted Glycoside	Product[a] ⑤, x 10^3M	Product[b] ⑥, x 10^3M	Product[b] ⑦, x 10^3M
		Reaction 6MBR		
0.3	7	--[c]	0.2	0.3
0.5	15	--[c]	1.6	0.6
1.0	33	0.4	3.7	1.8
1.5	46	2.1	4.6	3.8
2.0	55	2.8	5.8	5.0
4.0	66	3.1	7.5	6.2
10.0	77	3.3	7.9	6.1
35.4	90	3.8	10.3	6.5
		Reaction 8MBX		
0.5	3	--	0.4	--
1.5	14	0.4	1.4	0.5
3.0	23	0.7	2.5	0.9
6.0	34	1.1	3.7	1.3
9.0	41	1.4	4.6	1.7
15.0	50	1.6	5.3	2.0
35.0	64	1.8	6.2	1.8
59.0	73	1.4	5.8	0.7

[a] Methyl 3-C-carboxy-β-D-tetrafuranoside.

[b] Isomeric methyl 2-C-carboxy-β-D-tetrafuranoside.

[c] Unable to determine due to tailing methyl riboside peak.

APPENDIX III

MASS SPECTROMETRY ANALYSIS

The equipment utilized for the mass spectrometry was previously described (see Experimental). The GLC conditions were identical to Conditions C (Appendix I, Table VII) except helium was used as the carrier gas instead of nitrogen. The operating conditions for the mass spectrometer are given in Table XVII.

TABLE XVII

MASS SPECTROMETER OPERATING CONDITIONS

Jet separator temperature: 300°C
Separator block temperature: 300°C
Oven temperature: 115°C
Source temperature: 180°C
Ionization voltage: 70 eV
Vacuum: 2×10^{-7} torr
Filament: GC mode
Scan: 10 sec/decade

The mass spectral data are presented in Tables XVIII-XXV. Fragmentation patterns for the methyl glycosides and the methyl C-carboxyfuranosides are presented in Fig. 30 and 31, respectively. The product numbers referred to in the table headings correspond to the product numbers assigned in the Results section.

TABLE XVIII

MASS SPECTRAL DATA FOR METHYL β-D-XYLOPYRANOSIDE (MBX) AND METHYL β-D-RIBOPYRANOSIDE (MBR) (TMS DERIVATIVES)[a]

m/e	Relative Abundance, %	m/e	Relative Abundance, %
	MBX		
73	93	149	5
74	10	189	5
75	6	191	4
89	7	201	6
101	5	204	100
102	34	205	20
103	5	206	11
116	4	217	81
117	5	218	11
129	7	219	5
133	42	233	4
135	5	305	4
146	7	349	1
146	27		
148	6		
	MBR		
73	63	159	3
74	11	189	8
75	13	191	3
89	12	201	4
101	8	204	69
103	5	205	20
116	10	206	8
117	4	217	100
129	7	218	35
131	4	219	20
133	56	233	4
134	6	247	3
143	5	305	6
146	4	349	<1
147	33	365	<1
148	6		
149	5		

[a] Figure 30 gives a fragmentation pattern for some of the major ions.

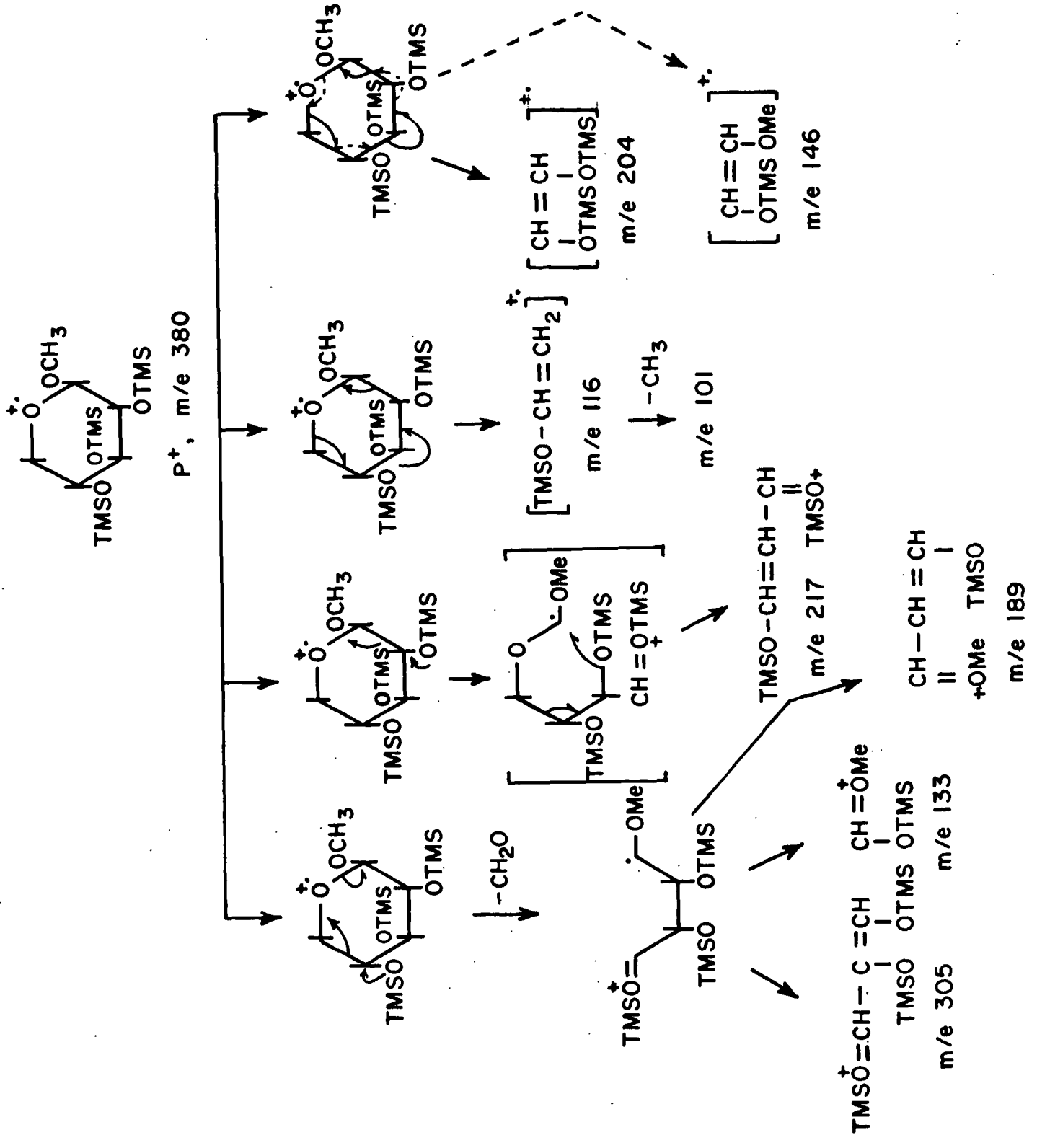

Figure 30. Fragmentation Pattern for Some Major Ions in the MBX and MBR Mass Spectra

TABLE XIX

MASS SPECTRAL DATA FOR METHOXYACETIC ACID (TMS DERIVATIVE) (MBR AND MBX PRODUCT ①)

	Relative Abundance, %			
	Product ①		Known Methoxyacetic Acid	
m/e	A[a]	B[b]	A[a]	B[b]
73	100	94	100	100
74	14	17	78	13
75	42	9	64	8
83	15	--	--	--
85	12	--	--	--
86	--	11	--	5
87	4	--	--	--
88	--	8	7	4
89	75	--	80	12
90	--	--	31	--
91	3	3	60	3
100	--	37	--	11
101	--	6	6	--
102	--	17	--	4
103	--	--	51	--
104	--	5	10	--
105	--	3	6	--
113	--	6	--	--
114	--	4	--	--
115	--	4	--	--
116	--	9	4	--
117	57	4	72	3
118	4	3	51	--
119	--	4	11	--
130	--	75	--	27
131	4	26	--	4
132	--	14	14	3
133	21	--	--	--
146	--	9	--	--
147	44	17	70	25
148	7	14	14	10
162,P^+	10	27	1	5
163	3	6	--	--
164	--	3	--	--
177	--	72	--	21
178	--	35	--	6
179	--	23	--	3
191	--	100	--	70
192	--	87	--	27
193	--	70	--	18
205	--	8	--	--
206	--	67	--	10
207	--	16	--	4
208	--	10	--	--

[a] Derivatized without the use of $NaHSO_3$.
[b] $NaHSO_3$ used in sample work-up.

TABLE XX

MASS SPECTRAL DATA FOR LACTIC ACID (TMS DERIVATIVE) (MBR AND MBX PRODUCT (2))[a]

m/e	Relative Abundance, %	m/e	Relative Abundance, %
73	100	133	6
74	12	147	70
75	18	148	9
89	7	149	6
101	3	190	7
117	49	191	8
118	5	192	4
119	3	219	2
131	3		

[a]Spectrum taken on MBX product sample.

TABLE XXI

MASS SPECTRAL DATA FOR GLYCOLIC ACID (TMS DERIVATIVE) (MBR AND MBX PRODUCT (3))[a]

m/e	Relative Abundance, %	m/e	Relative Abundance, %
73	100	147	96
74	18	148	59
75	22	149	28
89	3	161	25
101	4	162	4
102	4	177	43
103	10	178	5
115	6	179	5
117	9	191	4
131	13	205	63
133	18	206	10
134	5	207	8
135	3	220, P^+	1

[a]Spectrum taken on MBX product sample.

TABLE XXII

MASS SPECTRAL DATA FOR GLYCERIC ACID (TMS DERIVATIVE) (MBR AND MBX PRODUCT ④)[a]

m/e	Relative Abundance, %	m/e	Relative Abundance, %
73	100	147	21
74	7	148	5
75	14	189	8
89	3	205	3
102	7	292	4
103	10	307	1
107	7		
131	3		
133	4		

[a] Spectrum taken on MBX product sample.

TABLE XXIII

MASS SPECTRAL DATA FOR METHYL 3-C-CARBOXY-β-D-TETRAFURANOSIDE (TMS DERIVATIVE) (MBR AND MBX PRODUCT (5))[a]

m/e	Relative Abundance, %	m/e	Relative Abundance, %
73	100	207	4
74	12	215	14
75	15	216	7
89	12	217	28
101	3	219	3
113	3	221	7
116	9	231	3
117	4	232	3
127	3	233	4
129	10	243	4
131	14	244	5
133	10	245	8
134	7	259	5
143	7	276	5
147	54	277	3
148	7	291	11
149	9	316	3
157	4	319	6
159	3	334	45
162	4	335	12
174	4	336	13
177	10	363	1
189	3	379	8
191	4	380	4
201	8	381	4
204	5	394	1
205	6		

[a]Mass spectra taken from the MBR and MBX systems were identical within the operating limits of the mass spectrometer.

TABLE XXIV

MASS SPECTRAL DATA FOR METHYL 2-C-CARBOXY-β-D-TETRAFURANOSIDE (TMS DERIVATIVE) (MBR AND MBX PRODUCT (6))[a,b]

m/e	Relative Abundance, %	m/e	Relative Abundance, %
73	100	215	6
74	11	216	19
75	15	217	10
89	11	219	4
101	3	221	4
103	3	229	5
116	4	230	5
117	3	231	3
118	3	233	4
119	6	244	6
127	4	245	10
128	4	246	4
129	4	247	17
132	16	262	4
142	5	276	16
147	41	283	3
148	18	289	5
149	10	291	10
157	5	308	3
163	16	319	7
173	7	320	3
177	6	334	67
190	6	335	19
191	3	336	11
201	6	363	2
207	4	379	19
208	6	394	2

[a] Mass spectra from MBR and MBX systems were identical within the operating limits of the mass spectrometer.

[b] Fragmentation pattern for some major ions are given in Fig. 31.

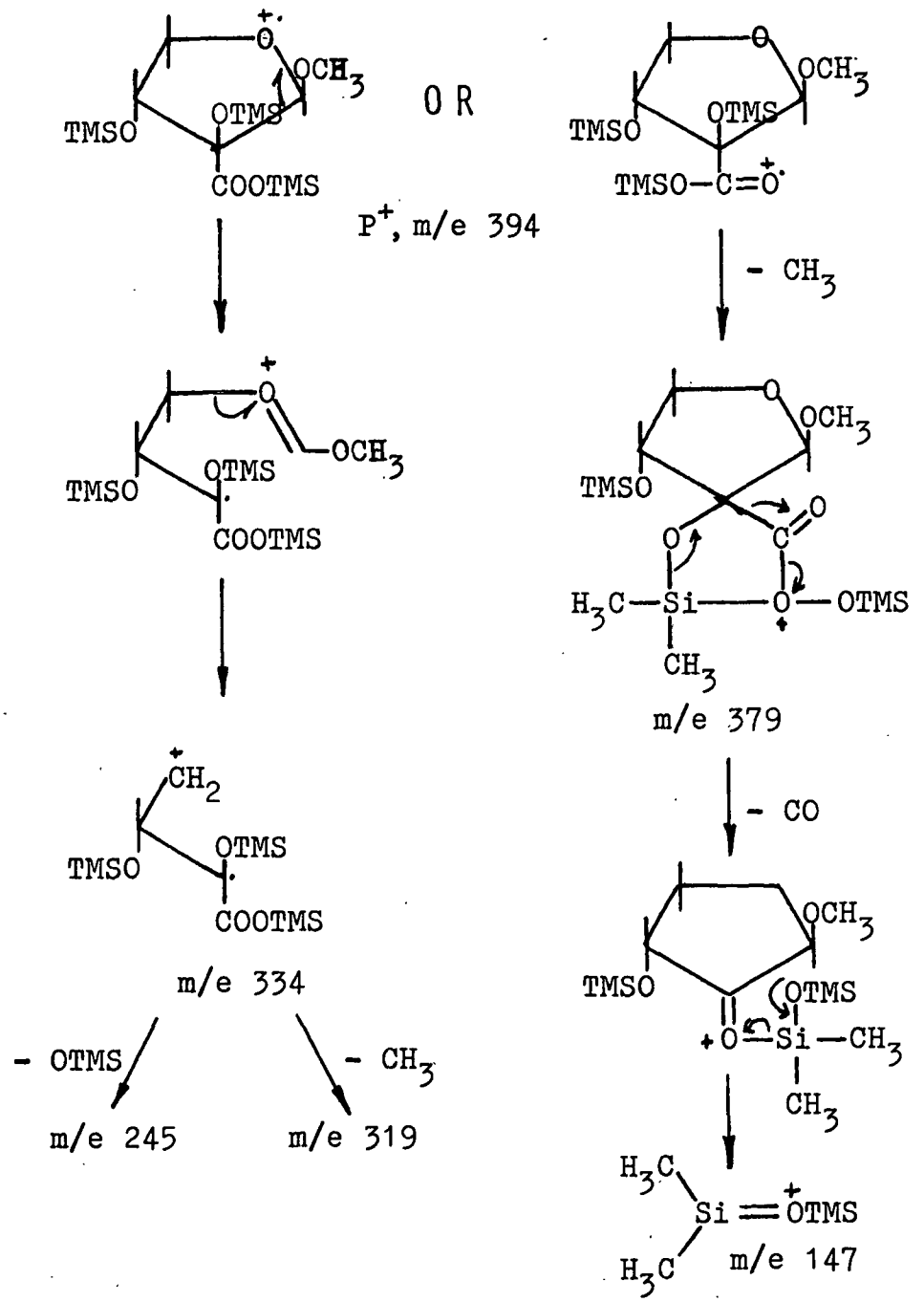

Figure 31. Fragmentation Pattern for Some Major Ions in the Mass Spectrum of MBX and MBR Products (6) and (7)

TABLE XXV

MASS SPECTRAL DATA FOR METHYL 2-C-CARBOXY-β-D-TETRAFURANOSIDE (TMS DERIVATIVE) (MBR AND MBX PRODUCT ⑦)[a,b]

m/e	Relative Abundance, %	m/e	Relative Abundance, %
73	100	219	3
74	20	221	6
75	30	229	4
89	17	230	4
101	3	231	12
114	5	232	4
116	6	233	6
117	4	244	6
119	5	245	5
129	10	246	24
131	10	247	7
132	5	259	4
133	31	262	4
141	4	277	21
142	5	288	4
145	4	289	3
147	58	291	8
148	12	292	4
149	12	293	4
156	5	319	15
161	9	321	8
175	8	334	57
186	5	335	19
190	12	336	6
191	15	337	5
201	7	347	14
205	8	348	3
208	5	351	6
211	4	363	2
215	13	379	25
216	4	380	5
217	13	381	5
218	5	394	6

[a] Mass spectra from MBR and MBX systems were identical within the operating limits of the mass spectrometer.

[b] Fragmentation patterns for some major ions are given in Fig. 31.

APPENDIX IV

REACTOR SYSTEM

REACTION VESSEL

The reaction vessel was the same as described by Millard (1) and the reader is referred to his thesis for a detailed description of the vessel. The inside of the reactor was completely Teflon lined which minimized the possibility of surface catalysis. Agitation in the reactor was accomplished by an air-driven magnetic stirrer also described by Millard (1).

OIL BATH AND TEMPERATURE CONTROL APPARATUS

The oil bath pan design was patterned after the pan described by Brandon (83). Insulation was provided by calcium silicate and the reaction vessel was raised and lowered by a rack and pinion mechanism. The bath was heated by a Polyscience 73 immersion circulator (0-1000 w; Polyscience Corp., Niles, Illinois) equipped with a pre-set thermostat (120°C; J. L. Stortz Div., PSG Industries, Inc., Perkaskie, Pennsylvania) to insure temperature reproducibility. As a safety precaution, the heater was plugged into an Over-Temp Guard (Instruments for Research and Industry, Cheltenham, Pennsylvania) set at 130°C.

Reactor temperature was sensed by an inconel clad, copper constantan, grounded thermocouple (Omega Engineering Inc., Stamford, Connecticutt). The signal from the thermocouple was referenced to a type T thermocouple reference junction (Charles T. Gamble Ind., Riverside, New Jersey) and the output recorded by a Leeds and Northrup Speedomax Flatbed 628 recorder. As sensed by the thermocouple, the reactor temperature was controlled to ± 0.2°C.

SAMPLING SYSTEM

The reactor was sampled under pressure through Teflon lines (0.063 inch OD x 0.031 inch ID, Chromatronix, Inc.) and a series of pressure tight, inert valves (Chromatronix, Inc.) (Fig. 32). The Teflon line was backed by stainless steel tubing for the first 12 inches leading from the reactor. The sampling system could be arranged to take either a small sample (kinetic or methanol sample, ca. 0.8 ml) through the sample loop or a large sample (peroxide or product sample, ca. 4-5 ml) through the bypass to the sample loop. In all cases, sample valve ports B2, B3, and A2 were blanked.

GLYCOSIDE AND METHANOL SAMPLING PROCEDURE

1. The three-way valve was positioned to connect ports C2 and C3.
2. The sample valve was placed in position B. This connected ports A3, A4, C2, and C3 filling the sample loop with reaction solution.
3. The sample valve was placed in position A. By use of the syringe attached to port A1, the sample was blown out port B4 into the sample vial.
4. With the sample valve in position A, the sample loop was back-flushed by drawing solvents through port B4 and out port A1 with a vacuum.

PEROXIDE AND PRODUCT SAMPLING PROCEDURE

1. The three-way valve was positioned to connect ports C2 and C1.
2. The sample valve was placed in position B. Pressurized reaction solution then flowed from the reactor through ports A3, A4, C2, and C1 directly into the sample vial.
3. When the desired sample size was obtained, the sample valve was returned to position A.

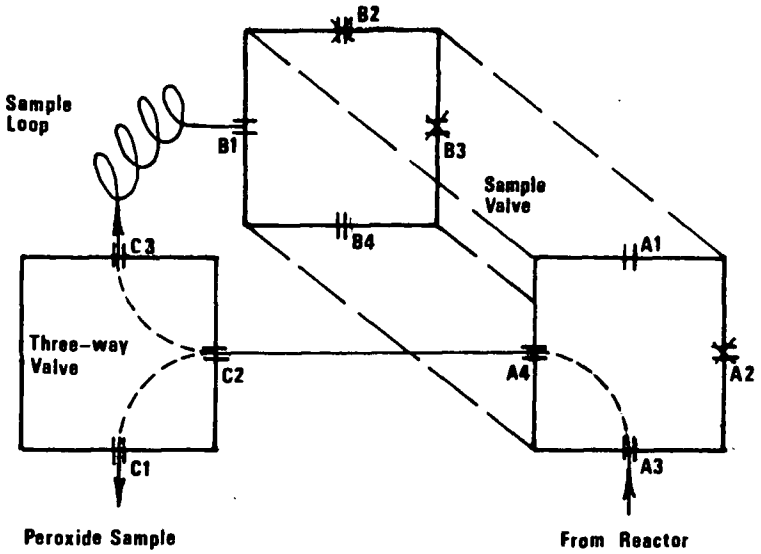

Position B

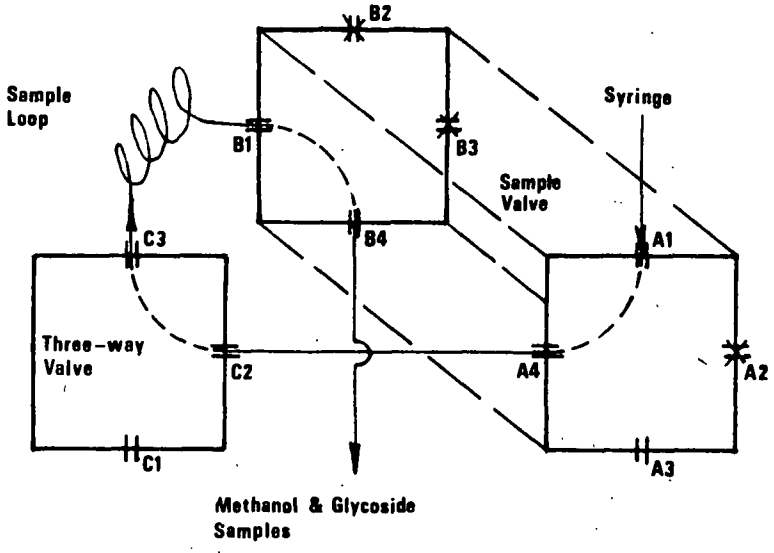

Position A

Figure 32. Schematic Representation of Reactor Valve System